Title
High biofuel production of Botryococcus braunii using optimized cultivation strategies

Author
Yu, Wei

Publication Date
2014

Peer reviewed|Thesis/dissertation

UNIVERSITY OF CALIFORNIA

Los Angeles

High biofuel production of *Botryococcus braunii* using optimized cultivation strategies

A dissertation submitted in partial satisfaction of the

requirements for the degree Doctor of Philosophy

in Biomedical Engineering

by

Wei Yu

2014

ABSTRACT OF THE DISSERTATION

High biofuel production of *Botryococcus braunii* using optimized cultivation strategies

by

Wei Yu

Doctor of Philosophy in Biomedical Engineering

University of California, Los Angeles, 2014

Professor Pei Yu Chiou, Co-chair

Professor Chih Ming Ho, Co-chair

This thesis describes how using a heterotrophy-recovery-autotrophy route (called the green cycle) for the cultivation of *Botryococcus braunii* results in high biofuel production. Our experiments show that the addition of citrate to a culture can increase cell numbers by up to 20 times compared with the control in the first week. A metal solution was then added to help cells synthesize chlorophyll, enabling *Botryococcus braunii* to regenerate

the chlorophyll content in the plastids and become autotrophic. In our experiments, high cell numbers were obtained after two weeks and biofuel production was enhanced.

We also developed an N-N-A source media which could achieve enhanced cell growth as opposed to using nitrate as the only nitrogen source. This N-N-A source media was able to balance pH variation due to nitrate uptake, so as to maintain the pH level in the media solution without the use of buffer.

By applying these techniques to the *Botryococcus braunii* culture, we found that cell growth could increase by up to 58 times in comparison with the control.

The dissertation of Wei Yu is approved.

Jacob J. Schmidt

Andrea M. Kasko

Pei-Yu Chiou, Committee Co-chair

Chih Ming Ho, Committee Co-chair

University of California, Los Angeles

2014

TABLE OF CONTENTS:

Acknowledgements

First of all, I would like to express my thanks to my faculty advisor, Prof. Chih Ming Ho, who gave me great support and helpful direction in this research. He has been a role model for every member in our group, encouraging innovation and persistence. I am very grateful for the learning experience provided by Prof. Ho over many years.

Secondly, I could not have completed this project without the support of my fellow committee members: Prof. Pei-Yu Chiou, Prof. Jacob Schmidt, Prof. Andrea Kasko and Prof. Chih Ming Ho. They are encouraging and inspiring my creativity along the project. In addition, I would like to thank faculty members Prof. James Liao and Prof. Laurent Pilon who acted as our research advisors.

I would also like to acknowledge the fund provided by the von Liebig Entrepreneurism Center for my DOE fellowship during 2012-2013 which supported the commercialization path of this project.

Finally, it has been a great honor to work with Prof. Ho's group in particular with Priscilla Zhao, Thang le Nguyen, Dr. Xianting Ding, Dr. Leong Wong, Dr. Leyla Sabet, Dr. Gauvain Haulot, etc. I appreciated everyone's help and was inspired by the group's dedication and motivation. I will carry this inspiration into my future life.

My heartfelt thanks.

Prof. Ho's group, 2012

VITA

WEI YU

Education

2005-2010 Bachelor of Engineering at Zhejiang University

Major: Biomedical Engineering GPA：3.7

2010-present Ph.D. candidate at University of California Los Angeles

Major: Biomedical Engineering GPA：3.533

Research

2007-2008 ZJU SRTP (Student research training program): "*A convenient system for preparation and measurement of bilayer lipid membrane*", directed by Prof. Xiaoxiang Zheng.

2008-2009 National Research Program: "Chip-based biosensors for functional analysis of ion-channels", directed by Prof. Ping Wang, Prof. Qiang Xia and Prof. Wei Liu.

2007-2009 Biosensor National Special Laboratory: "*Electrochemical characterization and biosensor application of gold-coated ZnO nanorod arrays electrode*", directed by Prof. Ping Wang. This was accepted for publication by the *Chinese Journal of Sensors and Actuators.*

2009 June-July The Joint Research Center of Photonics between Royal Institute of Technology in Sweden and Zhejiang University in China: photolithography and etching experiments for fabricating silicon chips, directed by Prof. Sailing He.

2010-Present Research Assistant in UCLA Microsystems Laboratories, advised by Prof. Chih Ming Ho.

Teaching

2011-2012 Teaching Assistant in UCLA Chemistry Department for Chemistry 14A-2 (Dr. Eric Scerri: Atomic and Molecular Structure, Equilibria, Acids, and Bases), Chemistry 20A (Dr. Kevin Barnese: Chemical Principles); and Chemistry 153A (Dr. Heather Tienson: Biochemistry).

Professional employment

2011-2012 Co-founded **Chihuo.org**. Chihuo is a commercial website focusing on the introduction of Chihuo cuisine and culture within the Greater Los Angeles Area.

2012-Present Founded **Lyxia Corporation** with Dan Zhang in the state of Delaware. Lyxia is an early stage biotechnology company working in the area of commercialized microalgae cultivation and biofuel production (www.lyxia.com).

Projects & Products & Publications

US patent application No. 61720942 "*Enhanced oil and protein production in microalgae and cyanobacteria".*

Award

Southern California Clean Energy Technology Acceleration Program

Department of Energy June 2012.

North America Chinese Startup Contest

UCAHP, TEEC, HYSTA January 2013.

FloW Competition Regional Final

Department of Energy May 2013.

Finalist in regional final of FloW Competition sponsored by US Department of Energy.

UCLA ITA SEVC FINAL

UCLA ITA May 2013

Patrick Soon Shiong Innovation Award 2013 Nominee

Patrick Soon-Shiong, M.D; Los Angeles Business Journal, NantWorks September 2013.

Additional Honors & Awards

Fellowship of Southern California Regional Renewable Energy Technology Acceleration Program, sponsored by the U.S. Department of Energy

Chapter 1. Introduction to the microalgae industry

1.1 Environmental issues and the hunger for energy

Worldwide climate change is today's most urgent global environmental problem. Hundreds of millions of people could lose their lives and up to one million species in nature could become extinct if the average global temperature rises by more than 2°C [1]. It is widely believed that burning fossil fuels accounts for global warming; therefore the use of fossil fuels as a conventional energy resource should be gradually substituted with clean, renewable energy sources to reduce greenhouse gas emissions [2]. In addition, global warming could lead to other environmental hazards including a potential increase in sea levels and the subsequent submerging of lowlands, deltas and islands, as well as changes to climate patterns [3].

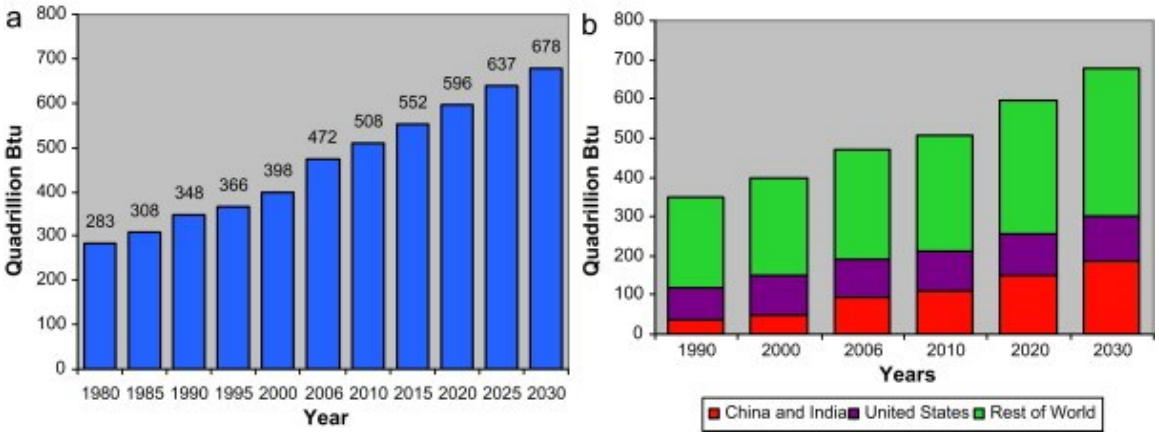

Fig. 1 (a) World energy consumption. (b) Energy use by region .Sources: Energy Information Administration (EIA), International Energy Annual 2006 and World Energy Projections Plus (2009). [117]

Despite rigorous efforts in predicting and exploiting new reserves of energy in the past, it turns out that the world cannot continue the luxury of maintaining the same energy consumption rate going forward. Global energy resources are limited. According “Energy in 2050” issued by HSBC Global Research in March 2011, oil supplies are calculated to last barely 49 years even if we assume that demand will not increase in the future [4]. Therefore, in order to solve these pressing and important issues, we need to develop new technologies to allow the substitution of fossil fuels with clean, renewable energy sources.

Fossil fuels – what's left?				
	Reserves		Years left at current production	
	Proven	Potential	Proven	Potential
Oil (bn barrels)				
Conventional	1333	3322	43	108
Unconventional*	143	6829	5	223
Total	1476	10151	48	331
Natural gas (bn barrels**)				
Conventional	942	1759	53	98
Unconventional***	200	5716	11	320
Total	1142	7475	64	418
Coal (bn tonnes)	826		176	

Table 1 HSBC estimates based on BP, USGS, H-H Rogner 'An assessment of world hydrocarbon resources' 1997 [5].

* According to the International Energy Agency's (IEA) World Energy Outlook 2001, unconventional oil includes "oil shales, oil sand-based synthetic crudes and derivative products, (heavy oil, Orimulsion®), coal-based liquid supplies, biomass-based liquid supplies, gas to liquid (GTL) - liquids arising from the chemical processing of gas."[6]

** Herein the "bn barrels" indicates the volume of natural gas equivalent to bn barrels of oil.

*** In terms of their chemical composition (primarily methane), these resources are identical to conventional natural gas. We call them "unconventional" because of their atypical geological locations. Unconventional gas is found in highly compact rock or coal beds and requires a specific set of production techniques.

1.2 Biofuel Technology

As the end of the age of fossil fuel is approaching, people are making persistent efforts in searching for new energy candidates. Various alternatives to coal, oil, and natural gas range from electricity generated by solar farms to biofuels brewed from plants. However, the progress that scientists are establishing the fundamental basis for the development of better alternatives is challenging, which potentially indicates the technical, political, and economic pitfalls associated with further scaling up [7].

To replace a substantial fraction of the petroleum supply with biofuel, feedstock that can grow in virgin soil without competing with the conventional food supply would be an attractive choice [8]. Nowadays, the process that turns lignocellulosic feedstocks into biofuels is encountering a matter of cost and efficiency, but scientists are trying to improve the approach on many fronts [9].

Biofuels are alternative transportation fuels in the form of liquid or gases that are predominantly produced from biomass. As a renewable resource, biofuels are bringing many interests, including sustainability, reduction of carbon dioxide (CO_2) emissions, regional development, and security of supply [10].

Biomass, as a primary renewable energy source to supplement diminished fossil fuels, are drawing more and more public and academic attention, driven by factors such

as oil price peaks, the need for enhanced energy security, concern over greenhouse gas emissions from fossil fuels, and government subsidies [11, 12]. There are three reasons for biomass to be an attractive feedstock. Firstly, it is a renewable resource that could be sustainably developed in the future. Second, it has positive environmental impact resulting in no net releases of carbon dioxide (CO_2) as well as very low sulfur content. Third, its economic potential could become significant provided that prices of fossil fuel increase in the future [13]. Lignocellulosic bioethanol has such low emissions because the carbons in alcohol are mainly derived from carbons that were sequestered in the biofuel feedstock during the growing period and are only being released back into the atmosphere [14].

In the next few decades, to address societal needs to reduce the net carbon emissions, it is imperative to develop biofuel as an alternative resource to supplement liquid transportation fuels. As a global energy survey showed that the potential of bioenergy ranges from 10% to 60% of world primary energy supply [15-18], biomass is poised to serve as a fundamental successor to fossil fuels. The International Energy Agency (IEA) [18] estimates that by 2050, 50% reduction in greenhouse gas emissions will require a factor of 4 increases in bioenergy production, reaching 150 EJ/year (1 EJ=10^{18} J) that could provide over 20% of global primary energy.

There are many studies target on the commercialization of concepts in the transportation sector, for example, regional deployment of clean energy resources,

creating supply chain for eco-friendly process, supporting sustainable development, etc. At present, using biofuels from a variety of biomass sources as cost-competitive substitutes to fossil fuel becomes popular trends in the developed countries, where they are apt to employ innovative technologies involving efficient bio-energy conversion [19]. Biofuels provide biodegradability and sustainability to the industry and society [20].

Currently, biomass could be converted to oil by fast pyrolysis and subsequently the oil turns into hydrogen (H_2) via catalytic steam reforming [21-23]. However, the H_2 productivity is still low, accounting for 16-18% of dry biomass weight [24]. By co-reforming of biomass-derived oil with natural gas, it is possible to increase the yield of H_2 in the process [25]. In biomass pyrolysis, a low temperature, high heating rate and short gas residence time process would favor the formation of liquid products while a high temperature, low heating rate, and long gas residence time would maximize the yield of fuel gas [26].

Biofuels from plant feedstock can be used when mixed with diesel fuels. In the past two decades, researchers have exerted great efforts to convert vegetable oils and animal fats into biodiesel that can be incorporated into diesel fuel. [27-32]. Chemically speaking, biodiesel is a mixture of long-chain alkyl (methyl, ethyl, or propyl) esters obtained from vegetable oils and animal fats. Plant feedstock includes soy, canola, corn, rapeseed, and palm while Animal fats are commonly considered involving those derived from poultry, beef, and pork [33].

Cellulosic biomass or sugar-based crops are also served as a feedstock for ethanol production. The feedstock includes carbohydrate-based crops such as corn, rice and sugarcane, fast-growing perennial grasses such as switchgrass and giant miscanthus, and woody crops such as fast-growing poplar and shrub willow [34, 35]. Although there is still a long way to go, bioethanol already made a relatively small but significant contribution to the global energy supplies.

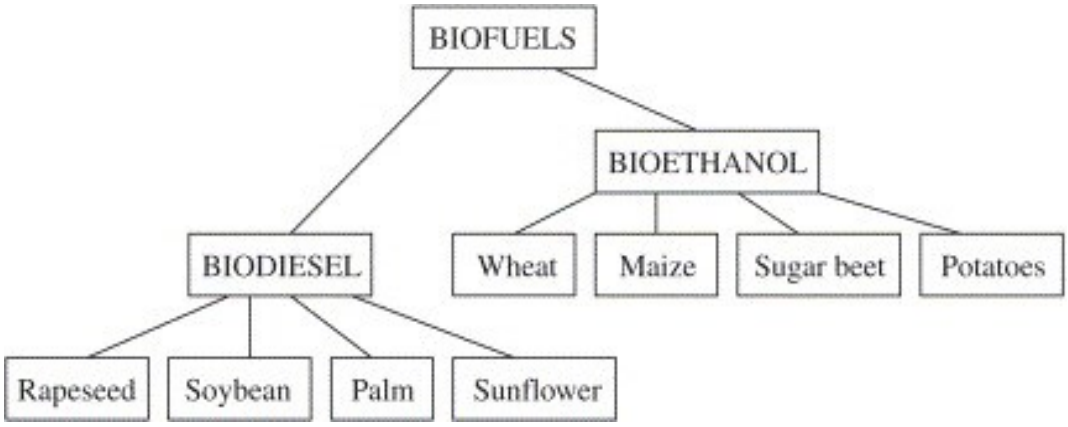

Fig. 2 Resources of main liquid biofuels for automotive. [36]

Lignocellulosic biomass is another source of biofuels that can be converted into cellulosic ethanol. The biomass is firstly compacted and transported to the ethanol refinery. A pretreatment is conducted to break it down into intermediates and remove the lignin from the biomass extracts. Then a detoxification and neutralization process is followed to separate the previous intermediate into its liquid and solid components. The

latter are then hydrolyzed using enzymes that are produced in microbial bioreactors. Finally, sugars are fermented to produce ethanol (Fig. 3).

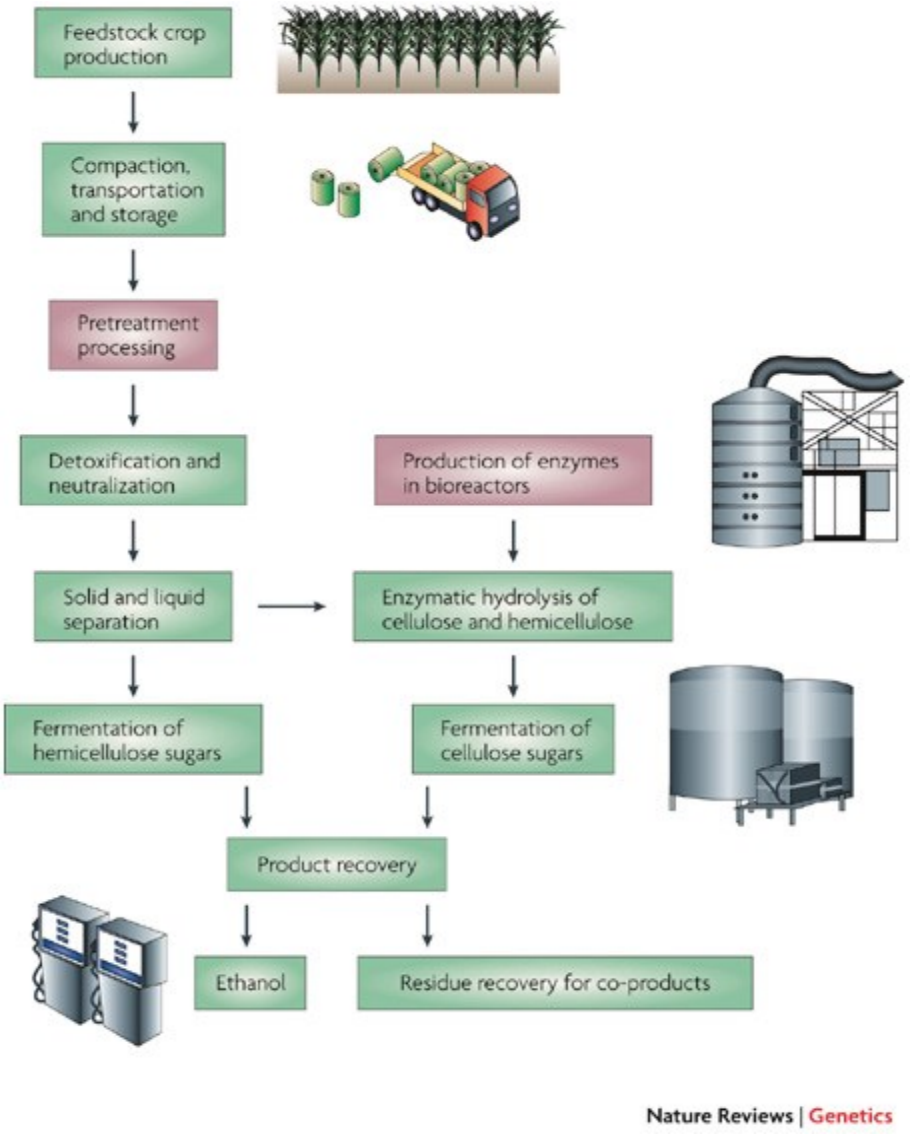

Fig. 3 Flow chart showing the steps in the production of cellulosic ethanol from feedstock crops. [116]

1.3 Microalgae biofuels and different engineering approaches

Since the 1960s, people started to discover the use of microalgae as sources of fuel [37], whereas, the real push on this subject took place with the 1970s' global oil crisis. The U.S. DOE funded a national project in 1978, in order to develop renewable liquid fuels from algae [38]. In the project, scientists aimed to generate microalgae-based biodiesel that were cultured in the open ponds using carbon dioxide from coal-fired power plants. In the 1990s, Japan started to realize the importance of carbon emission, and they launched a similar research program which use CO2 as sources of inorganic carbon to grow microalgae and cyanobacteria [39].

Microalgae accumulate oils during nutrient starvation [40]. Generally, there are generally two approaches to treat the oil extracted from algae. One way is converting oils into biodiesel by transesterification with short-chain alcohols [41]. And another method is to hydrogenate the fatty acids into aliphatic hydrocarbons [42]. Besides, algae can also produce hydrogen (H2) [43], ethanol [44] and long-chain hydrocarbons that resemble crude oil [45]. Alternatively, the biomass can be converted to biogas through anaerobic fermentation [37].

Most microorganisms do not produce considerable quantities of hydrocarbons. There is one obvious exception. *Botryococcus braunii* accumulates hydrocarbons in quantities that can amount to 80% of its cellular dry weight during the stationary phase of growth. Most of these oils are secreted and embedded in the extracellular matrix.

Debates that were surrounding inadequacy of microalgae commercialization and readiness for scale up persisted for the past few years. [45] Currently, productivity of microalgae is inferior to energy crop. In 2010, volume of the biodiesel market was €1.25 billion, indicating an average market price for microalgae at $318.5/kg dry biomass [46]. On the other hand, the world production of palm oil in 2010 approximated 40 million tons, with a market value of $0.64/kg [47].

Thereby large scale cultivation of microalgae is imperative. In Europe, 0.4 billion m^3 biodiesel would be needed per year if all transport fuels were to be substituted by biodiesel in Europe [48]. This accounts for an algae cultivation area of 9.25 million ha (almost the surface area of Portugal).

Very few microalgae strains had been sequenced [50], e.g., *Chlamydomonas reinhardtii* [51], *Thalassiosira pseudonana* [52], and *Phaeodactylum tricornutum* [53]. However, only *C. reinhardtii* had been proven as a common model for sophisticated metabolic engineering.

As well as other plants, sunlight, water, CO_2, nitrogen, and phosphorus are required for microalgae cultivation. Large-scale cultivation of microalgae for biofuel production must rely on sunlight as the sole source of light energy. When culturing in summertime

and/or culturing at lower latitudes, sunlight intensities are too high and often oversaturate the photosynthetic cycle, which will limit growth and lead to a drop in productivity. Recently, much researches were into increasing photosynthetic efficiency of microalgae under oversaturating light (the normal condition on a sunny day) by developing new strains with smaller antenna sizes [54] and by decreasing the light path of photobioreactors while increasing mixing (turbulence) in high cell density cultures [55,56]. However, turbulence requires high energy input and, therefore, is not suitable for large-scale production of biofuels from microalgae. One strategy to obtain high photosynthetic efficiencies under bright sunlight in systems with lower energy requirements is to reduce the light intensity at the reactor surface. For instance, stack the reactor unit vertically (Fig. 4): Narrow spacing in the stacks minimizes loss of light to the ground surface [57]. But, this setup will lead to voluminous reactor systems with low volumetric productivity and low biomass concentration with a long light path [58]. To reduce investment costs of these systems, vertical panels can be made from thin plastic films such as polyethylene (Fig. 5). There are examples of thin film systems submerged in large water volumes for good temperature control and a lower associated energy requirement for cooling [59]. We expect that in the future more systems will be developed based on these design principles (Fig. 5).

Fig. 4 Vertically aligned photobioreactor units in Arizona State University.

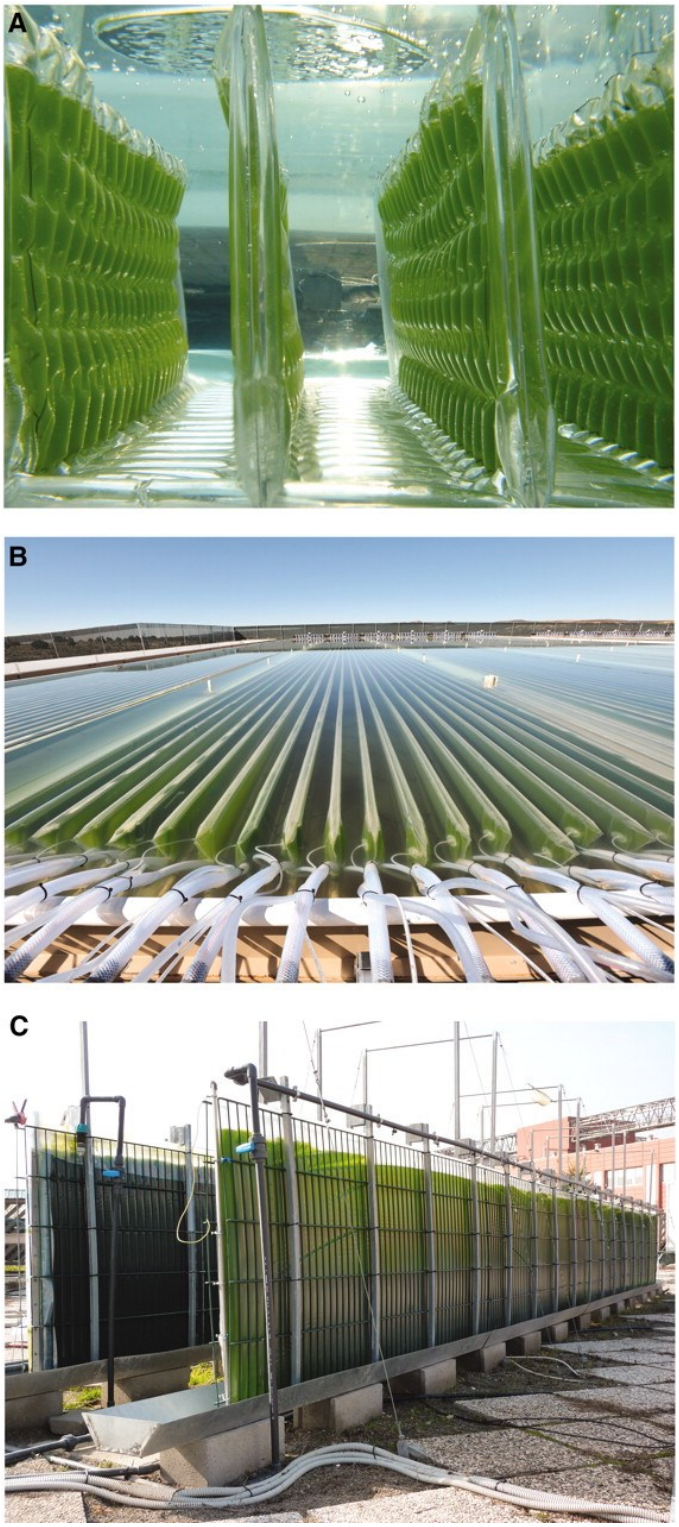

Fig. 5 Development of low-cost photobioreactors [61]. Flat-panel reactorsfrom (A) Proviron, Belgium reproduced with permission from [60], (B) Solix Biofuels, USA (reproduced with permission from Biomass Magazine), and (C) Green Wall Panel reactors from Fotosintetica & Microbiologica S.r.l., Italy.

Nitrogen and phosphorus are two main nutrients needed for the production of microalgae. The algal biomass consists of 7% nitrogen and 1% phosphorus As a result, biofuels in European market will need 25 million tons of nitrogen and 4 million tons of phosphorus, which is estimated approximately twice the amount of the current fertilizer productivity in Europe [60]. Therefore, using culture residual as recycled nutrients to feed microalgae for sustainable biofuel production became a solution. It reveals that the protein could be used as a nitrogen-source, and go through to recycle the nitrogen.

Besides microalgae oils, coproduction of proteins from algae is another promising field. The algal biomass which is used for fuel production typically consists of 40% protein. Assuming microalgae could supply 0.4 trillion liters biodiesel to the European market; protein content as a by-product would reach approximately 0.3 billion tons. This number is about 40 times as much as the amount of soy protein (18 million tons of soybeans with 40% of proteins in 2008) currently imported into Europe [47]. Therefore, an integrated technology platform is needed for complete development and usage of various cell compounds from microalgae.

1.4 Proteins as a source of biofuels

Carbohydrates and lipids are commonly used as biofuel sources. Proteins, however, have not been used to make fuels because of the barrier to deaminate

protein hydrolysates. However, conventional bio-refinery methods for carbohydrates and lipids are inferior for several reasons [126]. First, microalgae are subject to nitrogen starvation for higher lipid productivity, resulting in compromised cell growth and CO_2 fixation. Second, microalgae harvest schemes, lead to accumulation of protein by-products (Fig. 6), currently delivered to the limited feedstock market [61]. Third, it is essential to recycle the reduced nitrogen otherwise could cause a net decline of reduced nitrogen in nature [62,63] and plus a lift in the atmospheric level of nitric oxide, which is greenhouse gas almost 300 times severer than CO_2 [64]. Furthermore, the lost reduced nitrogen must be replaced by supplementing crops with reduced fertilizer nitrogen, which is generated by the energy-intensive and environmentally unfriendly Haber-Bosch process [65].

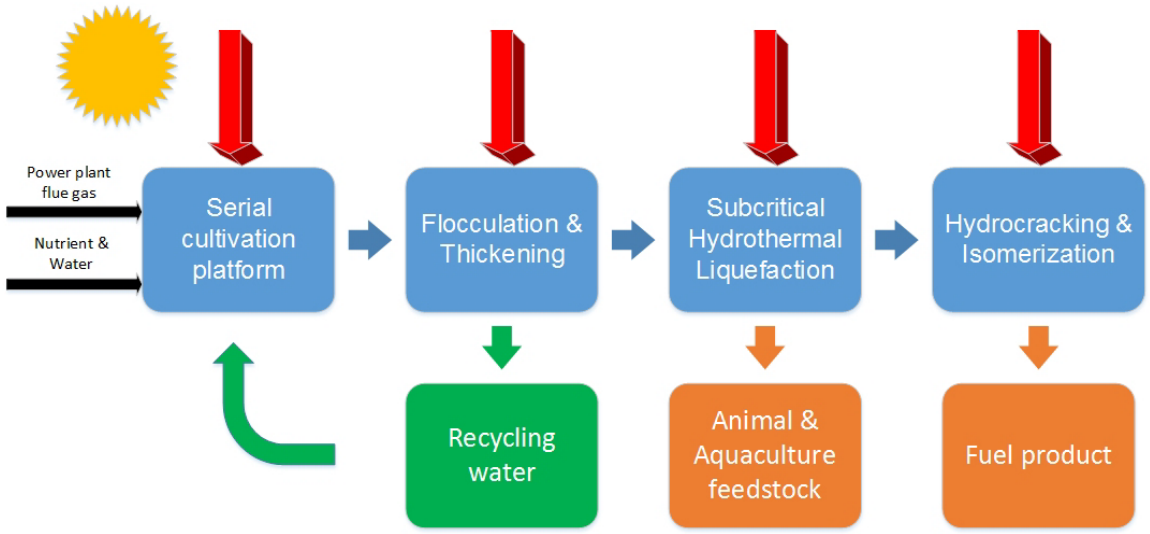

Fig. 6 Fuel and feedstock combined path for microalgae production. Currently, Proteins as extraction residues are sold as animal feedstock.

Proteins are the dominant fraction in photosynthetic microorganisms [38, 66] and industrial fermentation residues. To begin with, the peptides and amino acids are subject to enzymatic reactions, including deamination, transamination or dehydrogenation. And these reactions must happen in order to release the carbon skeletons prior to protein hydrolysis. However, thermodynamic irreversibility and metabolic regulation that favors anabolism over catabolism becomes the major barrier to deaminate proteins hydrolysates [67]. If we could properly engineer the metabolic regulation, some amino acids could be directly deaminated to 2-keto acids, which can be converted to aldehydes and then further to alcohols by alcohol dehydrogenases [68].

One possibility of utilizing proteins as a source of biofuels is associated with the sugar-lipids process. As a pivot metabolite in cell machinery, pyruvate can be further extended to longer keto acids by acetohydroxy acid synthase or isopropylmalate synthase chain elongation pathways, which both provide potential for proteins to be used for fuel production [68, 69]. But the native productivity of converting amino acids to higher alcohols is far from sufficient [67]. Therefore, we need to engineer a metabolic driving force to suit those hydrolysates for fuel production.

In order to effectively deaminate protein hydrolysates, the transamination and deamination cycles were first engineered in *E.coli* [126]. With a simple process of pretreatment and enzymatic hydrolysis, microbial proteins can be readily hydrolyzed.

Additionally, this process does not produce furfural and 5-hydroxymethylfurfural that inhibit microbial growth, as lignocellulose hydrolysis does.

Proteins could come from several sources. Fermentation, food processing and biofuel production can generate proteins (Table 2). Because proteins are the major component of microalgae [65] in open-pond cultures that are not artificially induced to accumulate lipids (Fig. 7), even with contamination by heterotrophic bacteria, the combined protein sources are still usable as raw material.

Source of biomass feedstock	Annual accumulation (million metric tons)	Protein content in biomass (%)	Potential protein leftover (million metric tons)	Potential biofuel production (billion gallons)
Corn ethanol	110	9.8	10.8	2.14
Fermentation	1.5	40	0.6	0.12
Total			11.4	2.26

Table 2 Proteins are rich in the industrial fermentation residues [126]. Potential protein leftover from current biofuel production and bio-fermentation was calculated. Current US annual corn ethanol production is over 11 billion gallons [70].

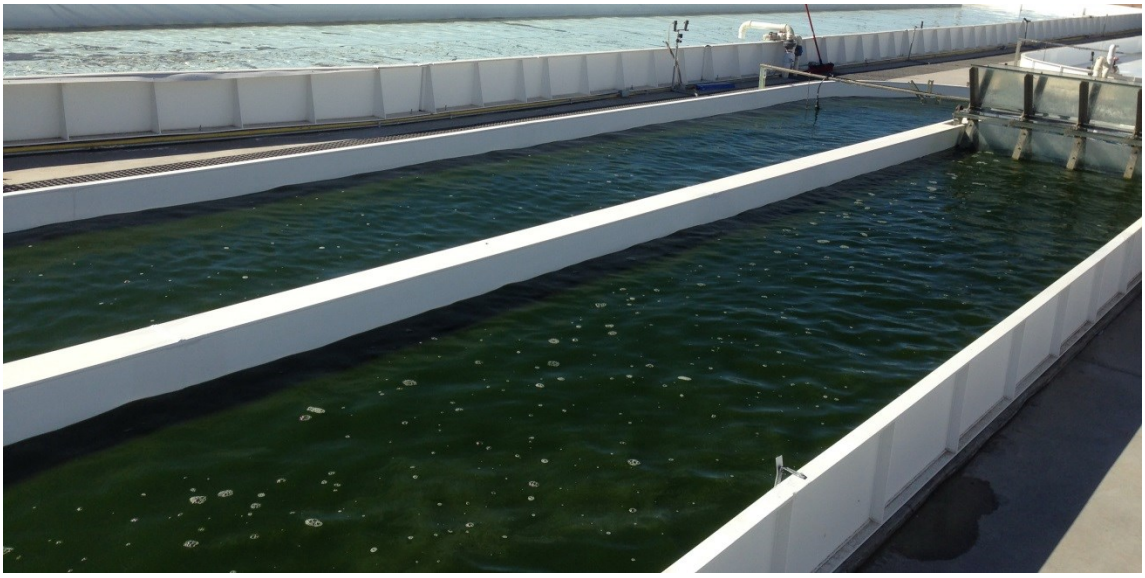

Fig. 7 An open raceway pond in Arizona State University

1.5 Summary

As the high technology industry and energy market continues to thrive, biofuels are poised to become the right candidate for petroleum. Considering the very significance and indispensability of liquid transportation fuels in the current world, microalgae biofuels provide such an attractive solution to this situation. Before 1990s, lots of academic research and pilot scale demonstration have been done to show the potential and productivity of microalgae biofuel. Since 2000, commercial scale production of microalgae biofuel has found its way to flourish. There are many microalgae biofuel companies emerge in the United States, such as Sapphire Energy, Synthetic Genomics, Solix, and etc.

Regardless the high cost and low productivity of biofuel obtained from microalgae right now, scientists are searching for other valuable products from algae which can be commercially deployed. Protein, as a major component in algae, has undergone further development for the past few decades. Intense efforts have been made to explore alternative protein sources such as food supplements, mainly in anticipation of an insufficient future protein supply. Examples include yeasts, fungi, bacteria and microalgae.

The gross chemical composition of different microalgae species has been published in research literature. To give a general overview of the major constituents, selected data of various microalgal species are compiled in Table 3. Up to now, very few have been selected for commercial-scale deployment (i.e. *Chlorella* sp., *Scenedesmus obliquus*, *Spirulina* sp. and *Athrospira* sp).

Algae	Protein	Carbohydrates	Lipids
Chlamydomonas reinhardtii	48	17	21
Chlorella pyrenoidosa	57	26	2
Chlorella vulgaris	51-58	12-17	14-22
Dunaliella salina	57	32	6
Scenedesmus obliquus	50-56	10-17	12-14
Arthrospira maxima	60-71	13-16	6-7
Spirulina platensis	46-63	8-14	4-9
Synechococcus sp.	63	15	11

Table 3 General composition of different algae (% of dry matter) [63]

Many nutritional and toxicological examinations have revealed the superiority of using algal protein as a high-value food supplement. On the other hand, utilization of microalgae as feed in aquaculture becomes trends. Currently 30% of current world algal production is sold for use of animal feed. Furthermore, by converting proteins into fuels, we could make use of *E.coli* to process the microalgal proteins into bioethanol.

Chapter 2. Preliminary results showing citrate effects on *Botryococcus braunii*

2.1 *Botryococcus braunii* and its chemical composition

The colonial alga *Botryococcus braunii* is widespread in freshwater environments and can be also found in brackish lakes, reservoirs, ponds in subtropical or tropical zones [71-77]. This alga is famous for a notable ability to synthesize a variety of lipids. It produces a high amount of hydrocarbons, excretes them outside the cells, and accumulates them in its extracellular matrix [78, 79]. Some strains of *Botryococcus braunii* can also produce several certain ether lipids [76, 80].

Botryococcus braunii is traditionally subclassified into three different races, in which they can be distinguished based on their specific hydrocarbons. Race A is characterized by n-alkadienes and n-trienes with odd-numbered carbons (C23 to C33). Race B synthesize triterpenoid hydrocarbons known as botryococcenes (C30-C37), and methylated squalenes (C31-C34) [81]. Race L produces lycopadiene, a C40 tetraterpene.

The hydrocarbon content in *Botryococcus braunii* is significantly higher than that in other oil-producing algae. Race A produces linear olefins that can consist of up to 61% of cell dry weight during the green phase [82]. Botryococcenes (C_nH_{2n-10} triterpenes) that are specifically synthesized by the B race can exist as isomers. Based on the literature, botryococcenes can constitute from 27 to 86% of cell dry weight in Race B population

[78]. $C_{40}H_{78}$ (lycopadiene), which is produced by L race [83], accounts for 2 to 8% of the dry biomass [84].

On the other hand, the three races can be well defined based on the distinctions in certain morphological and physiological characteristics (Table 4). The cell size of the L race (8-9μm×5μm) is relatively smaller than those of races A and B (13μm×7-9μm) [85]. The L race also contains less pyrenoid [85]. On the other hand, color change in colony during the stationary phase varies over different races. When race B and L algae enter stationary phase, their colony turn red-orange and orange-brownish from green color during the active state. For race A, they change into pale yellow from green. It was found that accumulation of keto-carotenoids, e.g., canthaxanthin, echinenone, adonixanthin and etc. contributes to color change during the stationary phases of race B and L.

Botrycoccus braunii			
	Race A	Race B	Race L
Types of hydrocarbon	C_{25}-C_{31} odd numbered n-alkadienes/trienes	Botryococcenes (triterpenes) C_nH_{2n-10}, n=30-37	Lycopadienes (tetra-terpene) $C_{40}H_{78}$
Color in stationary phase	Pale yellow	Orange-brown	

Table 4 Distinctive Features of the three races of *Botryococcus braunii* [129].

2.2 Cell physiology and morphology

Microscope image of *Botryococcus braunii* show that they exhibit a typical morphology (Fig.8), characterized by a botryoid organization of individual pyriform-shaped cells held together by a refringent matrix containing lipids. Droplet can be squeezed from the matrix by the pressure of a coverglass. Ultrastructural studies reveal that the matrix surrounding the basal part of the cells consists of outer walls originating from successive cellular divisions (Fig.9). Furthermore, the bulk of *Botryococcus braunii* hydrocarbons are stored in these outer walls [86].

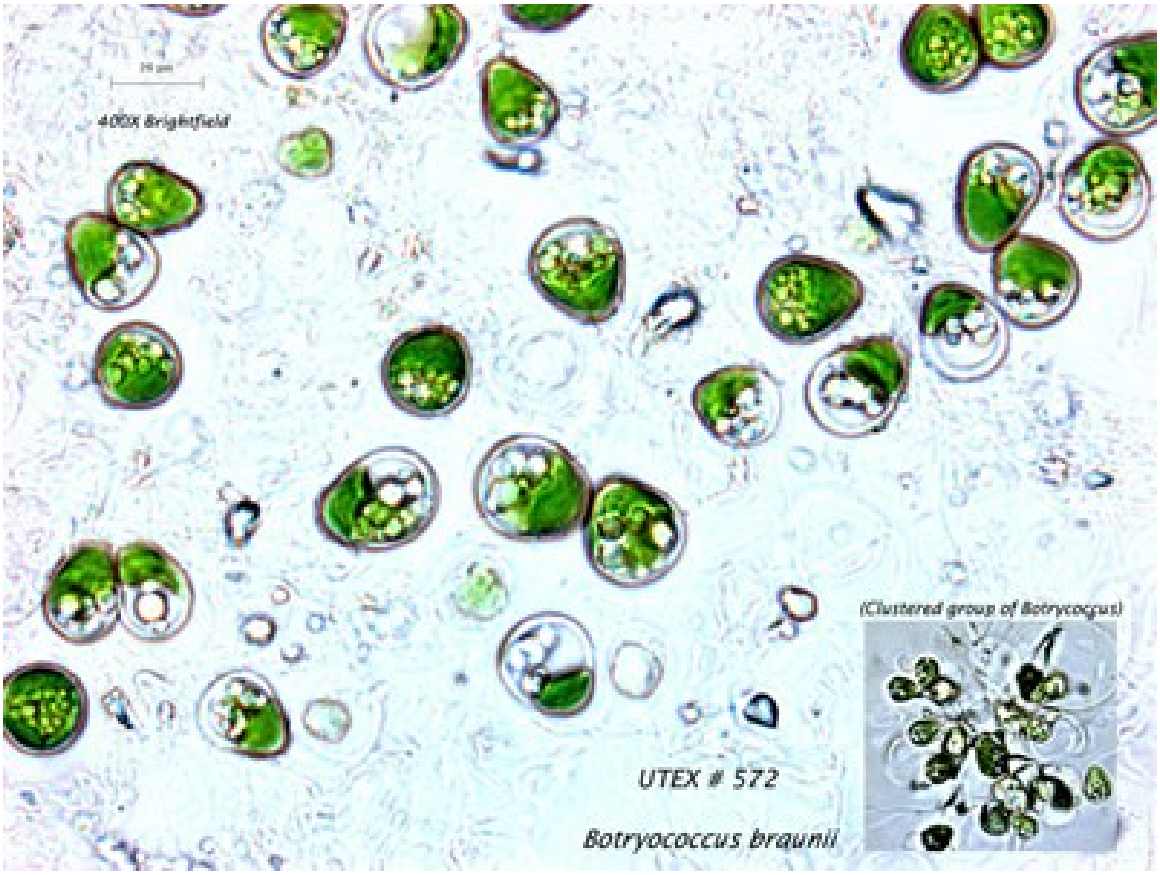

Fig.8 *Botryococcus braunii* under microscope observation (400x Brightfield), ruler bar 16um, right below is the clustered group of *Botryococcus braunii* (cited from UTEX webpage [128])

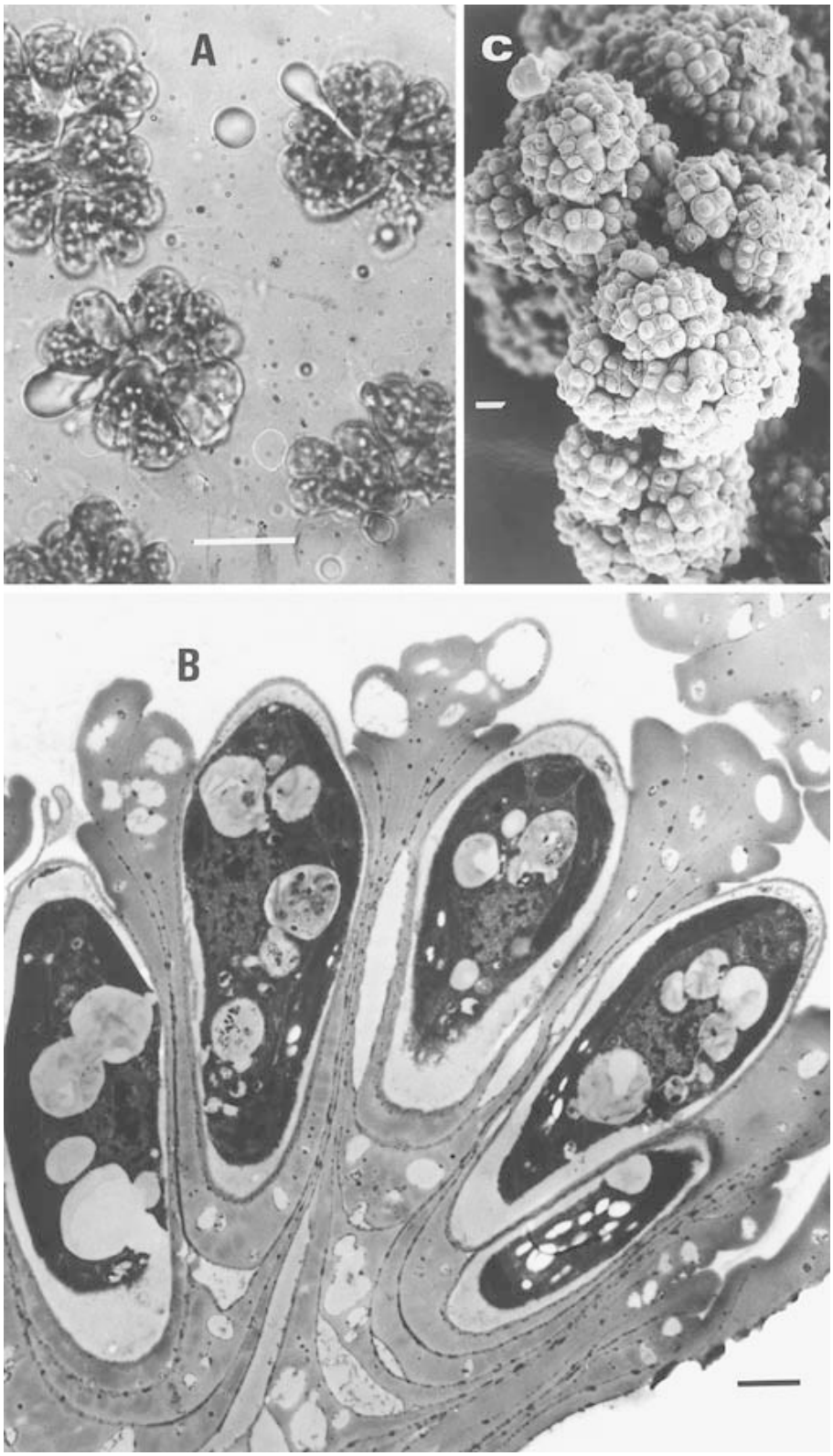

Fig. 9 Micrographs of *Botryococcus braunii* [127]. A light microscopy of a British strain (Maddingley Brick Pits, UK), race A: some refringent globules of lipids are ejected from the colonies by the pressure on the

cover glass. B: Transmission electron microscopy of a colony of a strain from Ivory Coast (Yamoussoukro), race L: the section shows successive outer walls surrounding the cells. c Scanning electron microscopy of a very large colony of a Martinique strain (La Manzo), race B. Scale bars: a, c 10 µm; b 1 µm

Nile red stained cell image under confocal microscope was shown in Fig. 10. While Nile red specifically binds to neutral lipids in the cells, it shows a high fluorescent signal at 525nm under an excitation at 485nm. The rubbery matrix containing oils shows a high lipid content, as well as the cytoplasm. During cell division, each cell secretes new matrix containing oil within the extracellular matrix of the mother cell. Thus, the rubbery matrix saturating with oils grows while the successive matrices gradually accumulate. The cytoplasm is filled with lipid globules [87, 88].

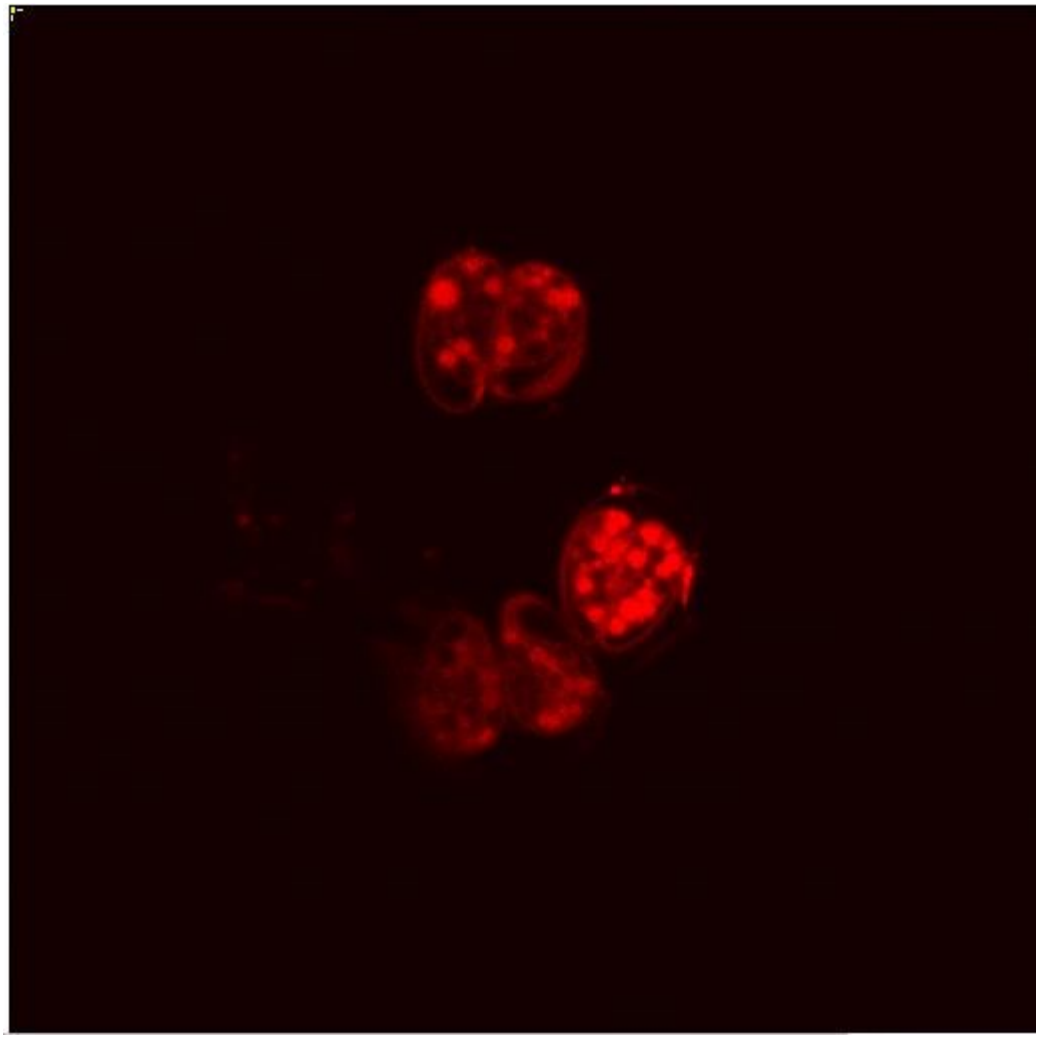

Fig. 10 Nile red stained cell image under confocal microscope. Nile red specifically binds to lipids molecules inside the cells. The rubbery matrix containing oils shows a high fluorescent signal, as well as the cytoplasm.

In the linear phase, *Botryococcus braunii* produce various types of carotenoids such as β-carotene, echinenone, 3'-hydroxy-echinenone, canthaxanthin, loroxanthin, lutein, violaxanthin, loroxanthin, zeaxanthin and neoxanthin. During the linear phase, lutein is the primary carotenoid (22% of total carotenoids in race B and 29% of total carotenoids in race L). Secondary carotenoids produced during the stationary phase are canthaxanthin (46% of total in both race B and L) and echinenone (20% and 28% of

total in race B and L, respectively) [89]. (3S, 3'R)–adonixanthin (42%) is found to present in a substantial amount in race L during its stationary phase [90].

Echinenone constitutes a substantial portion in extracellular carotenoids. As we discussed before, *Botryococcus braunii* undergoes a color change during stationary phase because of an accumulation of ketocarotenoids, mainly echinenone, which are overproduced under stress conditions such as nitrogen depletion and high light intensity. Another possible explanation is the simultaneous decrease in the amount of intracellular pigments in the plastids [91].

2.3 Culture of *Botryococcus braunii*

Much research has been carried out on investigating the optimal culture conditions for Botryococcus braunii. It is recognized that the production of hydrocarbons in Botryococcus braunii is positively correlated to the cell growth, regardless of the particular culture conditions and the media used. According to the algal biochemistry, it is such a substantial commitment for Botryococcus braunii to produce a considerable amount of hydrocarbons, the energetically expensive molecules. Therefore, the observed slow growth rate of this microalgae compared to other strains is apparently not the consequence of nutrient limitation, but the energetic consumption to synthesize and accumulate hydrocarbons.

Botryococcus braunii culture requires water, light, CO_2, and inorganic nutrients. Factors that govern the algae productivity include pH, pCO_2, light intensity, salinity and temperature. Modified Chu-13 medium is often used as growth medium for *Botryococcus braunii*. This medium has the following composition ($g \cdot L^{-3}$): KNO_3 (0.05), K_2HPO_4 (0.01), $MgSO_4 \cdot 7H_2O$ (0.025), $CaCl_2 \cdot 6H_2O$ (0.02), ferric citrate (0.0025), citric acid (0.025), boron (0.125 ppm), manganese (0.125 ppm), copper (0.005 ppm), cobalt (0.005 ppm), and molybdenum (0.005 ppm). The pH in the media is adjusted to 7.5 before sterilization [86].

CO_2 is necessary for Photosynthetic cultures of Botryococcus braunii. CO_2 enrichment favors the formation of lighter botryococcenes (C30–C32), while a substantial portion of heavier botryococcenes (C33–C34) are discovered in the cells sparged with ambient air [92]. Although under autotrophic cultivation, Botryococcus braunii could also utilize exogenous carbon sources for enhanced cell growth, as well as hydrocarbon production. A variety of carbon sources, such as C1-C6, lactose and sucrose, have been demonstrated to achieve a decrease in mass doubling time of the microalgae from 6-7 days to less than 2-3 days [93].

Even though we found that a deficiency of nitrogen supply favors lipid accumulation [94], nitrogen is still essential for growth. Studies on the nitrogen source as NO_3^-, NO_2^-, and NH_3 indicate that the critical factor in regulating nitrogen metabolism in *Botryococcus braunii* is the nitrate uptake system. Thereby nitrogen is generally

supplied as nitrate salts. An initial NO_3^- concentration of ≥0.2 g•L^{-3} favors hydrocarbon production [95]. Brenckman et al. found that with 1 g•L^{-3} KNO_3 the hydrocarbon production after 30 days was 4.8 g•L^{-3}, while about the same level of hydrocarbon production (4.5 g•L^{-3}) was obtained after 30 days if the initial concentration of KNO_3 in the culture media was 3 g•L^{-3}. This is because high concentration of nitrate interferes with hydrocarbon production of *Botryococcus braunii* [96].

Phosphorus is also essential for *Botryococcus braunii* growth, and usually supplied in the form of K_2HPO_4. However, active growth persists after complete depletion of phosphate in the medium. In the early exponential phase, phosphate levels in the medium can drop to below the detection limit (0.5 mg•L^{-3}) [97]. *Botryococcus braunii* can rapidly assimilate phosphate even over the cellular metabolic requirement. Cells store the excessive phosphate as intracellular granules. The excessive phosphate is stored as intracellular granules. When the extracellular phosphate is depleted, the cells will begin to use this phosphate reserve.

The light intensity to support *Botryococcus braunii*'s optimal growth and hydrocarbon production is still in study. As we discussed before, high light intensity may increase the carotenoid/chlorophyll ratio, and thus induce the color change in cell colony [98]. Experiments showed that when *Botryococcus braunii* UTEX 572 are exposed constantly to a light intensity within the range of 25 to 72 μE•$m^{-2}s^{-1}$, carbohydrate concentration, intracellular nitrogen, and phosphorus content drop [99]. *Botryococcus braunii* that is

exposed to a high light intensity during early stage of cell culture could reach a higher biomass density (7 g•L^{-3}) and hydrocarbon content (approximately 50% of cell dry weight) compared to cells that had been exposed to low light intensity (3 klx, or ~42 μE•$m^{-2}s^{-1}$) [100]. However, we showed that high intensity would induce accumulation of carotenoids over chlorophyll, where photoinhibition took place during the exponential phase of cell growth. In controlled close system, There are two approaches to overcome the overexposure of *Botryococcus braunii*;

1). Partial shading of the bubble column photo-bioreactor [100].

2). Adopting a diurnal light cycle (12 h light/12 h dark). However, compared with a diurnal illumination cycle, continuous light resulted in a 4-fold increase in hydrocarbon production [101].

The pH of culture medium is usually adjusted to between pH 7 and 7.5 before cultivation. A rise in pH is observed during active growth of *Botryococcus braunii*, and then a slight drop will be seen later [97]. Similar trends in pH are commonly observed in CO_2 enriched cultures during exponential growth. Experiments showed that the optimal temperature for cell growth is 25°C [102]. Sodium fluoride could stimulate cell growth when added at an initial concentration of 0.1 mg•L^{-3} [103].

2.4 Biotechnological value of *Botryococcus braunii*

It is known that hydrocarbons from *Botryococcus braunii* can be used as direct substitute of petroleum-based fuel products without the complexity of tranesterification and low temperature gelling, which showed an inherent superiority of producing hydrocarbons over biodiesel.

There are two ways to utilize these oils, either by directly pressing out or by solvent extraction of the biomass. Pressing has only been attempted on a laboratory scale, but no reliable information is available on the extent of recovery. *Botryococcus braunii* has a thicker cell wall than most strains, and usually the wet biomass contains a lot of water which cause the efficiency of hydrocarbon recovery to be rather low.

A non-destructive solvent extraction can extract the hydrocarbons without damaging the cells. Hexane is a good choice for extracting algal hydrocarbons [104,105]. For efficient extraction, cells need to be concentrated in order to remove water in the pastes, because presence of abundant water around the cells will reduce contact between the nonpolar solvent molecules and the outer cell wall where the hydrocarbons accumulate.

Cell growth and hydrocarbon productivity will not be affected by repeated extraction with hexane. However, the yields of hydrocarbon recovery are highly contingent upon the condition of cell culture. For instance, in the early exponential phase, cells reached

higher recovery of hydrocarbons when cultured in an airlift photobioreactor compared with those cultured in standard stirred bioreactor [104]. This correlated to the smaller average size of algae colonies in the stirred bioreactor [104]. A higher turbulence in the stirred reactor resulted in the smaller average colony size [106].

Enzymes regulates the unique pathways of triterpene biosynthesis in *Botryococcus braunii* have attracted many interests. It was possibly composed of three squalene synthase-like genes that functionalized separately but collaboratively, instead of catalyzing a two-step reaction within a single enzyme unit without intermediate release as other squalene synthases [107].

As mentioned in the previous chapter, due to the efficient protein production of *Botryococcus braunii*, we could take advantage of the protein content as a feedstock for animals. However, the conversion of algal protein into fuels also facilitates scientists in the use of the proteins which are produced by *Botryococcus braunii*.

Botryococcus braunii possesses a lot of biotechnological value regarding to its each component. Currently, scientists are seeking ways to increase the cell growth, in order to exploit the tremendous benefits from this species.

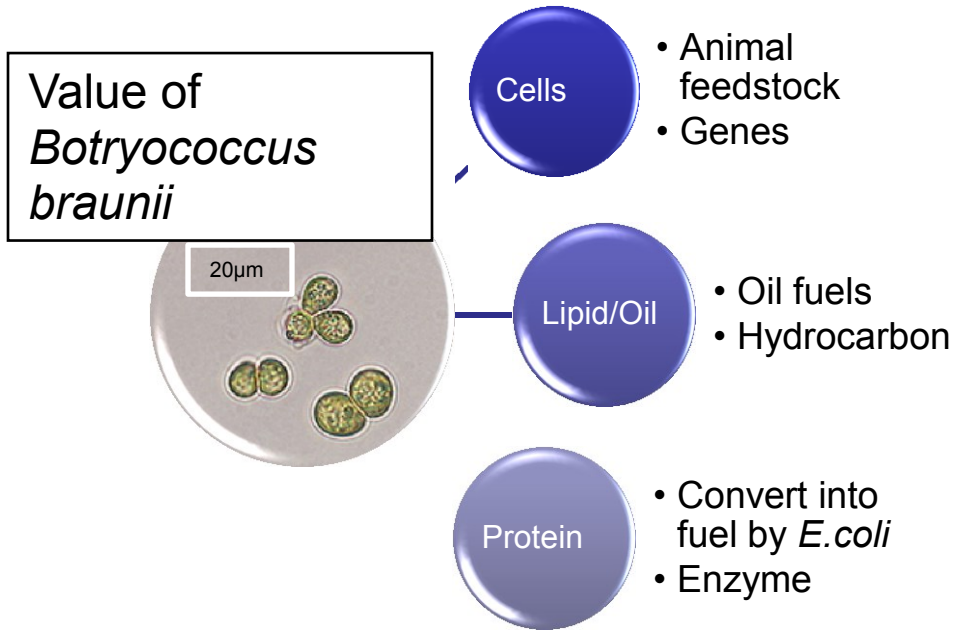

Fig.11 Biotechnological value of *Botryococcus braunii* the cells could be used as feedstock and gene host; lipid/oil could be used as fuels and hydrocarbon source; protein could be converted into fuels such as alcohol by *E.coli*, and algal enzymes could be screened and extracted.

2.5 Our experimental culture condition

In this study, *Botryococcus braunii* has been chosen as a suitable target to investigate the biofuel model (Fig.12). Metabolism modifications were applied in order to intentionally change some key reactions in the metabolic pathways. In addition, optimization strategies were carried out to achieve an optimal condition for autotrophic cultivation of *Botryococcus braunii* with an eye to outdoor cultivation in the future.

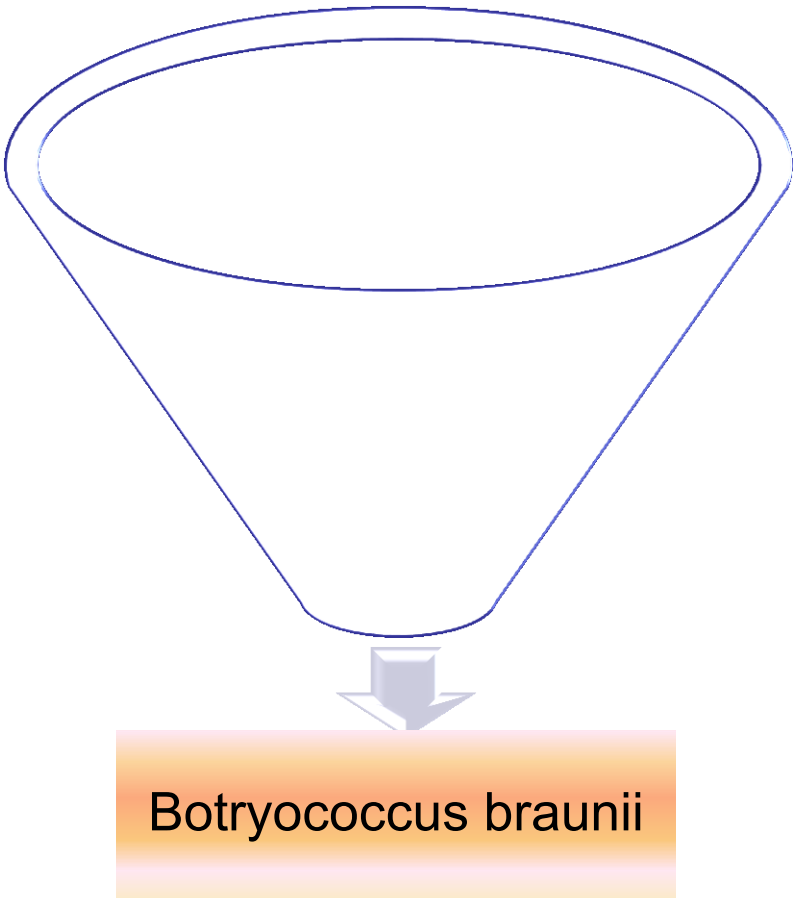

Fig.12 *Botryococcus Braunii* study model.

For this study, we chose *Botryococcus braunii* race A (UTEX 572), originating from Cambridge, as our experimental case (Fig. 13). The desired media for this strain is Modified Bold 3N Medium. Cells are loaded in a tube with agar to maintain an axenic environment.

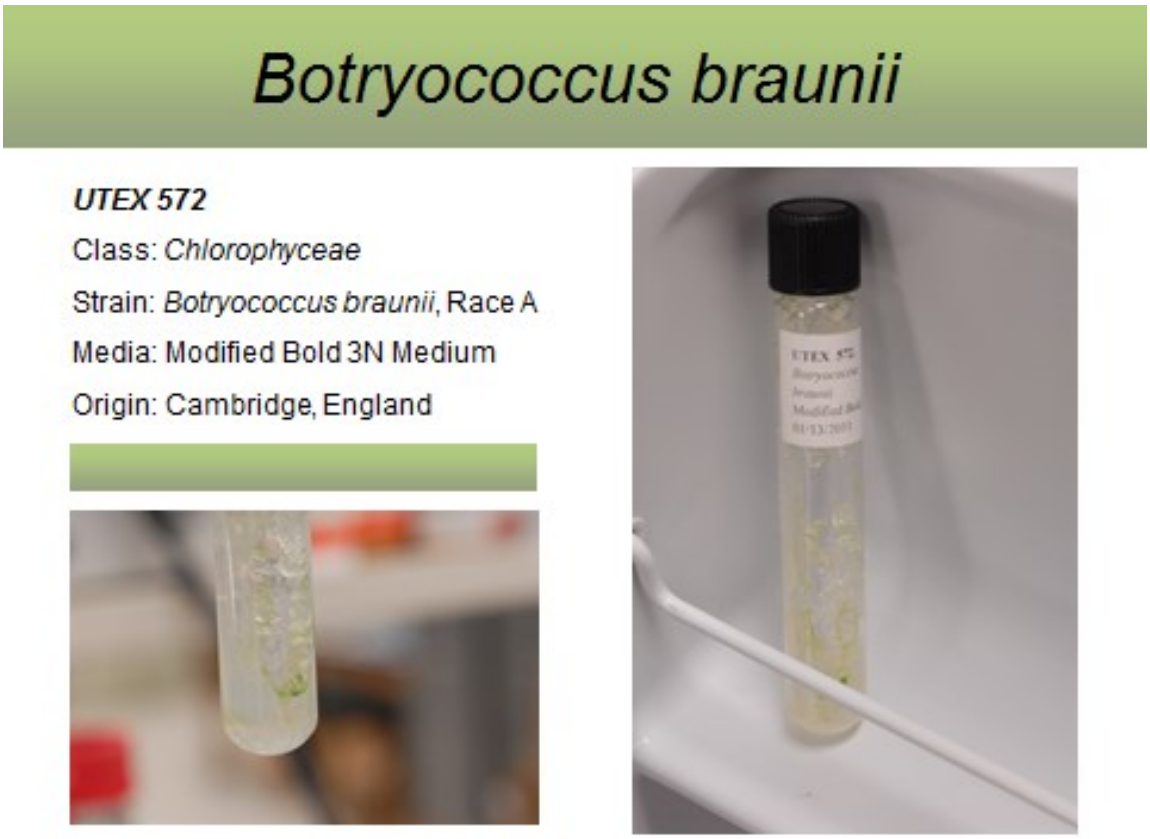

Fig.13 *Botryococcus braunii* race A (UTEX 572) strain in the tube with agar to keep axenic

The strain was kept under constant light exposure in the incubator for 24 hours a day with a constant temperature of 20°C. At the very beginning, cells with a mild green color could barely be seen from outside. Gradually as the cells grew in the agar, some green spots could be seen in the agar. This indicated that *Botryococcus braunii* cells were growing in the tube.

The Modified Bold 3N Medium [108] is comprised of various elements (Table 5), including:

#	Component	Amount	Stock Solution Concentration	Final Concentration
1	$NaNO_3$ (Fisher BP360-500)	30 mL/L	10 g/400mL dH2O	8.82 mM
2	$CaCl_2 \cdot 2H_2O$ (Sigma C-3881)	10 mL/L	1 g/400mL dH2O	0.17 mM
3	$MgSO_4 \cdot 7H_2O$ (Sigma 230391)	10 mL/L	3 g/400mL dH2O	0.3 mM
4	K_2HPO_4 (Sigma P 3786)	10 mL/L	3 g/400mL dH2O	0.43 mM
5	KH_2PO_4 (Sigma P 0662)	10 mL/L	7 g/400mL dH2O	1.29 mM
6	NaCl (Fisher S271-500)	10 mL/L	1 g/400mL dH2O	0.43 mM
7	P-IV Metal Solution	6 mL/L		
8	Soilwater: GR+ Medium	40 mL/L		
9	Vitamin B_{12}	1 mL/L		
10	Biotin Vitamin Solution	1 mL/L		
11	Thiamine Vitamin Solution	1 mL/L		

Table 5 The component and concentration of Modified Bold 3N Medium [108].

Directions [108]

This is a modification of Bold's recipe. A general purpose freshwater medium was used for xenic cultures, especially blue-greens and reds.

For 1 L Total pH 6.2:

1.To approximately 850 mL of dH_2O, add each of the components in the order specified (except vitamins) while stirring continuously.

2. Bring the total volume to 1 L with dH_2O.

*For 1.5% agar medium, add 15 g of agar into the flask; do not mix.

3. Cover and autoclave medium.

4. When cooled, add vitamins.

*For agar medium, add vitamins, mix and dispense before agar solidifies.

5. Store at refrigerator temperature.

The culture systems are based on the basic photosynthetic rules for plant cells (Fig. 14). Light, water, and CO_2, are supplied with an appropriate parameter. The media contains different element sources such as nitrate (nitrogen source), sodium, potassium, calcium and magnesium. Various metal ions are required to support several key metabolic reactions and organelle functions For example, chloroplast formation requires iron ions. Soil water, whose content is still not well known, is normally used as a grounded component. Several vitamins, often mixed with proteins, are provided to maintain essential cell activity. However, although culture systems try to mimic the biological plant system, there remain some differences such as light cycle, closed

cultivation, gas diffusion and media component. In general, optimal conditions were considered to apply for our experiment.

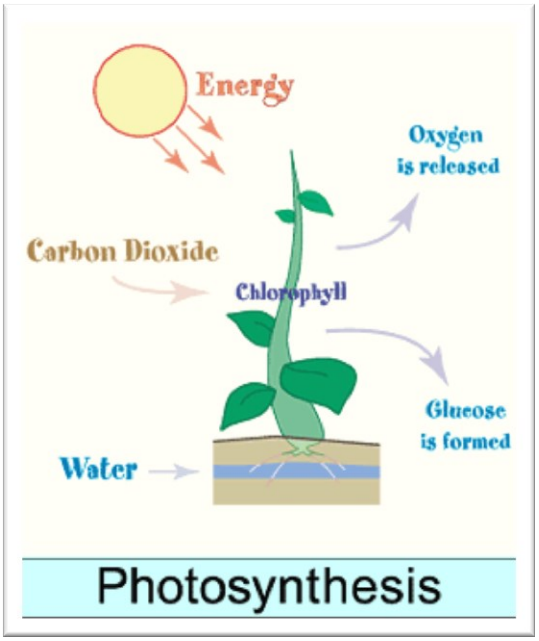

Fig.14 Photosynthetic model for plant [132]

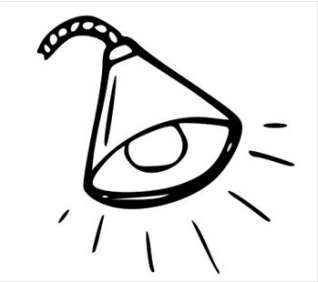

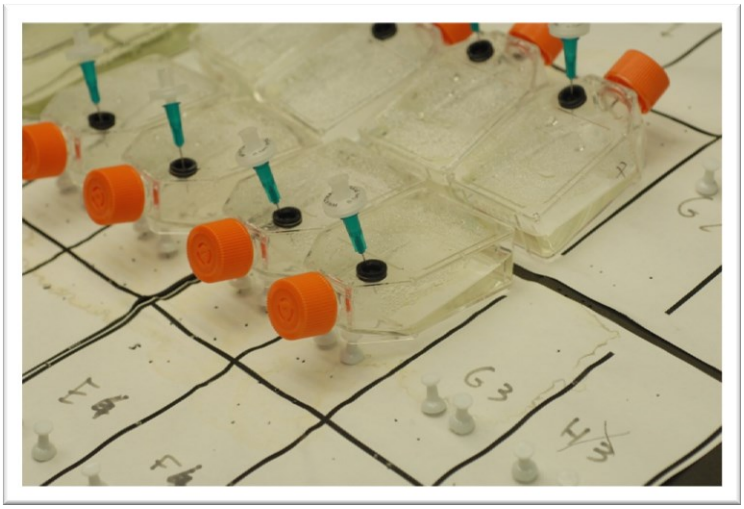

Fig.15 Culture system of cells in polystyrene bottles

In the case of CO_2 diffusion, vented caps were chosen for polystyrene bottles (Fig. 16). 25cm^2 flask canted, polystyrene bottles with 0.2μm vented caps were ordered from Corning Inc. A rounded hole was processed and then attached with a syringe rubber plunger to make it closed. 23G ¾ needles from Becton Dickinson Inc. with a 0.1μm PTFE filters from Whatman Inc. were inserted into the rubber to provide a gas tunnel for the exchange of CO_2 and O_2.

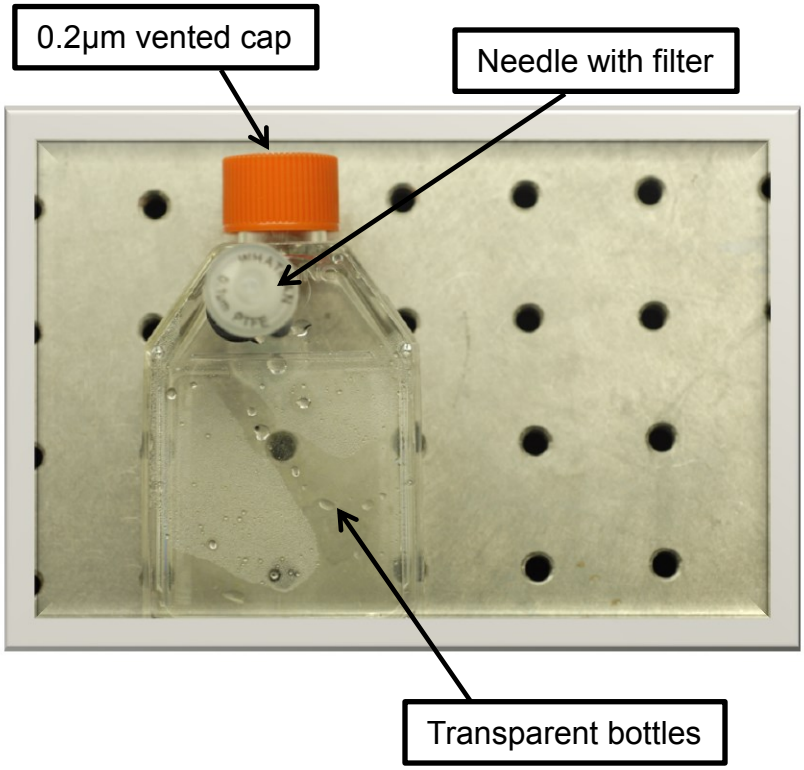

Fig. 16 Polystyrene bottles with a specific treatment were used to culture *Botryococcus braunii*. Model is shown in practical size. Plastic bottles with low reflection are good for photosynthesis since light can easily travel through them.

Constant light exposure for 24 hours a day (with no dark cycle) was applied and with constant shaking frequency. The most suitable position was in a slope from the horizontal (Fig. 17) because the algae cells tend to form colonies in the bottles and attach to the surface gradually. Gravity with constant shaking helped to prevent the algae from sticking to the bottles.

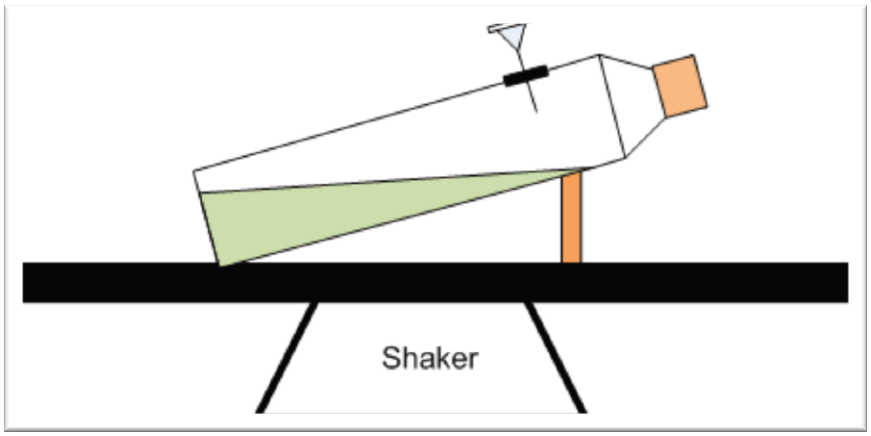

Fig. 17 The bottles were kept in a slope on the shaker board which could take advantage of gravity to prevent the algae cells from attaching to the bottles.

2.6 Preliminary results of citrate on *Botryococcus braunii*

The entire metabolic blueprint of *Botryococcus braunii* is still unknown; however, based on the genomic studies and species similarities, several general approaches to adjust universal reactions in the metabolic pathway could be carried out. At the same time, knowledge about the cell condition after treatment would be gained, enabling us to record the effect of each chemical to the reactions.

The reaction of Acetyl-CoA to Malony-CoA is regarded as a committing step in the metabolic pathway (Fig. 18). This reaction forms Malony-CoA, which could be used as the source for synthesizing many bio-products such as fatty-acids, hydrocarbon and amino acid.

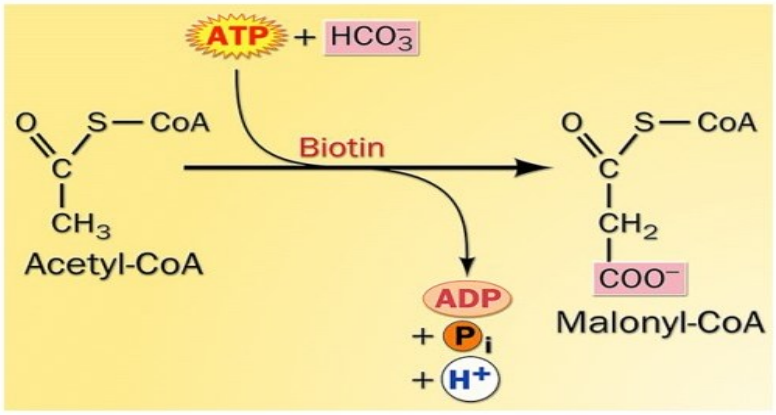

Activation of acetate : Acetyl-CoA to malonyl CoA

Fig. 18 The metabolic pathway from Acetyl-CoA to Malony-CoA is shown above. A biotin-dependent carboxylase catalyzes the irreversible reaction of Acetyl-CoA to produce Malony-CoA [131].

This reaction is catalyzed by an enzyme called acetyl-CoA carboxylase (ACC) which contributes to the biotin-dependent carboxylation of acetyl-CoA to form malony-CoA [109-112]. Active ACC combines with ATP to form inactive ACC by catalysis of an enzyme called AMPK.

Through a feed-forward loop, citrate allosterically activates ACC [113]. Citrate may increase ACC polymerization to increases enzymatic activity; however, it is unclear whether polymerization is citrate's main mechanism of increasing ACC activity or whether polymerization is an artifact of in vitro experiments. Other allosteric activators include glutamate and other dicarboxylic acids [114]. Long and short chain fatty acyl CoAs are negative feedback inhibitors of ACC [115].

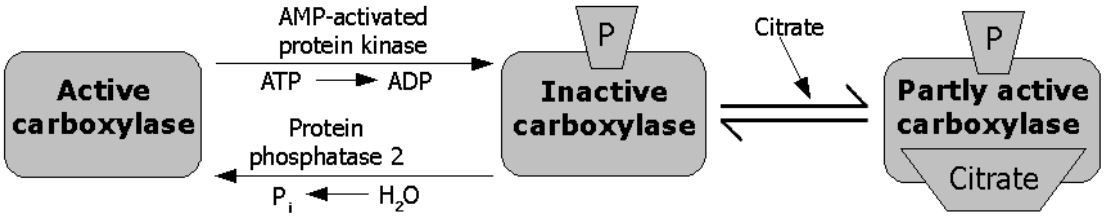

Fig. 19 AMPK and citrate functionalize in the reaction flows of ACC. This figure shows the control of Acetyl CoA Carboxylase. The AMP regulated kinase triggers the phosphorylation of the enzyme (thus inactivating it) and the phosphatase enzyme removes the phosphate group. [132]

Our experiment included treatment on *Botryococcus braunii* to modify the metabolic pathway. Cell number (optical density at 750μm), lipid content (Nile red fluorescent intensity) and protein production (Sulforhodamine-B fluorescent intensity) were measured during two weeks cultivation in the polystyrene bottles (Fig. 20, 21).

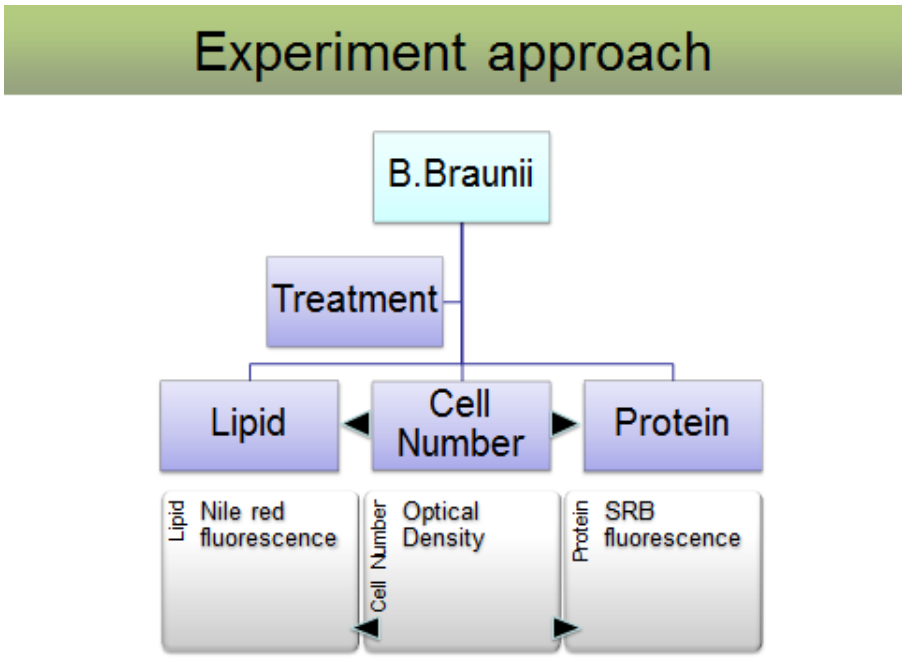

Fig. 20 Experiment approach to study cell growth and lipid/protein production. *Botryococcus braunii* cells were treated under a variety of media conditions. Samples were taken on a two-day basis and cell numbers, lipid content and protein content were measured after sampling.

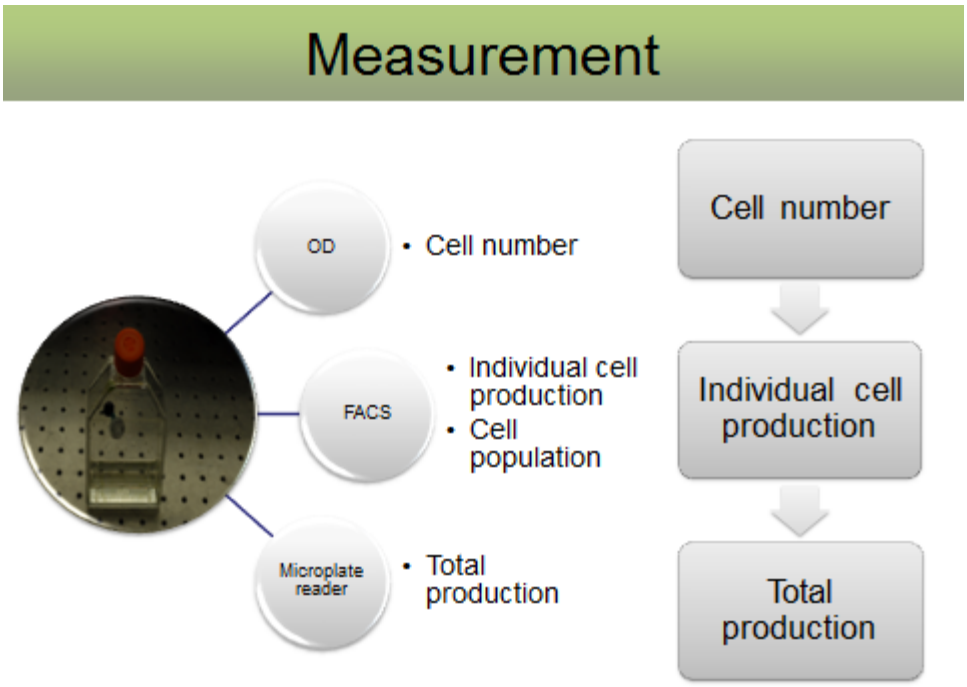

Fig. 21 Measurements carried out in our experiment. Optical density at 750nm of each cell sample was measured on the 96-well plate by spectrophotometer (SpectraMax M5 microplate reader, Molecular Devices). Individual cell population and production were measured under flow cytometer (BD FACSCANTO II Cell analyzer, BD Bioscience). Cell samples were stained by a variety of dyes and fluorescent intensity measured afterwards by spectrophotometer (SpectraMax M5 microplate reader, Molecular Devices).

UV–vis spectrophotometric optical density (OD) is the most commonly-used technique for measuring chromophore formation and cell concentration in liquid cultures [118]. Within an appropriate range of measurements, analysis of the absorption and scattering of the measured optical density provides a quantitative evaluation of cell numbers in the liquid culture. Prior to the experiment, we calibrated the optical density at 750nm with the cell numbers observed under the microscope, from which we obtained a linear relationship on the above two parameters (Fig 22).

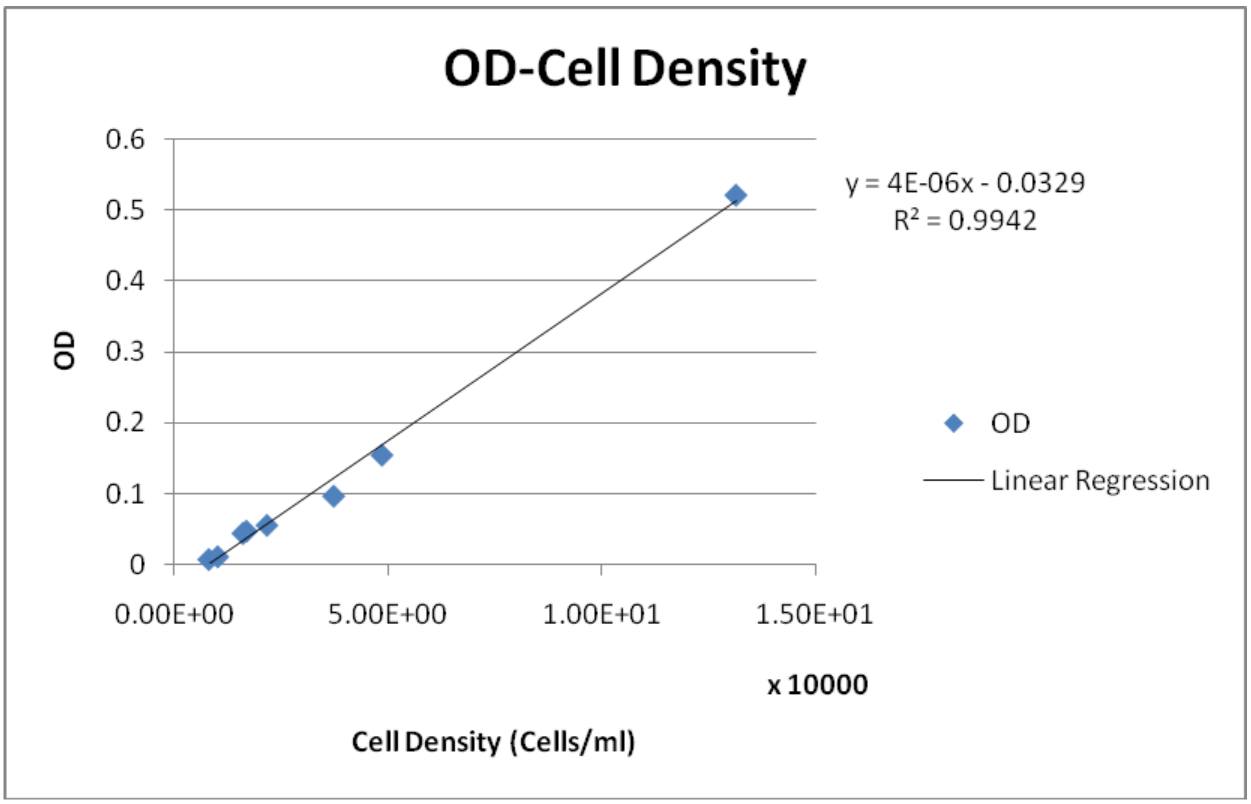

Fig 22 Calibration curve of optical density at 750nm and cell density measured under hemocytometer. Cell numbers were read within the 1mm*1mm area on the hemocytometer with a depth of 0.1mm, which formed a volume of 100nl. Cell density was read within the area and recorded at each level of optical density, measured by spectrophotometer. A straight curve could be fitted on the optical density - cell density graph to indicate a linear relationship between them.

For each culture with different media conditions, we extracted samples of 1.5ml using 3ml syringes to the 2ml centrifuge tubes every two days. Robotic pipettes (MICROLAB® STAR Liquid Handling Workstations, Hamilton Robotics) were used to handle the centrifuge tubes and distribute fixed volume from the tubes to each well on the 96-well plate with a clear flat bottom. 600ul of each sample was pipetted into two parallel wells (each well 300ul) on the 96-well plate to conduct a duplicate OD measurement. The remaining volume in the tube was used by lipid measurement.

Optical density at 750nm for each sample was measured on the 96-well plate by spectrophotometer (SpectraMax M5 microplate reader, Molecular Devices). We divided a sample volume of 600ul into two wells for each sample in the same rows in order to reduce colony-specific errors or errors from deposits forming in the tubes. We also measured readouts twice for each plate so that we could minimize system errors.

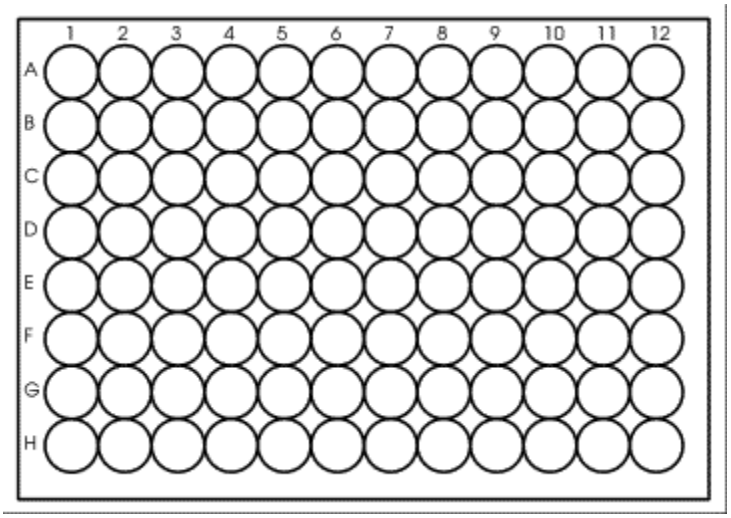

Fig. 23 96-well plates were used to measure OD for a variety of culture samples [137]. 600ul liquid samples were discharged into two parallel wells (e.g. A1 and A2) for duplicate measurement. We then measured twice in the spectrophotometer. Data were recorded in SoftMax and exported into txt files.

We designed several media conditions as shown in Table 6. Each media condition was prepared in duplicate. 1ml to 2ml fresh inoculum (depending on the available volumes of big bottles and the numbers of testing conditions) from the big bottles was transferred into each 25cm^2 flask canted, polystyrene bottle. Fresh culture media was then added to make a volume of 20ml in total.

Condition	Concentration
Citrate	20mM
Citrate per day	20mM per day
Acetate	20mM
Control	/

Table 6 Several different media conditions with chemical concentrations. “Citrate per day” indicates that 20mM citrate was added on a daily basis based on the remaining volume in the bottles.

For each measuring point, we aspirated 1.5ml samples from each polystyrene bottle into a 2ml centrifuge tube by 3ml syringe. These tubes were moved onto the MICROLAB® STAR liquid handling workstations for accurate and automated multi-pipetting. 650ul of each sample was aspirated and transferred into a low-bind tube which was prepared for lipid measurement. The remaining volume was used to determine the optical density for the measurement of cell numbers.

600ul from the remaining volume was subsequently divided and transferred into two parallel wells (each well 300ul) on a 96-well plate with a clear flat bottom. A violet rectangle which was designed to offset the influence from visible absorbance other than violet light was placed beneath the 96-well plate into the drawer holder.

Optical density at 750nm was measured twice for each well plate. For each measuring point we obtained four data points of optical density for each sample from

the polystyrene bottles, and eight data points of optical density for each media condition (in duplicate).

The average value of each set of four data points was calculated to determine the gross optical density of each sample at each measuring point. Then each value was deducted by 0.0445 which were the blank readouts of a clear well and this value was the optical density of each sample at each measuring point. For each experiment (each experiment has many measuring points), we selected average optical density at Day 0 as the base value, and normalized the averaged optical density at each measuring point (or at Day i) to the base value. Therefore the normalized cell numbers at each measuring point or at Day i are expressed as follows:

$$\text{Normalized Cell Numbers at Day i} = \frac{\text{OD at Day i}}{\text{OD at Day 0}}$$

The normalized cell numbers at each measuring point were then averaged according to the duplicate media conditions to obtain the averaged value of the normalized cell numbers of each media condition. Eventually the normalized cell numbers of each media condition at each measuring point were calculated and plotted to make the cell growth curve. In the following chapters, we will use normalized optical density to Day 0 as a reference of normalized cell numbers.

Several rounds of preliminary experiments were carried out to test the effect of the citrate on cell growth and lipid/protein production. We chose citrate and acetate as the growth stimulus for *Botryococcus braunii*. The cell growth curve is shown below. The *Botryococcus braunii* in the citrate per day group had a sharp increase in the early period. Normalized cell numbers reached 23 within six days which was about 20 times that of the control. After Day 6, cell numbers started to drop and finally reached a plateau as the citrate and acetate group responded.

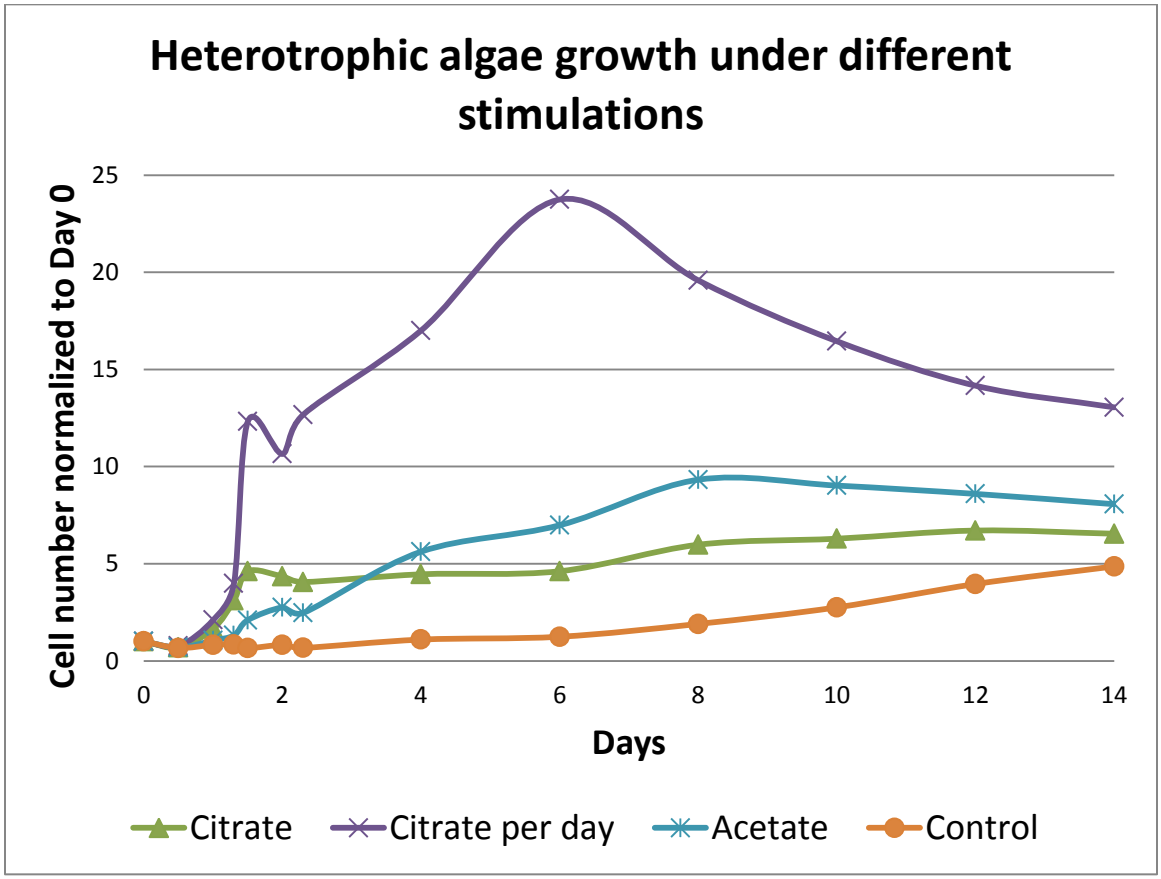

Fig. 24 Optical density normalized to Day 0 at 6th round experiment. Optical density measured at 750μm indicated the cell numbers in the solution. Citrate-treated cells showed a sharp increase after 1-2 days, and once we added citrate on a daily basis, the cell growth continued. The increase stopped after Day 6.

To sum up, in our preliminary experiment we designed a sophisticated culture platform for *Botryococcus braunii* and discovered that citrate could induce the cells into heterotrophic growth giving a high biomass yield.

Chapter 3. Solving data inconsistency: determining the initial cell condition

3.1 Data inconsistency associated with our preliminary experiments

In the previous chapter, we showed that citrate could trigger cell growth and enable cells numbers to increase up to 20 times more than the control at Day 6. However, we were unable to repeat these results in the next few experiments because of the data inconsistency

We repeated the preliminary experiment three times and there were two major issues in the growth curve of the citrate per day groups

1). Difference in peak level

Normalized cell numbers reached peak levels ranging from 15 to 24 at Day 6 and then plateaued. In Test 1, the *Botryococcus braunii* in the citrate per day groups reached 24 at Day 6, while in Test 3 it barely reached 15.

2). Difference in slope

The growth rate in the early period (the first two days) was unstable for all three tests. In Test 1, *Botryococcus* grew in a higher slope which was around five times more than the slope in Test 3.

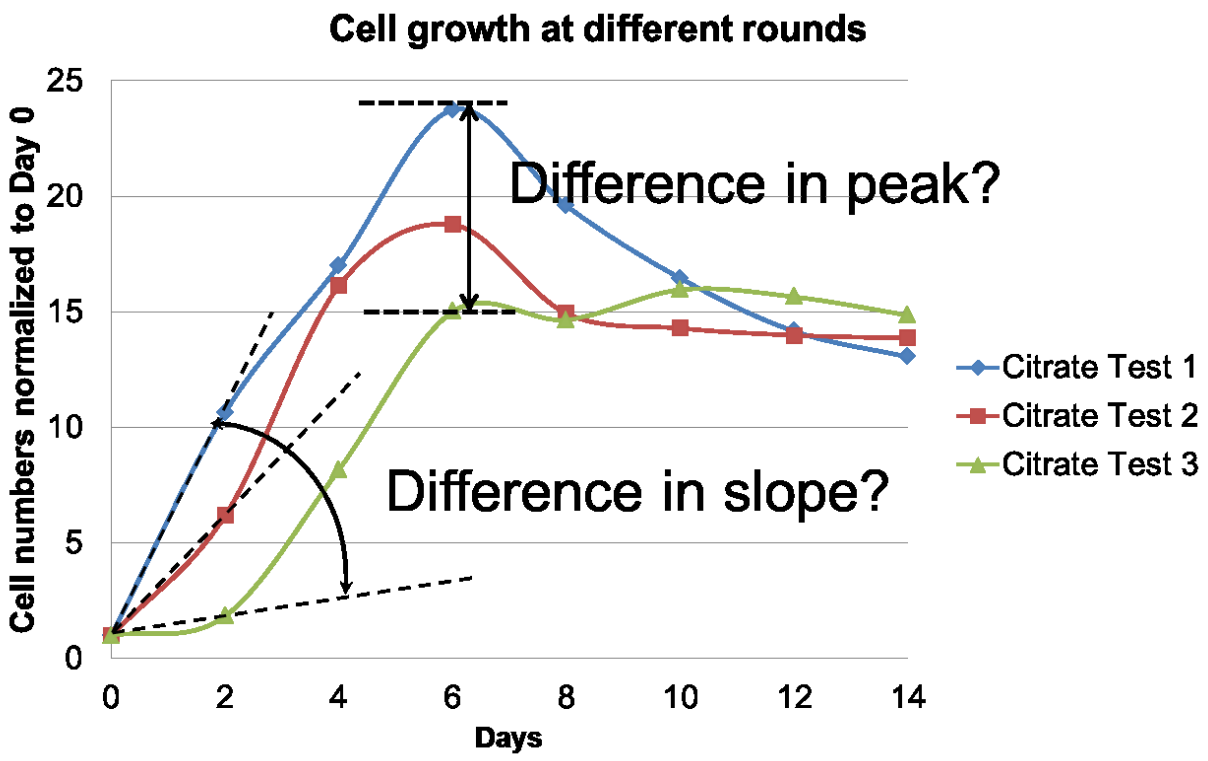

Fig. 25 Three repeated experiments were conducted and data inconsistency was observed. Difference in both peak and slope became the major issues for reproducing the same results as in the preliminary experiment.

These two differences resulted in the data inconsistency of cell numbers for *Botryococcus* growing under the same stimulus. The same results could not be reproduced by simply performing the same chemical treatment such as adding citrate each day.

3.2 Difference in initial cell density

The data inconsistency became a challenge for our microalgae study since our findings could not be repeated in a consistent way. For each experiment, the growth curves were different with different peak levels and different slope angles in the early period.

By comparing the data, we realized that the growth curves of normalized cell numbers were similar when the starting optical density was at a similar level. This finding focused our attention on the possible reasons for the data inconsistencies noted in the previous experiments. Normalized cell numbers in those experiments that started with an optical density of around 0.008 could reach 23 at the peak and shared a similar slope in the early period. However, if the starting optical density at Day 0 was lower than 0.005, cell numbers grew more slowly in the early period and entered the exponential phase only after the optical density exceeded certain amounts.

After analyzing the data, we concluded that the difference in the initial cell density of each experiment could explain the data inconsistencies in the repeated experiments.

We therefore designed a parallel experiment to examine whether the difference in initial cell density could cause a different growing pattern of *Botryococcus braunii*. First we defined the low and high initial cell density in Table 7.

Initial cell density	Low	High
Optical density at Day 0	0.002-0.005	>0.007

Table 7 We defined optical density at Day 0 ranging from 0.002 to 0.005 as low initial cell density, while anything higher than 0.007 was defined as high initial cell density.

The parallel experiment showed that normalized cell numbers which started with low initial cell density were significantly lower than cell growth starting with high initial cell density (Fig 26). This was represented by the cell growth curves where the low initial cell density group showed a lower slope and peak level compared with the high initial cell density group. It appeared that the growth curves of the low initial cell density group were likely to fit as a linear function, while the growth curves of the high initial cell density group appeared to fit as an exponential function.

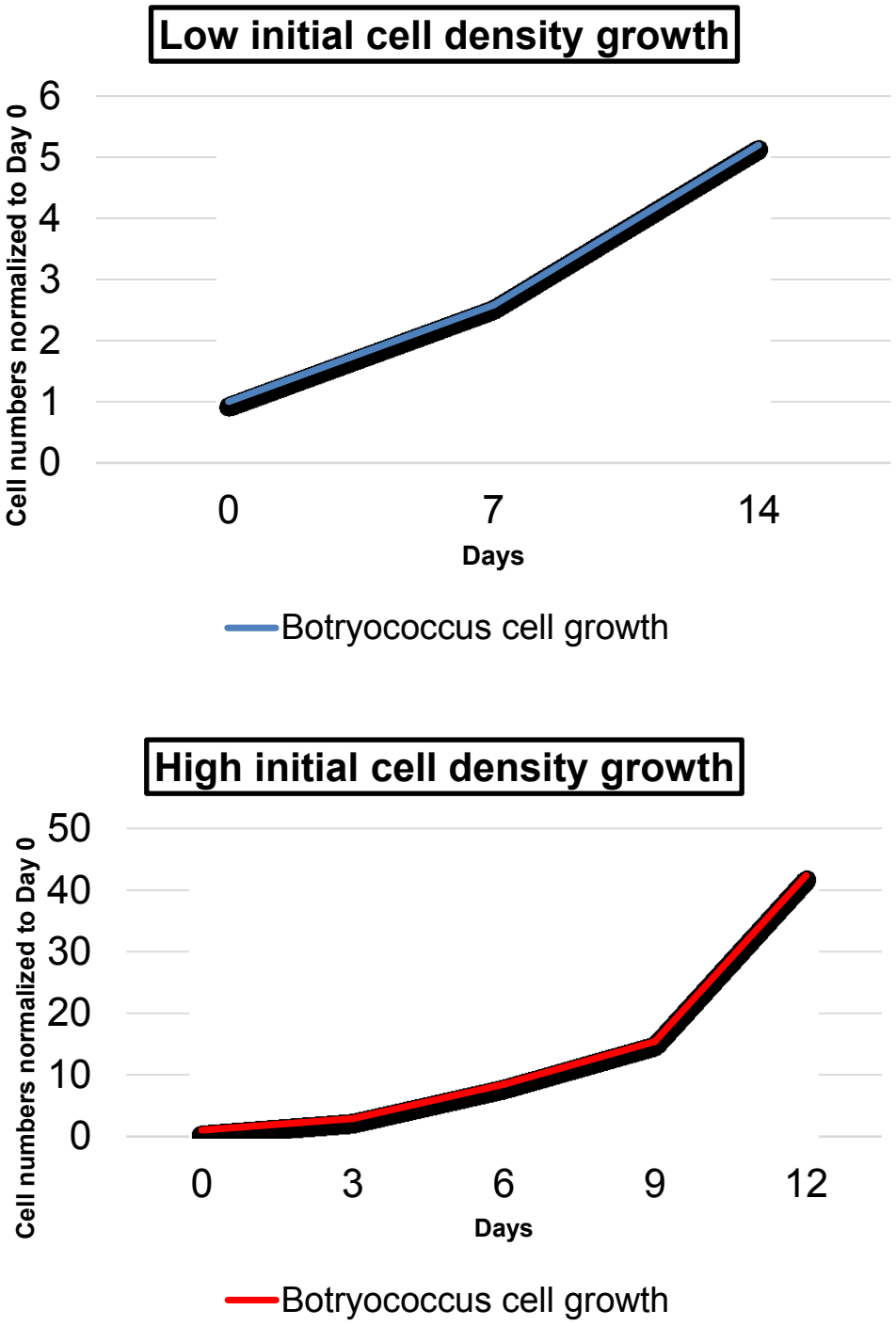

Fig. 26 Difference in initial cell density showed a different pattern in cell growth for *Botryococcus braunii*.

Unlike the previous data, there were no plateaus for these growth curves within the two week period because these cells were treated with pH-balanced media so that pH was kept constant as the cells grew in the liquid media. We will discuss this further in Chapter 5. The reason for selecting these growth curves is due to the clear difference in growing patterns and slope between the low initial cell density group and the high initial cell density group.

We realized that the difference in the initial cell density of each experiment could be the reason for the data inconsistency in the repeated experiments. We could therefore overcome this difficulty.

3.3 Solving the data inconsistency

In order to reduce the difference in initial cell density for each experiment, a pre-culture protocol (Fig. 27) was developed to meet the same initial condition for *Botryococcus braunii* before we started the experiments.

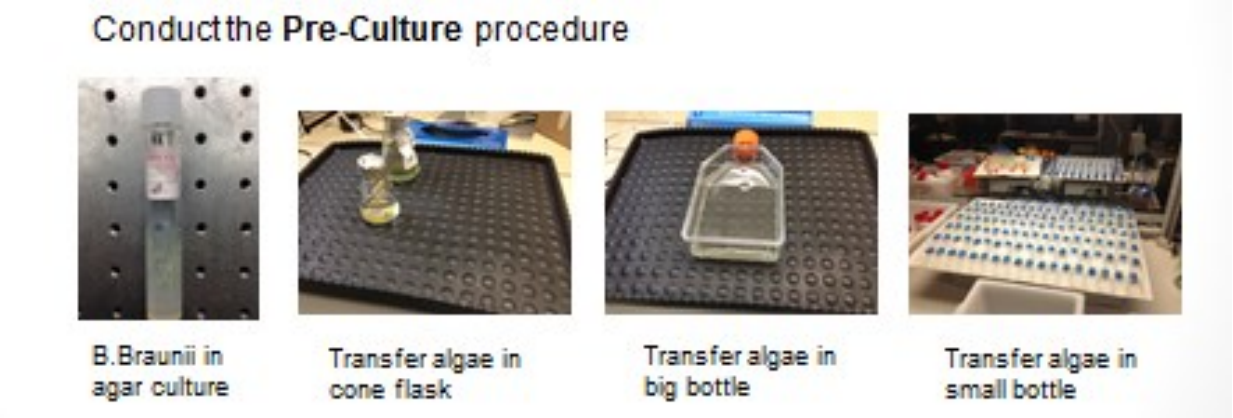

Fig. 27 Pre-culture protocol was designed to meet the same initial conditions for *Botryococcus braunii*. It consisted of a multi-stage culture that enabled cell accumulation in the liquid media before we diluted them into the new experimental bottles.

The pre-culture procedure was conducted to reduce the difference in the initial cell density for each experiment. There were two parameters to adjust during this procedure:

1). Adjust the length of each pre-culture period

Pre-culture protocol usually was composed of several periods, including inoculation from agar culture, culture in the cone flask, culture in the big bottle, and finally transfer to the small bottles for experiments. Each period typically took one to three weeks depending on the cell density. This approach could be followed by monitoring the optical density in the liquid media during each pre-culture period. The growth of *Botryococcus braunii* in the control condition (commercial media) was predictable allowing us to control the length of each pre-culture period to meet the initial cell density.

2). Adjust the dilution rate for the sample

Dilution rate is the ratio between the volume of cell solution from the big bottles and the total volume of media solution in the small bottles. This directly determines the initial cell density in the small bottles. We used this as an alternative way to tweak the cells to meet the same initial condition.

By implementing the pre-culture procedure, the data fluctuations of cell growth in each experiment were significantly reduced. Three new tests on *Botryococcus braunii* were repeated. The data were far more consistent than in the previous repeated experiments (Fig. 28). For the citrate per day group experiment, the initial optical density started from 0.008 at Day 0. With each repeated experiment, cells numbers reached more than 20 with low deviation. Thus, we successfully solved the data inconsistency issue.

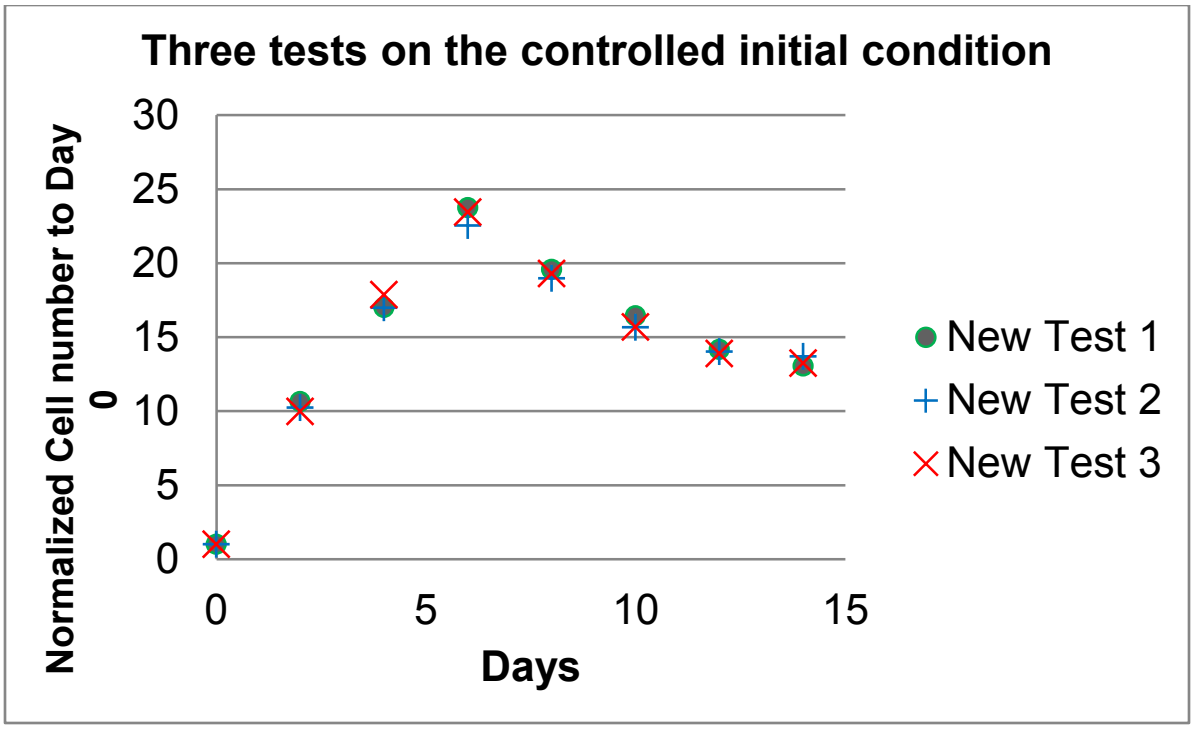

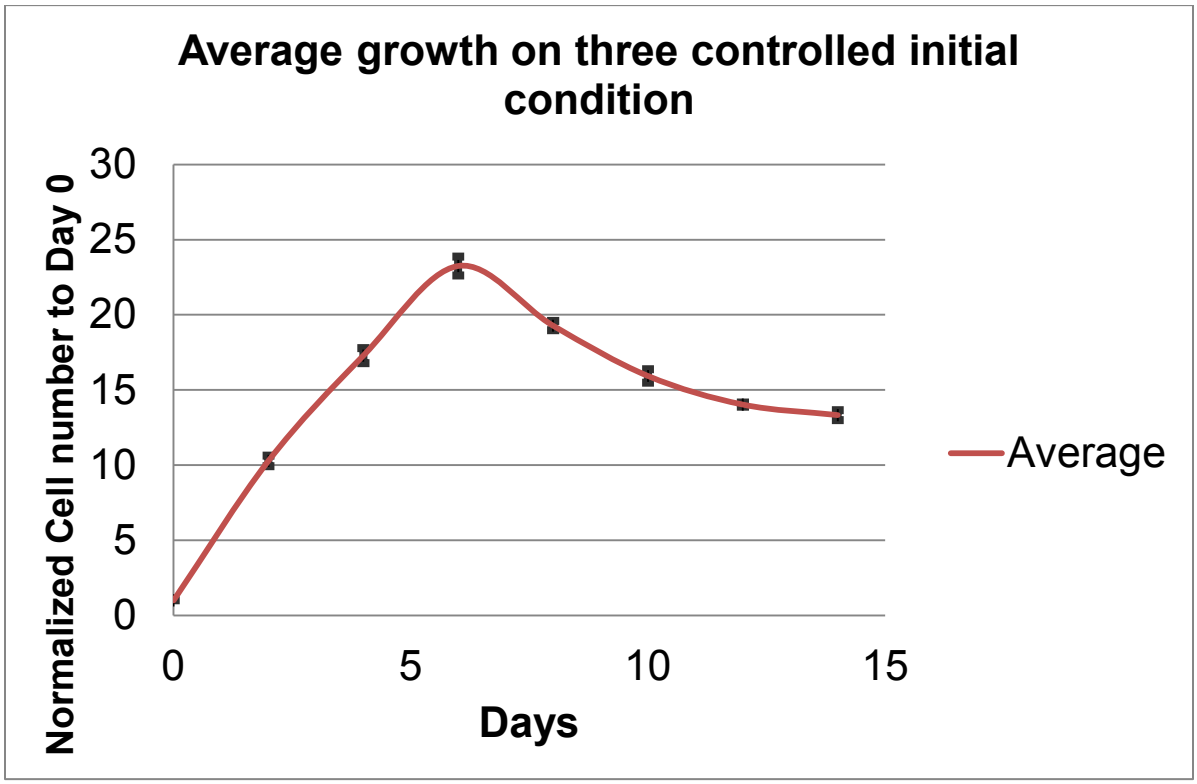

Fig. 28 Three new tests on citrate per day groups showed minimized scatter in growth curves between several repeated experiments. The first graph showed the relationship between normalized cell numbers and days in three repeated experiments on the controlled initial condition. The second graph showed the

average normalized cell numbers and error bars on normalized cell number according to the first graph. It showed the data scatter is significantly reduced.

3.4 Determination of time reference for the experiment

Time reference suggests the duration of each experiment. It is important to the reliability and accuracy of the results since the time reference provides the observational window in which we looked into the data and compared the peak and slope of the growth curve.

Botryococcus braunii growing in small bottles tends to reach a plateau within two weeks. After two weeks, the culture starts to change color, from green to brown. One possible explanation for these phenomena is the depletion of the nitrogen supply in the liquid media (Fig. 29).

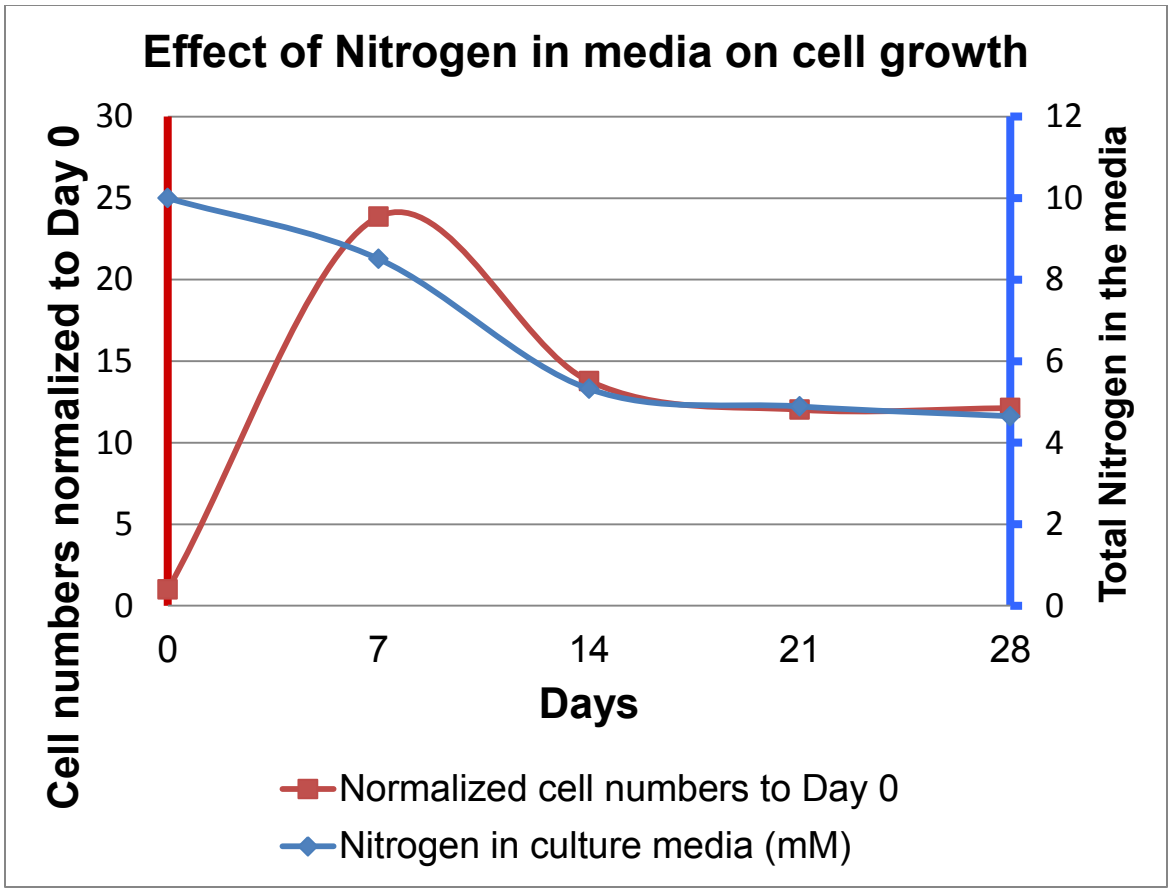

Fig. 29 This graph showed the depletion of nitrogen supply in the liquid media of *Botryococcus braunii* within four weeks. The red vertical axis on the left indicated the cell number normalized to Day 0 and the blue vertical axis on the right indicated the total nitrogen measured in the medium. X axis represented days. The drop in nitrogen content correlated with the plateau phenomena of cell growth. When the nitrogen in the medium was depleted,

We designed experiments to measure total N in a liquid media of *Botryococcus braunii*. Total nitrogen measurement is composed of four separate methods: Total Kjeldahl Nitrogen (TKN), Ammonia (NH_4^+), Nitrite (NO_2^-) and Nitrate (NO_3^-):

$$Total\ Nitrogen(TN) = R - N(Organic\ Nitrogen) + NH_4^+ + NO_2^- + NO_3^-$$

Samples were extracted and tested weekly by optical density and total nitrogen measurement (TN TNM-1 unit, Shimadzu) for four weeks. The results showed that after two weeks, nitrogen dropped to a certain level so that continuous algal growth was inhibited. This was when the plateau occurred. Consequently, we decided to select two weeks (i.e. 14 days) as the time reference.

Chapter 4. High cell growth and biofuel production of *Botryococcus braunii*: the green cycle from heterotrophy to autotrophy

4.1 Introduction to the green cycle

The main problem in using *Botryococcus braunii* to produce biofuel is its slow growth rate which hinders it becoming a commercially-competitive strain. Typically, the doubling time is about three to six days (Fig. 30) and the lag phase is longer compared with other microalgae strains. Regardless of the great potential and biotechnological value of *Botryococcus braunii*, scientists have suggested that this strain is unlikely to be used in any commercial-scale deployment.

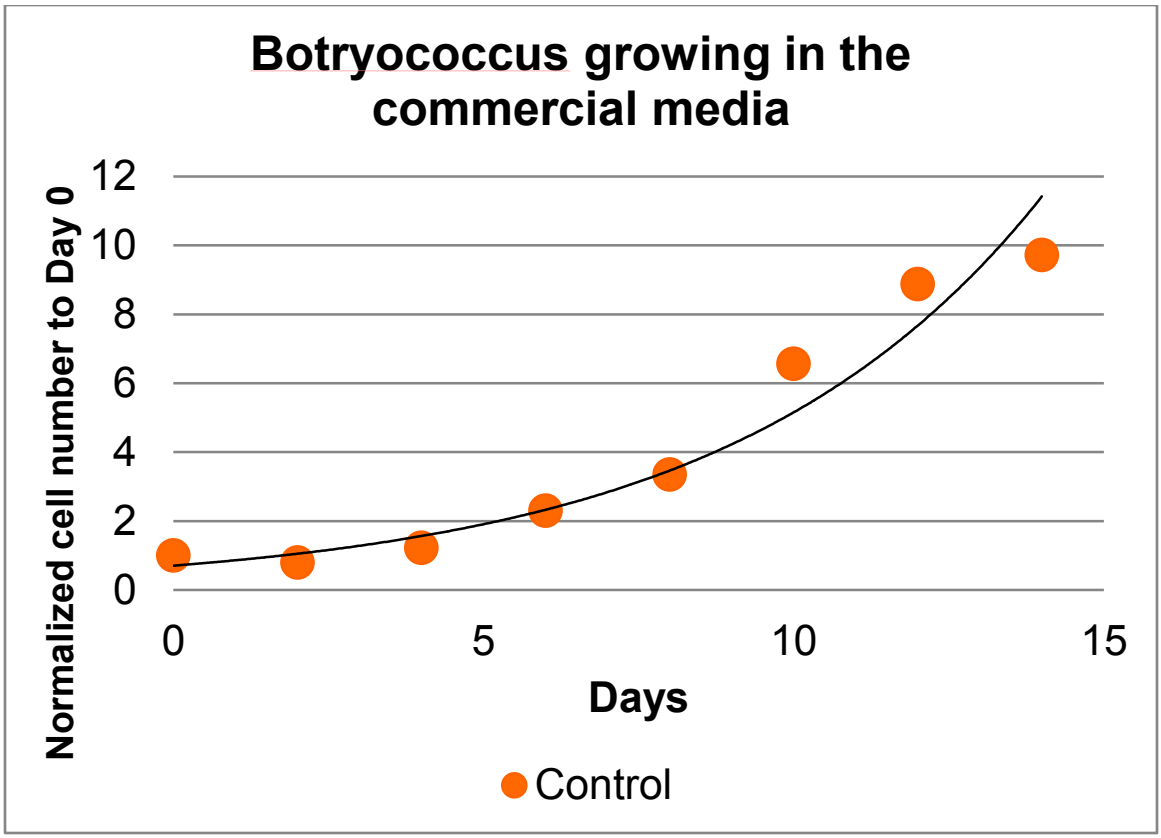

Fig. 30 A typical growth curve of *Botryococcus braunii* in the commercial media.

Since the 1980s, much research has been carried out on optimizing the media component and culture conditions of *Botryococcus braunii*. We discussed this research in an earlier chapter. The primary goal of these studies is to increase the cell growth which is positively correlated with biofuel production as well as protein content (Fig. 30).

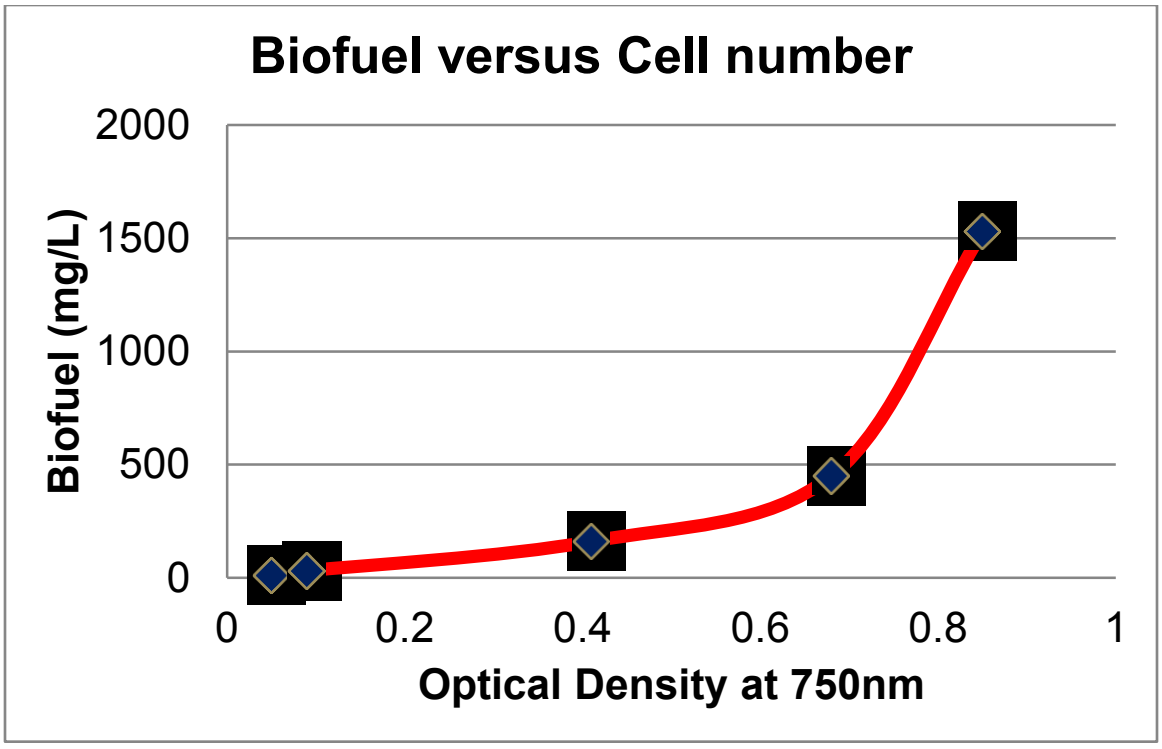

Fig. 31 A positive correlations between biofuel and cell numbers

A few microalgae strains such as *Chlorella* have been found to be capable of growing when supplied with organic carbons and using these as carbon sources other than for photoautotrophic growth. Microbiologists define this growth (in which cells are dependent on the supply of organic carbons such as sugar) as heterotrophic.

A heterotroph is an organism that cannot fix carbon and uses organic carbon for growth [119]. Heterotrophs act in the opposite way to autotrophs such as plants and algae which can utilize energy from sunlight (photoautotrophs) or inorganic compounds (litho-autotrophs) to synthesize organic compounds such as carbohydrates, fats, and proteins from inorganic carbon dioxide. These reduced carbon compounds can be used

as energy sources by the autotroph and provide the energy in the food consumed by heterotrophs.

Our preliminary results showed that citrate could induce *Botryococcus braunii* to grow in a heterotrophic way and therefore accelerate biomass accumulation. During the heterotrophic phase, cell numbers increased dramatically, up to 20 times more than with autotrophic growth. However, heterotrophic cells lose their ability to utilize sunlight and synthesize organic molecules from inorganic carbon. A high accumulation of heterotrophic cells were dependent on organic carbon sources and were unable to fix carbon dioxide from the air. Therefore the environmental merit and economic attraction of making microalgae biofuel was dramatically reduced. More importantly, heterotrophic cells cannot maintain their growth over time, due to rapid depletion of nutrients as well as causing crash with the culture due to low-chlorophyll cells.

To sum up, heterotrophic cells accumulate dramatically within a short period of time whereas autotrophic cells can perform photosynthesis subsequently to convert atmospheric carbon dioxide into biofuel. We wanted to find a way to bridge these two methods of growth; we therefore moved *Botryococcus braunii* from heterotrophic, organic carbon dependent growth to autotrophic, photosynthetic growth.

We defined this innovative growth method as the green cycle. The goal of the green cycle is to take advantage of high growth during the heterotrophic phase, thus creating a recovery method that enables heterotrophic cells to regenerate their photosynthetic function. The following chart (Fig. 32) shows a general pathway of green cycle. It starts from fresh inoculum in algae stock. Then a pre-culture procedure is followed to provide an early-growth period in which algae cells can accumulate their essential molecules. Cells are then induced to heterotrophic growth and algae biomass increases rapidly as well as the biofuel content. Heterotrophic growth is as fast as cell division and metabolism resulting in a deficiency of chlorophyll in the plastid.

The recovery process provides a transition period from the heterotrophic phase to the autotrophic phase which essentially helps cells regenerate their photosynthetic function. Heterotrophic cells with low chlorophyll appear pale gray from outside. After recovery, cells start to accumulate more chlorophyll which makes them look greener. Additionally, autotrophic cells reduce carbon dioxide and produce biofuel. This is why we called it the green cycle.

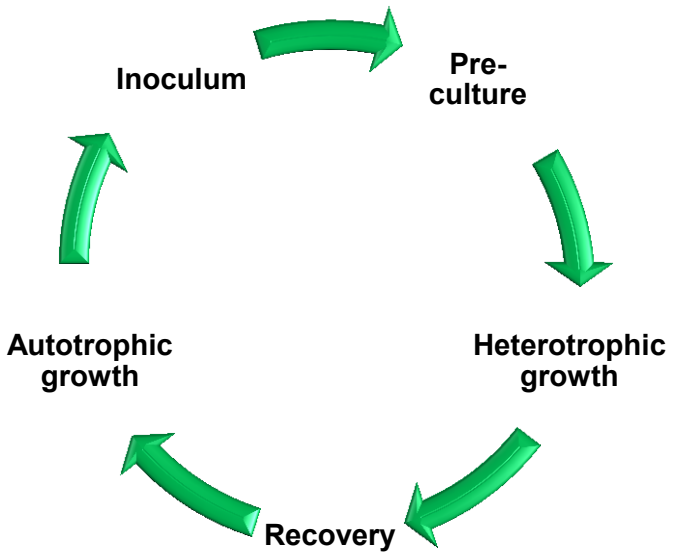

Fig. 32 A general chart for the green cycle.

Heterotrophic growth is important for the green cycle. However, almost all the algae strain will reach a similar plateau in the growth curve. Fan J, LI Y *et al*. have successfully used the “heterotrophy-autotrophy” approach to culture *Chlorella pyrenoidosa*. [120]

Based on the hypothetical idea of the green cycle, we developed “heterotrophy-recovery-autotrophy” for *Botryococcus braunii*. This method eliminated the plateau after the heterotrophic phase.

4.2 Enhanced cell growth and protein production during the heterotrophic phase

Our preliminary results showed that citrate triggered a high growth of *Botryococcus braunii* during the heterotrophic phase. Normalized cell numbers with daily citrate treatment could be 20 times higher than in the control group. (Fig. 33)

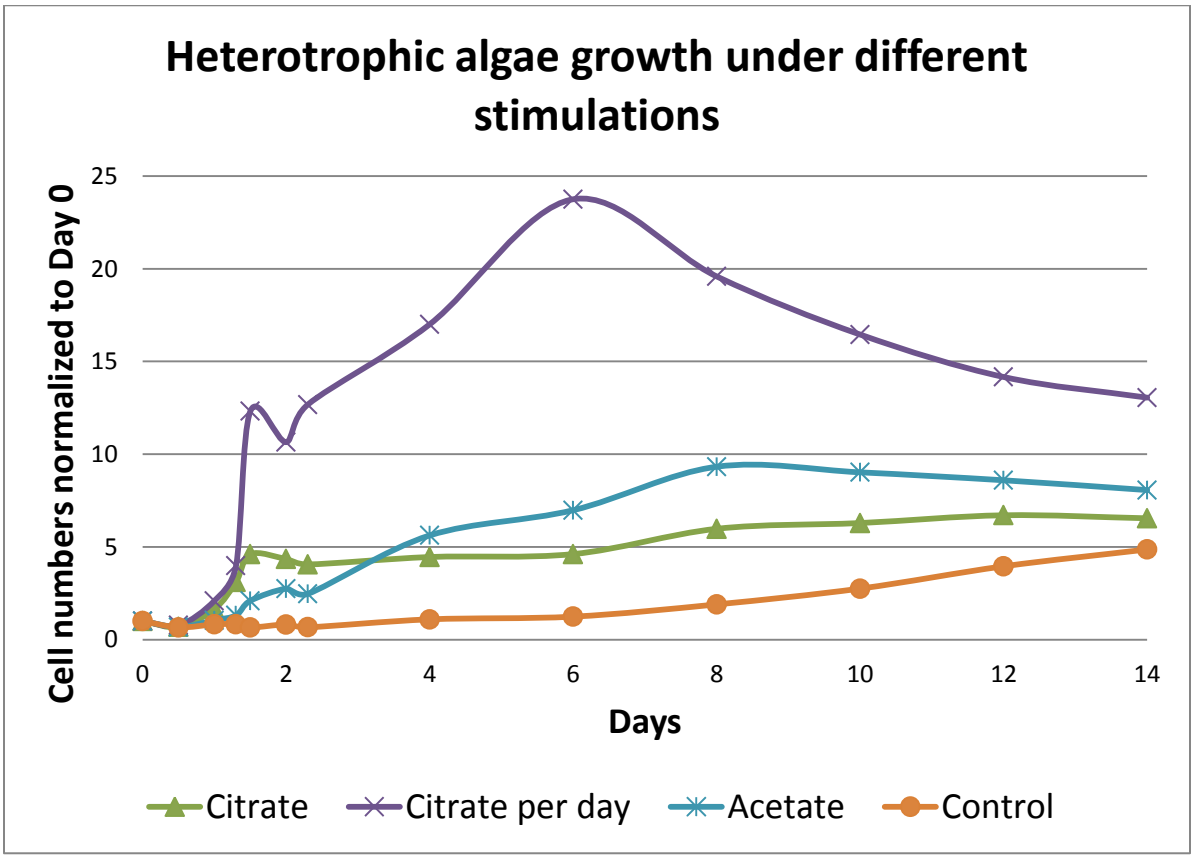

Fig. 33 Optical density normalized to Day 0 at 6th round experiment. Optical density measured at 750μm indicated the cell numbers in the solution. Citrate-treated cells showed a sharp increase in 1-2 days, and once we added citrate each day, the cell growth continued. The increase stopped after Day 6.

An agar test was conducted to observe the heterotrophic growth of *Botryococcus braunii*. 1.5% agar medium was prepared by adding (not mixing) the agar into liquid vitamin-free media. Autoclaving was followed with the top of flask covered. Vitamins were added during cooling, with mixing to make sure they dispersed before the agar solidified.

A parallel experiment was conducted to test the visible difference between citrate-treated agar culture and normal agar culture (agar culture with commercial media). Citrate-treated agar culture was made by adding 20mM citrate into liquid vitamin-free media before autoclaving.

Botryococcus braunii were inoculated on the citrate agar and normal agar respectively. At Day 4, cell samples were observed under microscope. Cells with citrate treatment grew as large colonies within the inoculation spots while the control group were still hardly to be seen (Fig. 34).

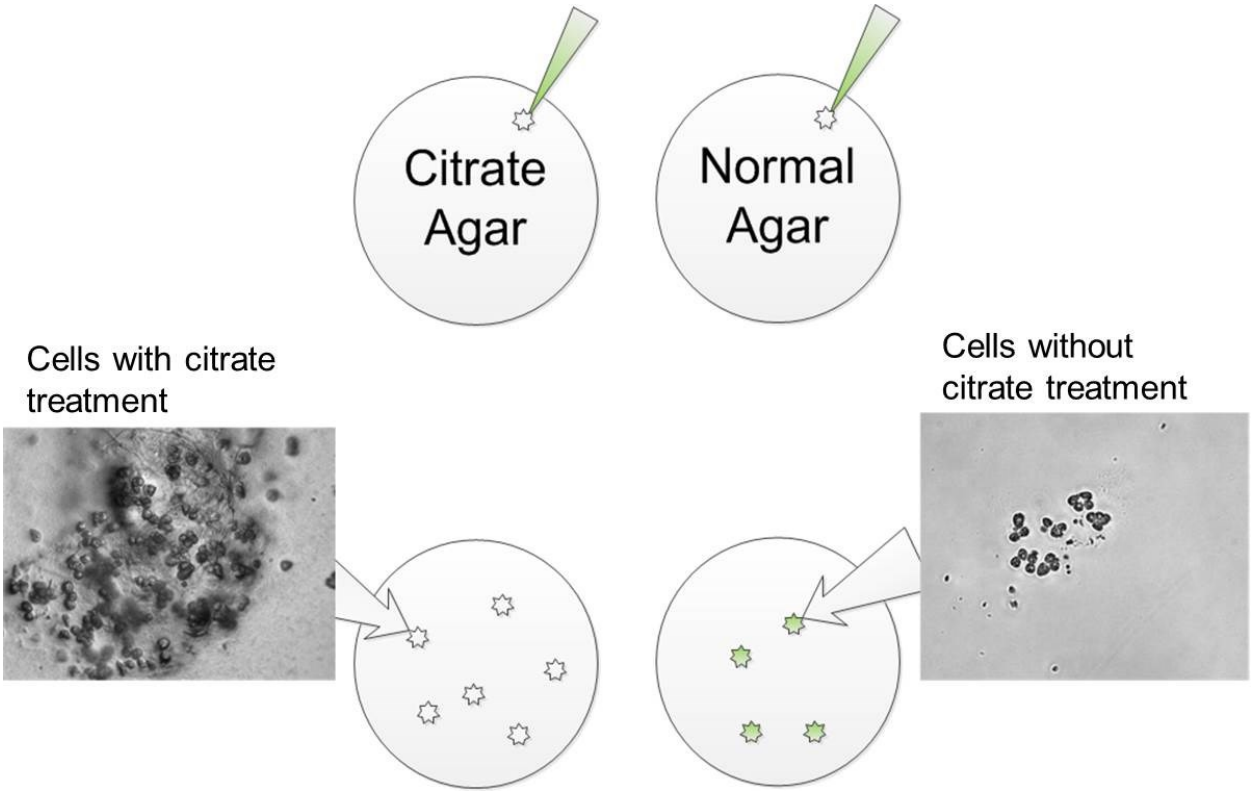

Fig. 34 An agar experiment shows the difference in cell growth between citrate-treated cells and normal cells.

Live-dead assays were conducted to examine the viability of *Botryococcus braunii* after citrate treatment. SYTOX® Green nucleic acid stain is an excellent green-fluorescent nuclear and chromosome counterstain that is impermeable to live cells, making it a useful indicator of dead cells within a population:

- Impermeable to live cells
- Excitation/Emission: 504/523 nm
- Use with 488 Argon-ion laser
- Works with mammalian cells and both Gram-positive and Gram-negative bacteria

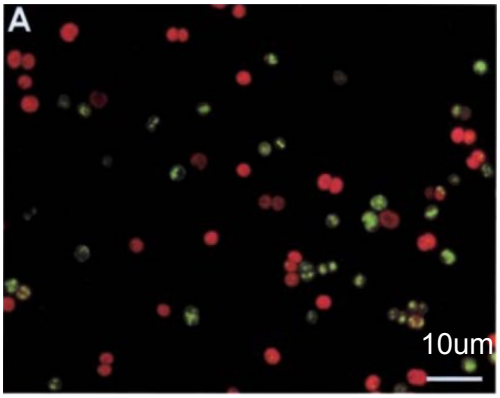

B

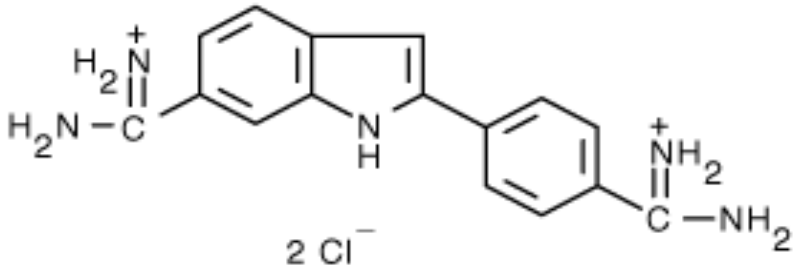

Fig. 35 Figure A was image of *Synechocystis sp. PCC 6803* showing SYTOX Green fluorescence (green) and autofluorescence (red) [133]. Figure was treated by photo-editing program to show the color. Figure B showed the molecular structure of SYTOX Green nucleic acid stain which binds to DNA abs [139].

Botryococcus cells were treated with SYTOX® Green Nucleic Acid Stain (Molecular Probes®, Invitrogen). Under a light field we observed that algae cells were present in several spots and we highlight two spots below (Fig. 36). Under green fluorescence, no excitation was seen which indicated that there were no dead cells present in the spots. Under red fluorescence, natural emissions of light by chlorophyll were seen indicating that the cells were intact containing plastids.

Live-dead assay showed that citrate-treated cells were alive.

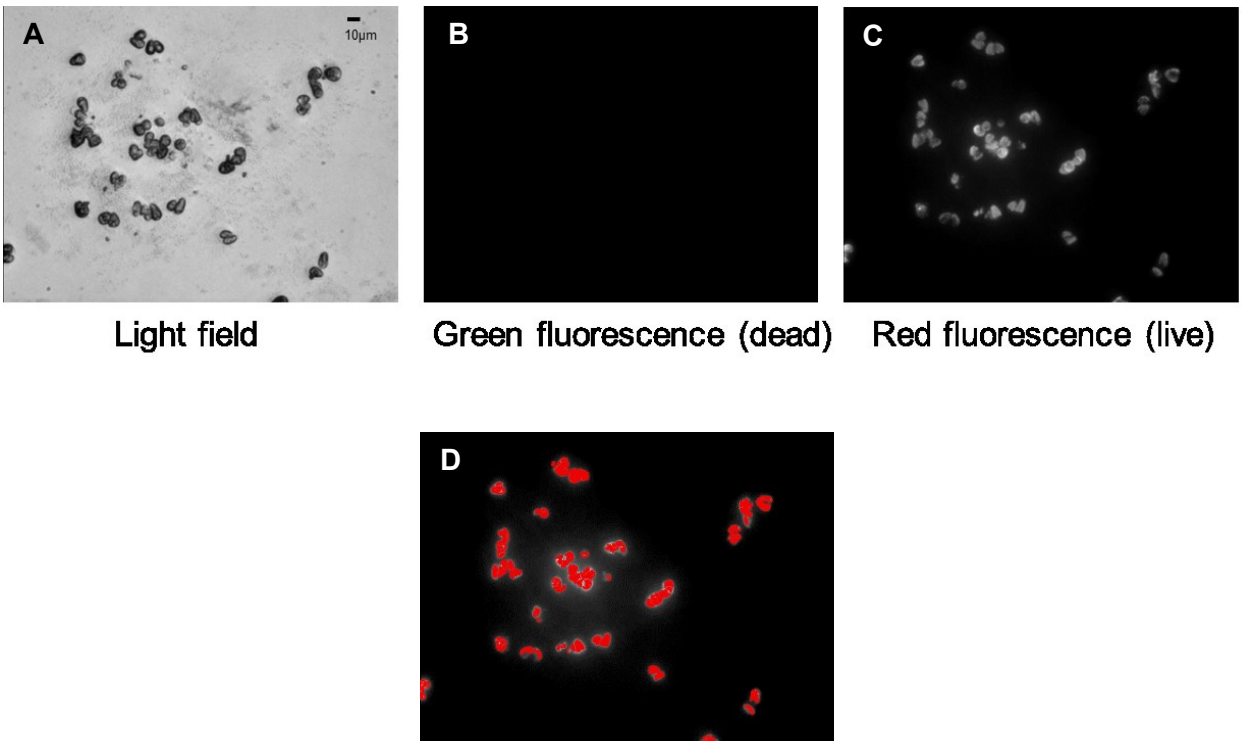

Fig. 36 Live-dead assays were deployed to study the cell viability after citrate treatment. SYTOX® Green nucleic acid stain is a green-fluorescent nuclear and chromosome counterstain that is impermeable to live cells. This delivered a green fluorescence with an emission peak of 523nm when excited by a 488nm Argon-ion laser. Camera loaded on the microscope (TE2000, Nikon) could only capture and record monochromatic images. Figure A was image of *Botryococcus braunii* under light field. Figure B was monochromatic image of *Botryococcus braunii* showing SYTOX green fluorescence which indicated dead cells. Since there were no dead cells present, we could not observe any green fluorescent signal. Figure C was monochromatic image of *Botryococcus braunii* showing autofluorescence. Figure D was the photo-stacking and colorized images of figure B and C. The red fluorescent cells showed the chlorophyll in the live cells, which indicated that cells were still viable.

Single cell analysis was examined by flow cytometers (BD FACSCANTO II Cell analyzer, BD Bioscience). Single cell analysis focuses on the distribution of cell population based on size, morphology, fluorescence intensity within certain ranges of light emission, etc. This indicates the cellular component of each individual cell,

representing a variety of morphological or photonic response from biochemical to physiological stimulus.

Cell samples were loaded into 5ml polystyrene tubes and aspirated successively through the channel. FITC and APC channels (Fig. 37) were used to measure the fluorescent signals from cells. All the samples were examined for one minute, medium flow rate. Fluorescence in the APC channel represents the chlorophyll content of microalgae cells. Forward-scattered light (FSC) is proportional to cell-surface area or size. FSC is a measurement of mainly diffracted light and is detected just off the axis of the incident laser beam in the forward direction by a photodiode.

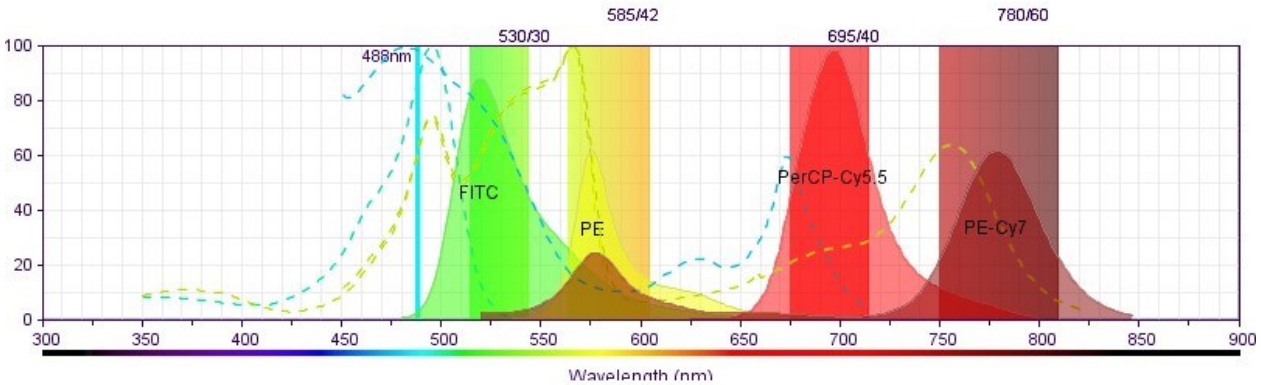

Fig. 37 A major fluorochrome chart on wavelength [134].

According to the distribution of cell population by size and APC fluorescence (Fig. 38), we divided the cell population into two parts: large cell size with high chlorophyll content which we defined as the “green” cell population, and small cell size with low chlorophyll

content which we defined as the “red” cell population. The green cell population acted as mature cells, functioning as the photosynthetic cells with complete biological activity, while the red cell population acted as newly-divided cells contributing to a fast cell accumulation and nutrient consumption.

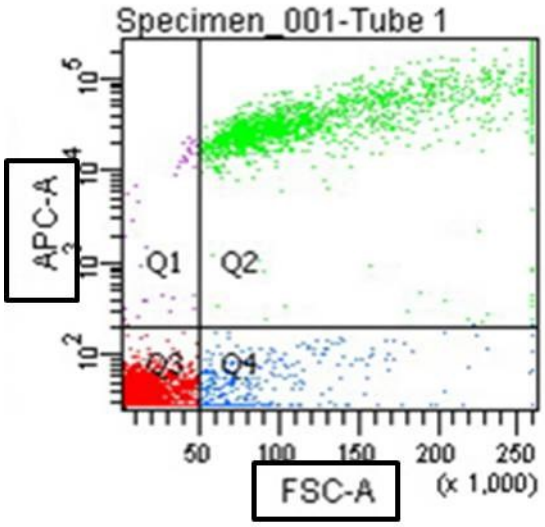

Fig. 38 Distribution of cell population by cell size and APC fluorescent intensity

Based on the distribution of cell population in Table 8, the cell numbers of the green population in the citrate-treated group were similar to those in the control group. However, cell numbers in the red population in the citrate-treated group were 20 times higher than those in the control group.

Citrate treated group		
Population	Numbers	%Total
Green	1,901	6.8
Red	25,425	91.5

Control group		
Population	Numbers	%Total
Green	1,747	56.3
Red	1,202	38.7

Table 8 Distribution of cell population by cell size and APC fluorescent intensity.

As we mentioned before, enhanced cell growth treated by citrate is associated with high production of biofuel and protein. A confocal microscope image is shown below (Fig. 39). It shows a colony with the high fluorescent signal of *Botryococcus braunii* stained by Nile red in which cells were grown under the stimulus of citrate.

Protein is another important component in microalgae, especially for high-value products and nutraceuticals. We used analytic methods to measure the protein content in *Botryococcus braunii*; enhanced protein production was achieved by the citrate treatment during the heterotrophic phase.

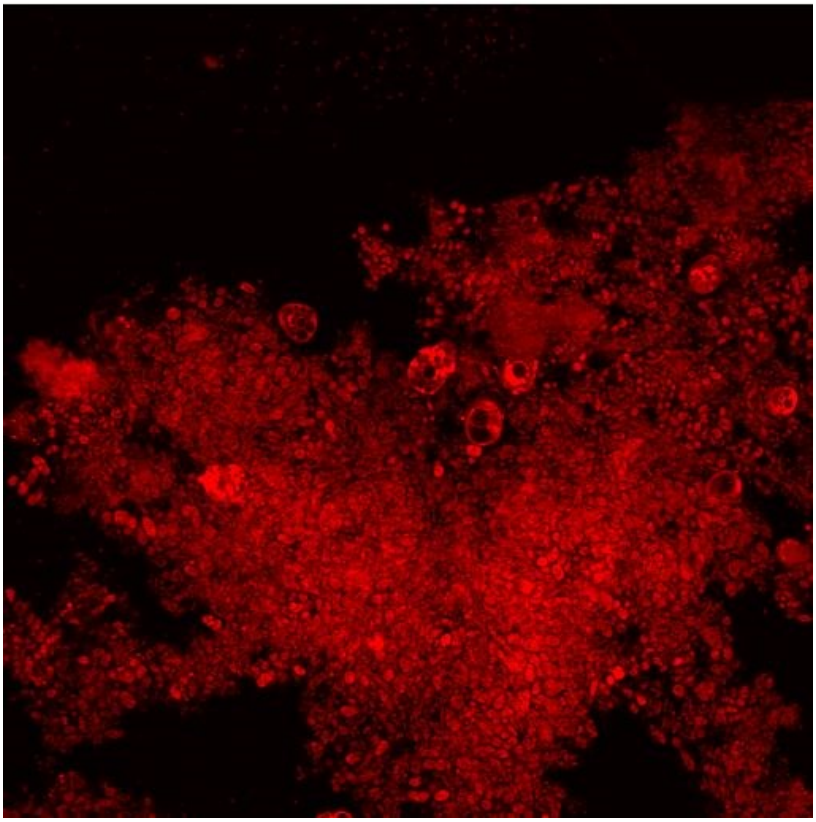

Fig. 39 Hydrocarbon and lipid molecules stained by Nile red under confocal microscope. These cells were treated by citrate.

Sulforhodamine B ($C_{27}H_{30}N_2O_7S_2$) is a fluorescent dye with uses spanning from laser-induced fluorescence (LIF) to the quantification of cellular proteins of cultured cells. The red, solid water-soluble dye is used primarily as a polar tracer. The dye has maximal

absorbance at 585 nm light and maximal fluorescence emission at 607 nm light. It does not exhibit pH dependent absorption or fluorescence over the range of 3 to 10.

Directions

The SRB staining prepared for the FACS (flow cytometry) experiment requires pretreatment of the cells:

1. Take 1ml cell into eppendorf tube. Centrifuge 6000rpm 3min, discard 500 ul supernatant and use the rest of the supernatant to resuspend the cells.
2. Add 250 ul 10% TCA (Trichloroacetic acid), vortex, keep at 4 degree for 1hr.
3. Centrifuge 6000 rpm 3min, discard all supernatant, use 1ml fresh media to resuspend the cells and add 30ul 0.057% SRB.
4. Keep at room temp for 30min covered by aluminum foil.
5. Centrifuge 6000 rpm 3min, discard all supernatant, use 1ml 1% acetic acid to resuspend the cells.
6. Repeat step 5. Prepare for FACS.

In the FACS experiment, SRB responded to the PE channel (Fig. 40).

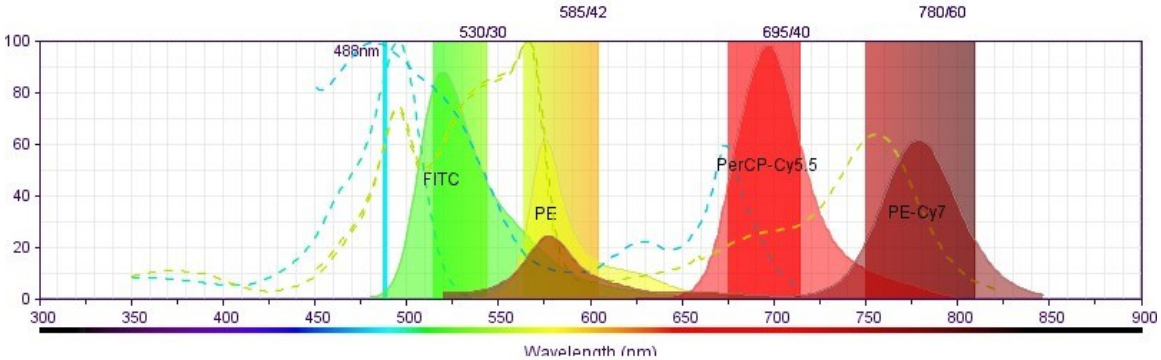

Fig. 40 Fluorescent dye wavelength spectrum in flow cytometer [134]. The PE channel ranges from 560 to 610nm while the APC channel usually ranges from 630 to 700nm.

From the FACS result (Fig. 41), with PE fluorescence intensity indicating the protein content, the citrate per day group showed a higher PE fluorescence intensity in both cell groups. This corresponds to higher protein production.

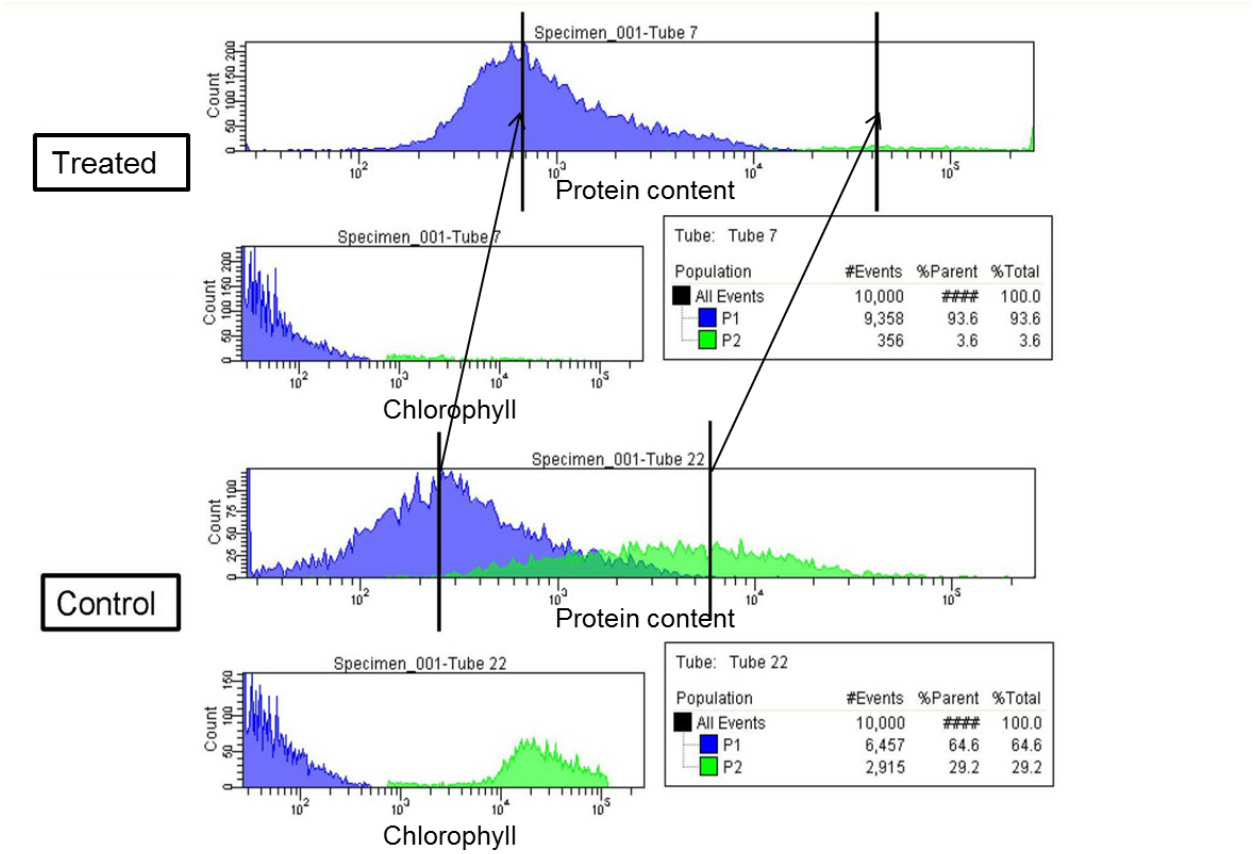

Fig. 41 Protein production from FACS. We could observe that the two peaks of cell populations have shifted to higher fluorescence intensity which reveals a higher protein production.

Total protein content was also measured by microBCA assays, indicating a dramatic increase in overall protein content. The BCA assay primarily relies on two reactions.

1) The peptide bonds in protein reduce $\mathbf{Cu^{2+}}$ ions from the cupric sulfate to $\mathbf{Cu^{+}}$. The amount by which Cu^{2+} is reduced is proportional to the amount of protein present in the solution.

2) Two molecules of **bicinchoninic acid** chelate with each Cu^{+} ion, forming a purple-colored product that strongly absorbs light at a wavelength of **562** nm.

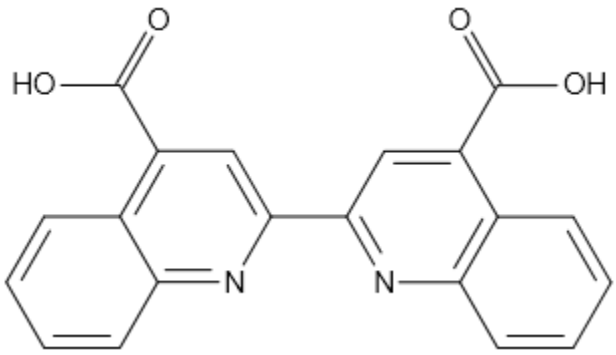

Fig. 42 Molecular structure of bicinchoninic acid [138]

A general step flowchart showing the microBCA assay is shown below (Fig. 43),

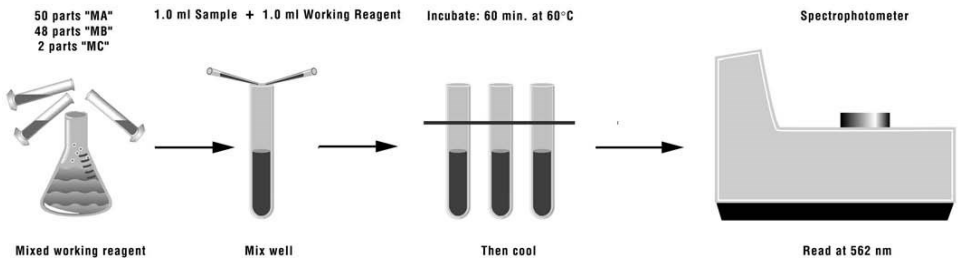

Fig. 43 General step chart of microBCA assay [137]

A protein standard assay of the protein sample with a serial of concentration was carried out to draw the standard curve (Fig. 44). Samples were then loaded on to 96-well plates in the microplate reader (SpectraMax M5, Molecule Devices) to measure the absorbance at 562nm of each sample.

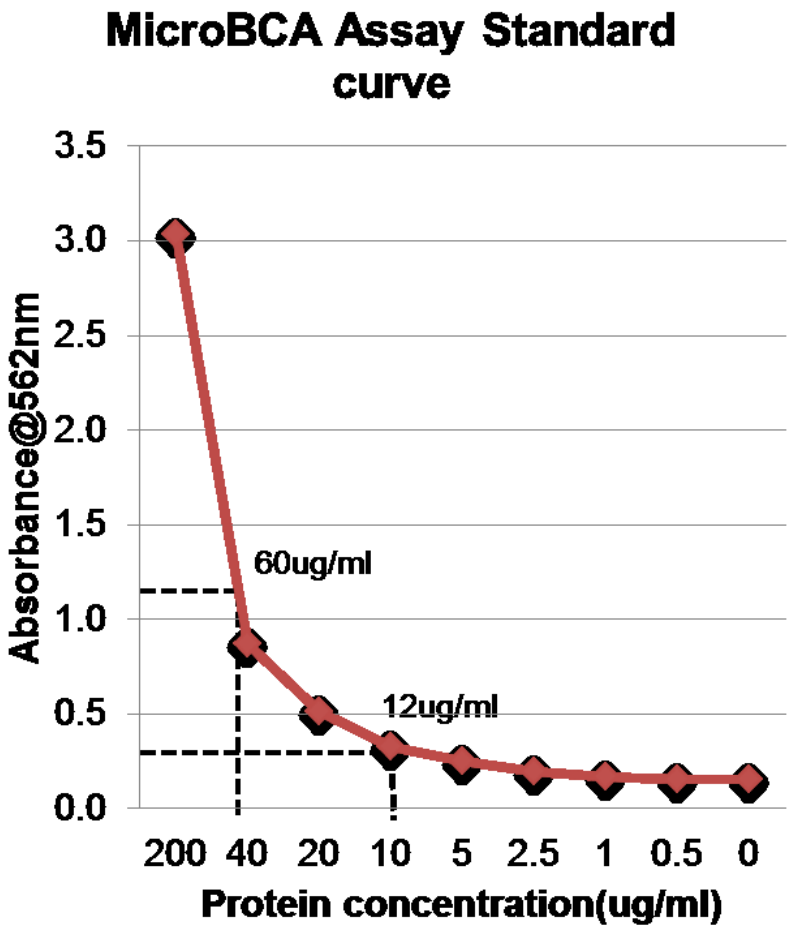

Fig. 44 MicroBCA assays of protein standard with a serial dilution of concentration. The absorbance on the y axis corresponds to the protein concentration on the x axis.

We then carried out a parallel BCA experiment. Cell samples were divided into two groups. One group was examined using the microBCA assay method, while the other group was homogenized by bead beater before the sample was loaded on the 96-well plate. After homogenization by bead beater, most of the cell walls and membranes were cracked. From the following graph (Fig. 45), it can be seen that there were no significant differences between intact cells and broken cells. We can also read the absorbance of the citrate group and the control group. These are then compared with the standard curve to calculate the protein concentration.

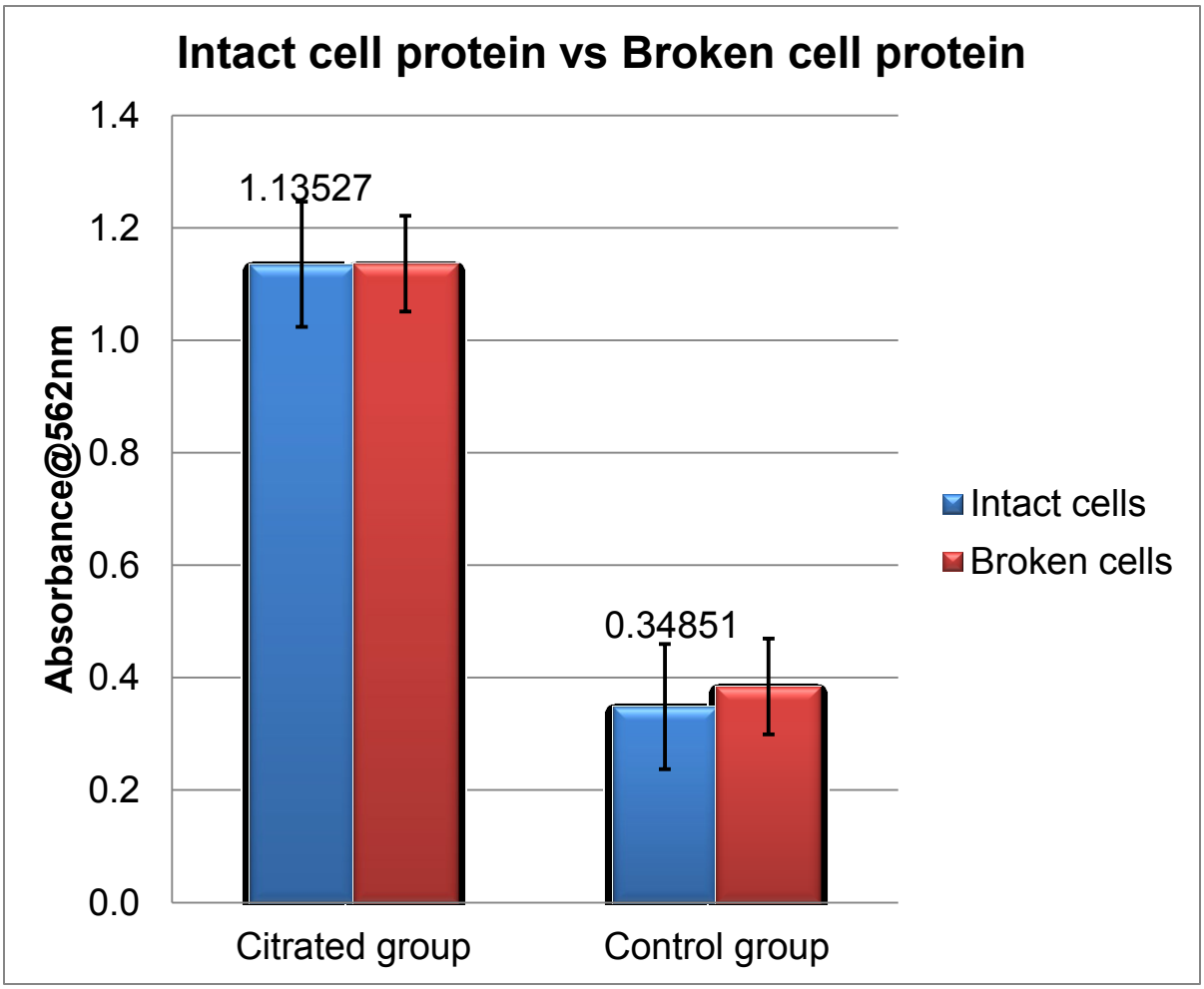

Fig. 45 MicroBCA assay of citrate group and control group. Each group was divided into intact cells and broken cells before mixing with BCA reagents. There was no significant difference between the intact cells and broken cells which meant the assays can reach a high accuracy of total protein without breaking the cell walls. The citrate group has a five-fold increase (60ug/ml compared to 12ug/ml) in protein content.

The citrate group has five-fold increase (60ug/ml compared to 12ug/ml) in protein content.

4.3 The hinge in the heterotrophy-autotrophy route: recovery

The objectives of the green cycle are to

1). Achieve high cell numbers

During the heterotrophic phase, cell numbers increase rapidly within a short period of time. However, the cell growth in the small bottles often reaches a plateau after a week. The culture then turns brown.

Typically the stationary phase is characterized by the brown color of the media solution which results from a nutrient depletion and culture crash.

One possible way to overcome the plateau is to recover cells from heterotrophy.

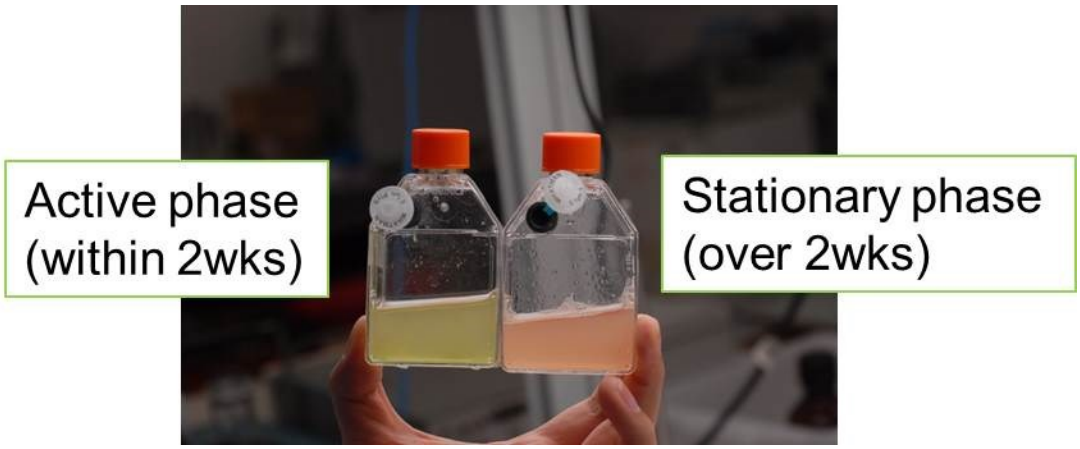

Fig. 46 The difference in color of *Botryococcus braunii* between the active and stationary phase

2). Enable cells to use inorganic carbon after the green cycle

Heterotrophic cells are dependent on organic carbon and are low in chlorophyll. They therefore lose the ability to fix carbon dioxide. It is important to apply the green cycle on heterotrophic cells so that they can synthesize chlorophyll and recover the photosynthetic mechanism.

A hinge is required to transition *Botryococcus braunii* from heterotrophic phase to autotrophic phase. At the end of heterotrophic phase, a high density of low-chlorophyll cells accumulated in the culture. Without recovery process, numbers of these heterotrophic cells would decline due to compromised metabolism and acute culture crash.

We developed a metal solution based on the elemental composition of chlorophyll and knowledge about the chlorophyll synthesis pathway. The solution component is shown in Table 9. An optimization experiment on the concentration was carried out. From this we found that the following concentration was best for recovering cells from heterotrophy to autotrophy.

Metal recovery solution	
Component	Final concentration
$FeCl_3 \cdot 6H_2O$	4.5uM
$MgSO_4 \cdot 7H_2O$	50uM
$CoCl_2 \cdot 6H_2O$	0.0425uM

Table 9 A component list of the metal recovery solution. The final concentration equals the concentration of each component in the media solution of *Botryococcus braunii.*

After the addition of the metal solution at Day 7 (Fig. 47), the cell growth of the citrate-treated group recovered from plateau while those without the addition of the metal recovery solution reached plateau.

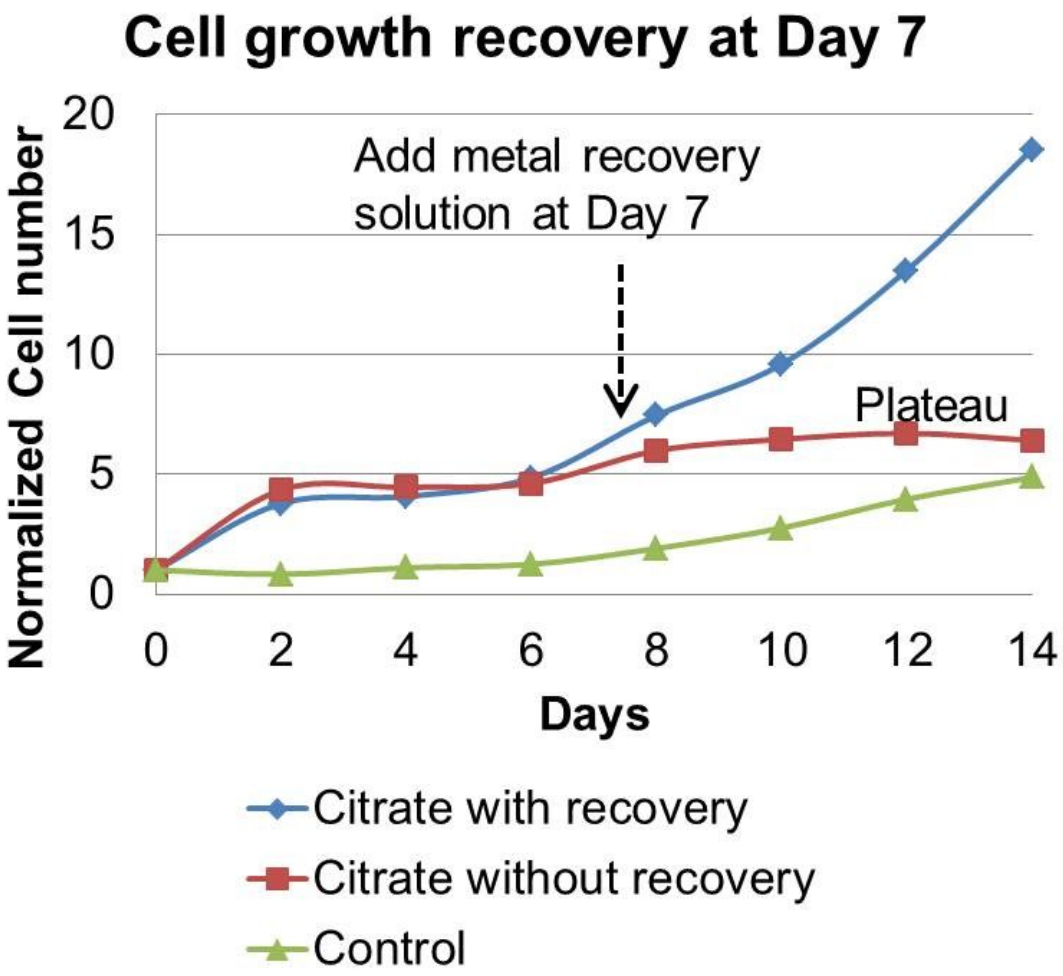

Fig. 47 A metal solution with reinforced Fe^{3+}, Mg^{2+}, Co2+ etc. ion components is added into the media for citrate-treated cells at Day 7. An increase in cell numbers is observed later.

The effect of the metal solution could be easily seen by observing the media solution from outside (Fig. 48). Once the metal solution had been applied after the stressed condition (addition of citrate ceased), the chlorophyll recovery was indicated by the clear green color in the solution. Compared to the control group and the citrate-treated group without the metal solution, these cells with more chlorophyll could continue to

photosynthesize and absorb CO_2. This could greatly enhance the environmental value of algae cultivation.

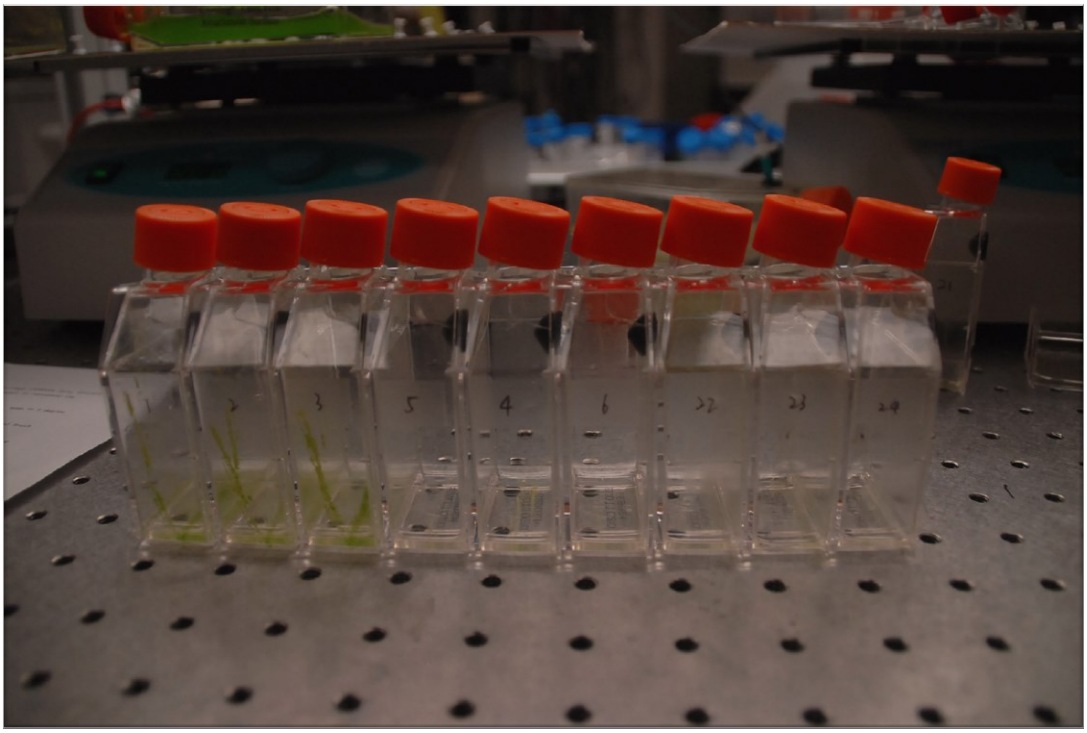

Fig. 48 The visible green color bottles treated with the metal solution after stressed condition (#1,2,3), compared to the citrate-treated group without the metal solution (#4,5,6) and the control (#22,23,24)

Apart from the growth and the color change of *Botryococcus braunii* after recovery, cell components varied due to the shift in metabolic function. We measured biomass, total cellular protein content, total lipid content and total carbohydrate content.

The algal cells were firstly washed with DI water, dried at 105°C for 24 hours and weighted to obtain the dry cell weight as biomass weight. The protein content was

measured using the Kjeldahl organically-bonded nitrogen method [121]. The carbohydrate content was analyzed according to anthrone-sulfuric acid colorimetric assay [122]. For lipid and fatty acid analysis, 0.5 g dried cells were extracted by a solvent mixture of chloroform and methanol (2:1, v/v), based on the procedures of Bligh and Dyer [123]. The supernatant was collected, and the solvent was subsequently removed using a rotary evaporator. The extracted oil was weighted to calculated lipid content. Then the oil sample was dissolved in KOH-CH_3OH. After 20 minutes heated at 75°C, 14% BF3 was added in and was heated at 75°C for 20 minutes. The sample was dissolved in hexane and was injected into Agilent GC-7980 for examination.

Botryococcus braunii were concentrated and inoculated in large bottles with media to which citrate was added each day. At Day 14, the metal recovery solution was added into the media solution and the total remaining volume was divided into five equal parts and diluted to five new media without citrate. Heterotrophic cells recovered from heterotrophy to autotroph and cell biomass increased again.

The measurement was carried out every five days and the results are shown in the following graph (Fig. 49). Carbohydrate was reduced from 50% to 20% after recovery, while protein and lipid content increased. This explained the fact that algae turned into mature, photoautotrophic cells after the accumulation of chlorophyll. Metabolic functions were recovered and algae cells started to utilize carbon dioxide other than citrate.

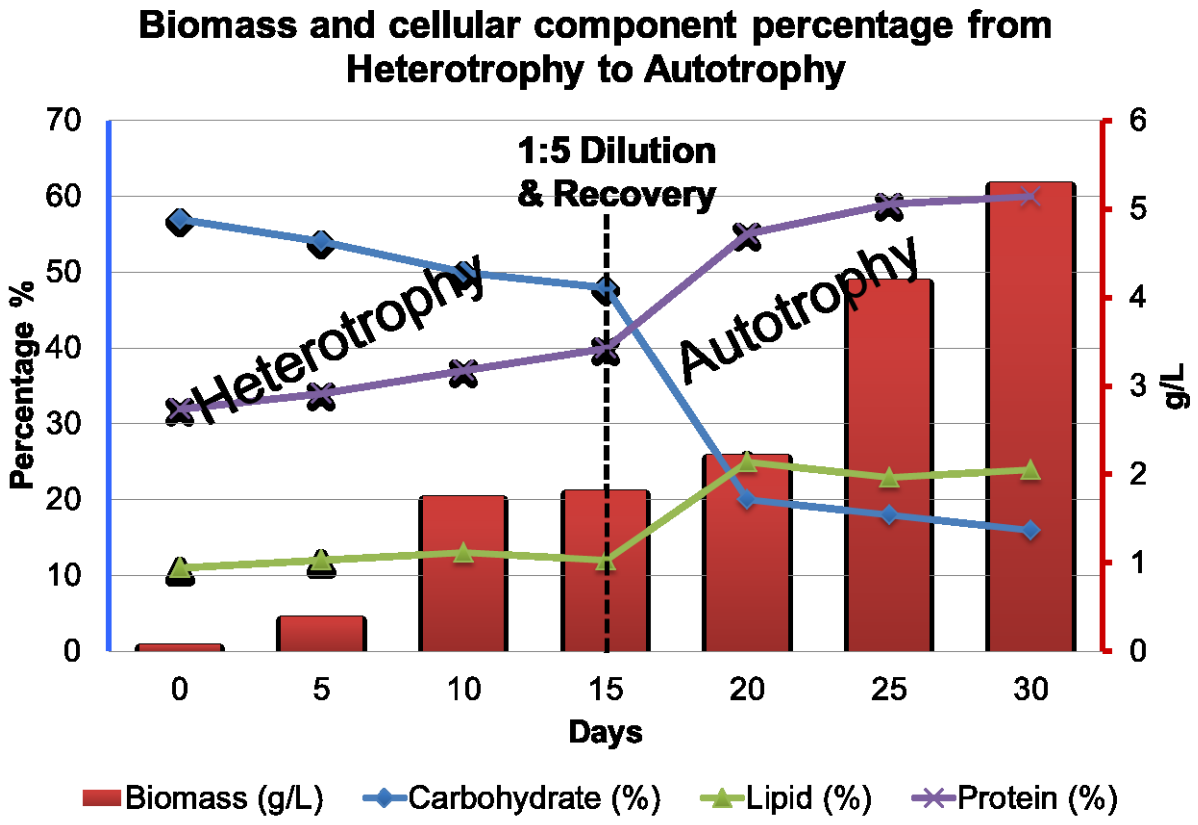

Fig. 49 A graph showing the biomass and cell component change from heterotrophy to autotrophy. Blue Y axis on the left showed the percentage of cell component such as carbohydrate, lipid and protein, Red Y axis on the right showed the concentration of biomass. X axis showed days.

In summary, the green cycle leads to a fast accumulation of heterotrophic cells and then converts them to autotrophy after recovery. This method is very significant for the commercial-scale of microalgae industry, providing as it does a shortcut for algae cultivation.

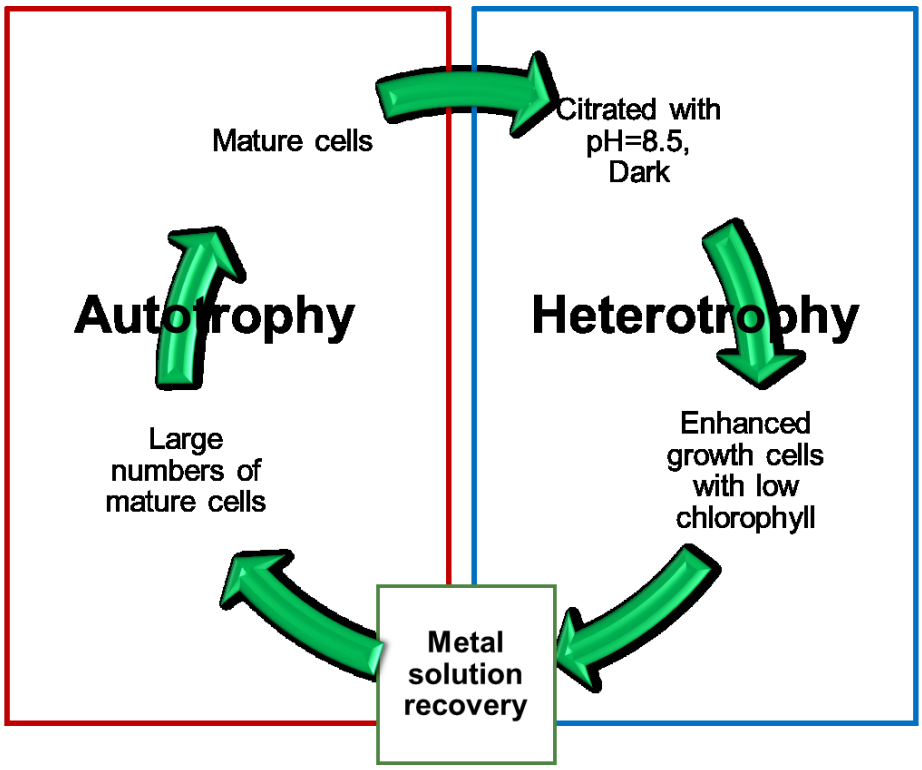

Fig. 50 A flow chart showing the green cycle for *Botryococcus braunii* from heterotrophy to autotrophy

Chapter 5. Optimizing the nitrogen sources of *Botryococcus braunii*

5.1 N-N-A Combined nitrogen sources versus a single nitrogen source

Aquatic organisms need nitrogen to live and can find it in different sources throughout nature. Nitrogen is the building material which makes proteins and nucleic acids for microalgae. It is 5% of algae cell dry weight. An adequate supply of nitrogen is imperative to ensure high growth rates of microalgae culture and biofuel productivity.

Currently all the culture media use a single source of nitrogen to feed algae, i.e. nitrate. There are several culture media for *Botryococcus braunii* such as Modified Bold 3N Medium, BG-11 Medium, Chu-13 Medium, etc. They use a variety of nitrate concentration ranges from 3.96mM to 17.6mM.

Culture Media	BG-11	MB3N	Chu13
Nitrate Conc (mM)	17.6	8.82	3.96

Table 10 It showed the nitrate concentration in different culture media for *Botryococcus braunii*

The metabolism of nitrogen source assimilation in some algae strains has been studied (Fig. 51). In *Chlamydomonas reinhardtii*, algae transports nitrate into cells through nitrate transporters on the cell membrane and then reduces cellular nitrate to

nitrite by nitrate reductase. Nitrite in the cells is transported into plastids through nitrite transporters and then reduced further into ammonium by nitrite reductase. Ammonium is finally used as the source to synthesize glutamate for biomass.

Besides the nitrate uptake pathway, scientists have found that some microalgae can utilize ammonium as their initial nitrogen source. For example, *Chlamydomonas reinhardtii* can transport aqueous ammonium from media through an ammonium transporter on the cell membrane (Fig. 51). Ammonium in the cells is then transported into plastids through an ammonium transporter on the plastid membrane. The ammonium in the plastids can be directly used as a metabolic source.

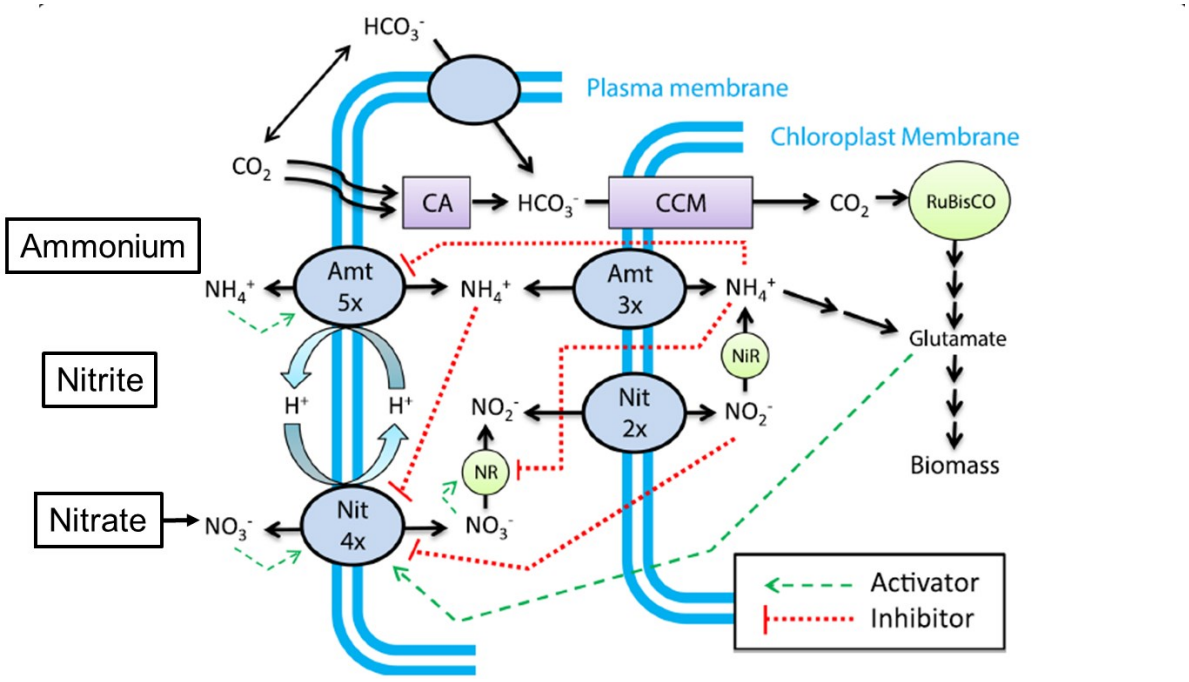

Fig. 51 Schematic of cellular regulation of nitrogen source assimilation in the algae *Chlamydomonas reinhardtii* [135]. The number of identified transporters is indicated on the respective membrane (i.e. 3x =

three ammonium transporters on the chloroplast membrane). Dashed lines in the legend represent the regulatory elements involved in nitrogen metabolism. Additional key notations: Amt = ammonium transporter, Nit = nitrate transporter, NR = nitrate reductase, NiR = nitrite reductase, CA = carbonic anhydrase, CCM = carbon concentration mechanisms.

Nitrate reduction is the committed step which limits the whole nitrogen-uptake process. It has to go through two membranes, two reductive reactions, and then finally be utilized as the building blocks. To study this mechanism in *Botryococcus braunii*, we examined each nitrogen component. The results are shown below (Fig. 52).

Nitrate and ammonium were measured after removal of the cell samples by filtration. The amount of nitrate was analyzed by measuring optical absorbance at 210nm [123] by the Griess method [124] (Griess Reagent, Promega). Ammonium was monitored by the Nesslerization method [125] (Nessler's Reagent, Sigma Aldrich).

10mM Nitrate was added into the culture media of *Botryococcus braunii* at the beginning of inoculation, with the presence of around 0.1mM of both nitrite and ammonium in the media solution after four hours of illumination. These phenomena substantiated that nitrate was transported into cells and converted into nitrite and ammonium.

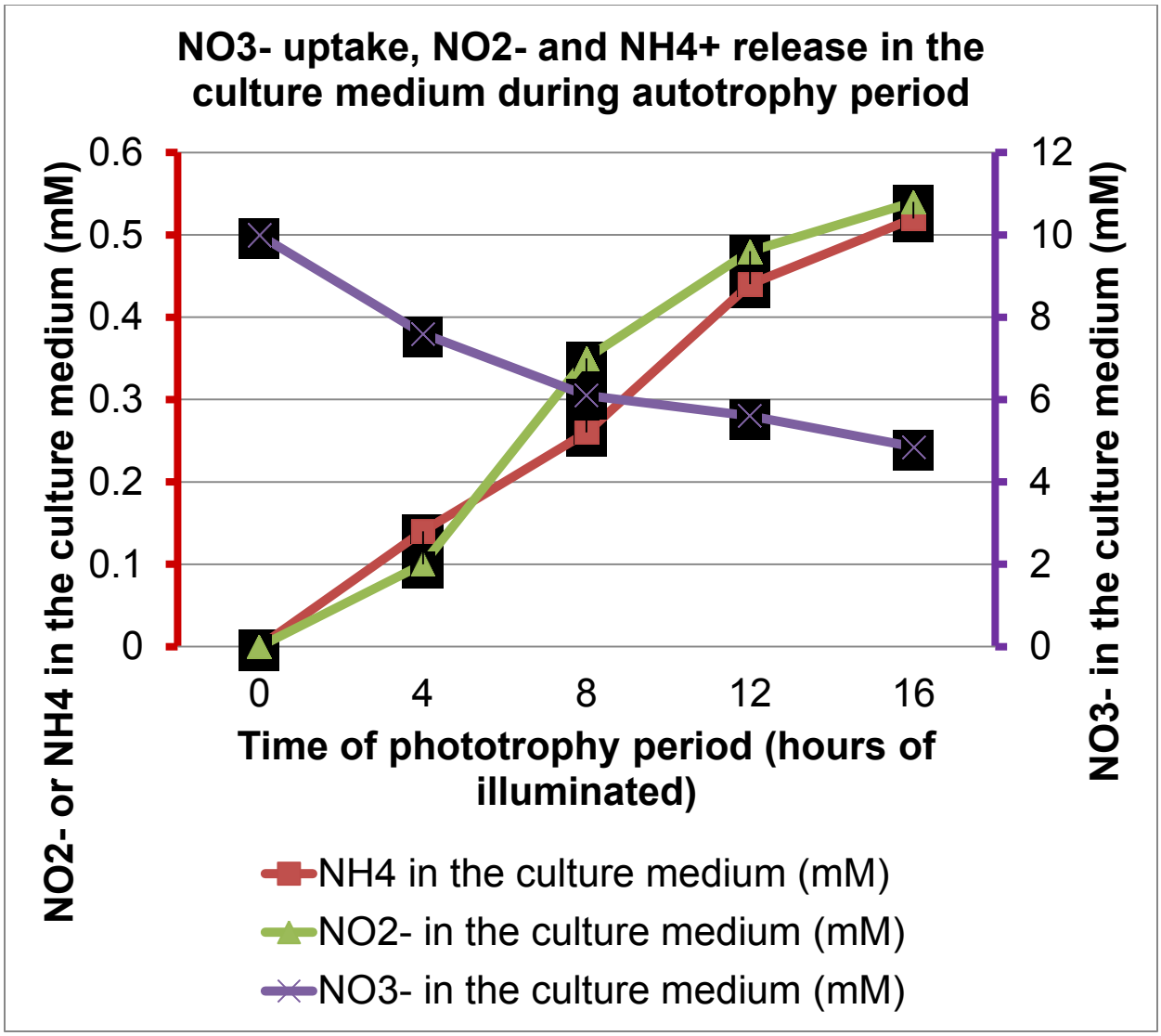

Fig. 52 Nitrogen component measurement in the culture media of *Botryococcus braunii*

Based on the current understanding of nitrogen assimilation in *Botryococcus braunii*, we developed a N-N-A (nitrate-nitrite-ammonium) combined nitrogen source feeding strategy over a nitrate only strategy, to increase the efficiency of nitrogen uptake.

The advantages of using N-N-A sources are based on the characteristic of each nitrogen sources showing in the following Table. 11:

Nitrate 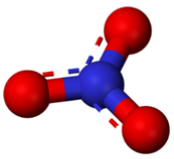	• Nitrate is effective for cell growth, but expensive. • All the culture media are using single source of nitrogen to feed algae.
Nitrite 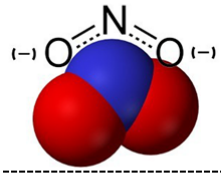	• Nitrite could inhibit foreign bacteria's growth • Nitrite coupling with ammonium, can facilitate nitrogen assimilation
Ammonium 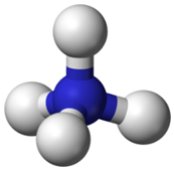	• Algae can utilize ammonium instantly. • Ammonium can balance pH variation

Table 11 The characteristic of each nitrogen source upon algae culture.

Ammonium was found to be an early triggering factor on cell growth (Fig. 53). Once ammonium chloride was added to the solution, an increase in cell numbers was evident on day 0. This proves that adding ammonium accelerates the citrate effect.

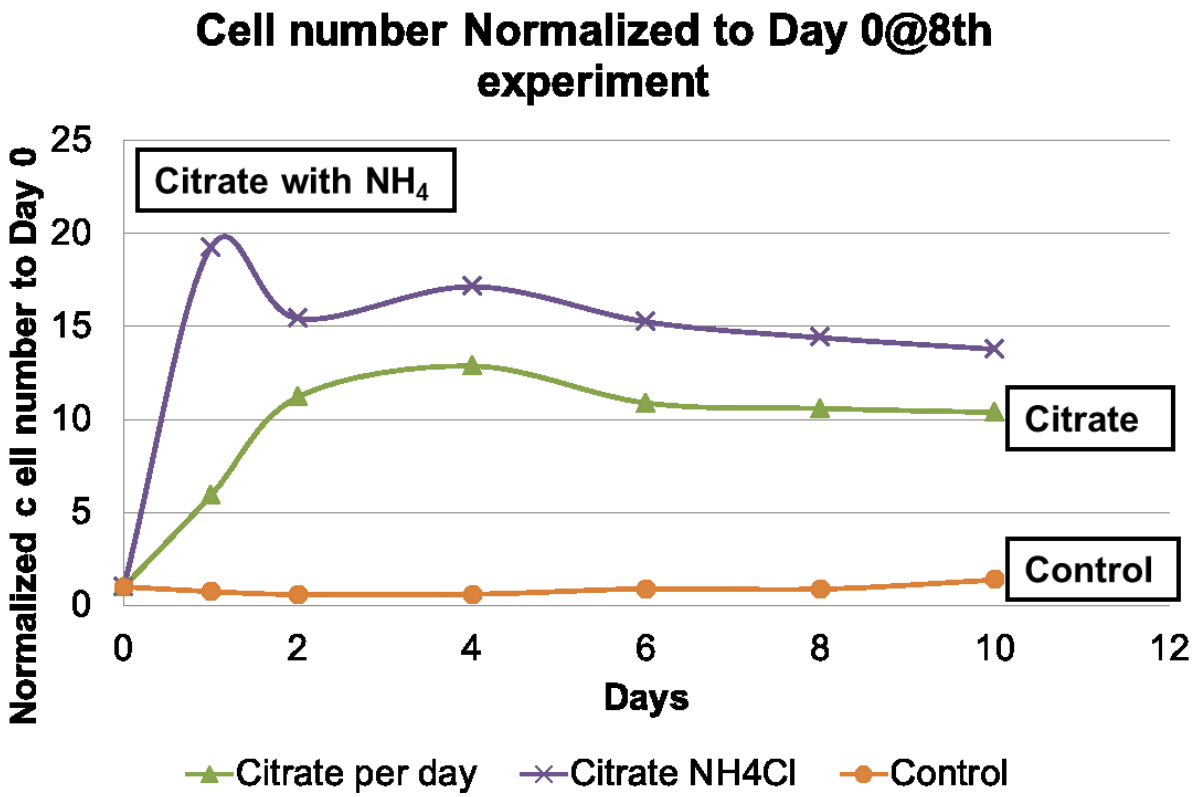

Fig. 53 Optical density normalized to Day 0 at 6th round experiment. Ammonium coupled with citrate can increase cell numbers at Day 0.

Various concentrations of ammonium chloride were investigated to achieve the concentration that triggered optimized cell growth immediately after day 0 (Fig. 54). 0.5mM ammonium chloride was found to lead to higher cell growth compared with other concentrations. However, the presence of higher ammonium ions seemed to deactivate the nitrate reductase enzyme which could cause the culture's pH to decline to less than pH=4 which would damage the cells [101].

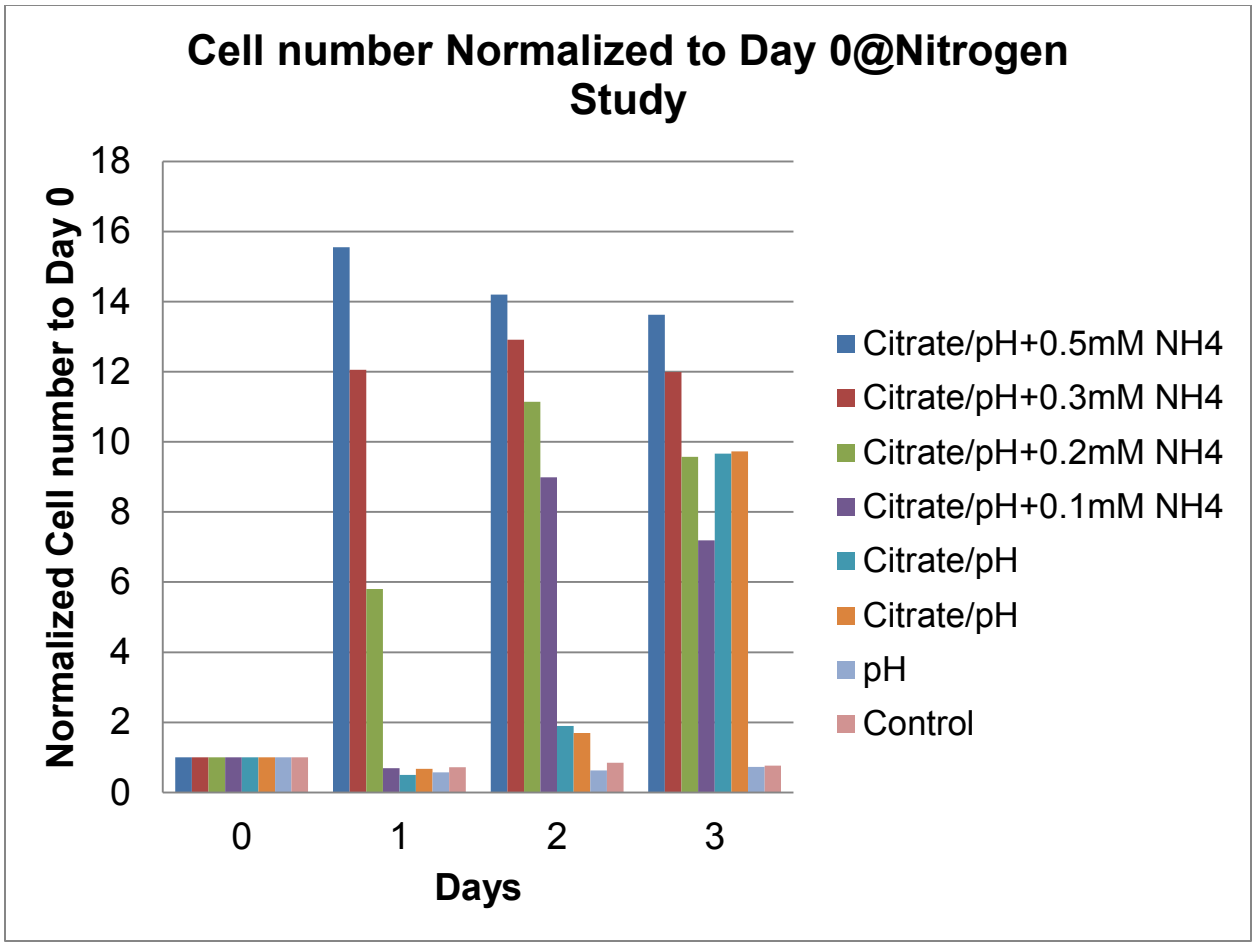

Fig. 54 This showed the cell growth result when using a combination of citrate and ammonium chloride. The first four bars (from blue to violet) used different concentrations of ammonium chloride with citrate (the same concentration) while the next two bars (cyan and yellow) used citrate (same concentrations) only. Use of ammonium chloride combined with citrate would effectively eliminate the lag-phase. The last two bars were control groups with no addition of citrate or ammonium chloride. In this experiment, the best concentration for ammonium chloride was 0.5mM.

The results from the above experiments showed there was an advantage in combining ammonium with nitrate during the heterotrophic phase before recovery. The optimized concentration of ammonium was given.

In order to investigate the effect of combined nitrogen sources upon cell culture of *Botryococcus braunii*, we first developed a nitrogen-free medium (Table. 12), based on the requirements of nutrients compositions and several optimized concentrations of different media component.

We calculated the use volume of each media component on the basis of final concentration of those components to be used in the nitrogen-free medium. Stock solutions of each media component were firstly prepared. We took the use volume of each ion component other than the vitamin components (vitamin solution needed to be added after autoclave) in the following Table. 12, and mixed them into a pre-sterilized glass bottle. After autoclave, the mixed medium and each vitamin components were then added in the filter bottles (Stericup® Filter Units, EMD Millipore). Finally, the nitrogen-free medium was prepared before the addition of nitrogen sources.

Ions

Chemical component	Stock solution concentration(M)	Final concentration(uM)	Use volume (uL)
K_2HPO_4	1	430	559
KH_2PO_4	1	1290	1677
$MgSO_4 \cdot 7H_2O$	0.1	300	3900
Citric acid	1	30	39
$CaCl_2 \cdot 2H_2O$	1	200	260
$MnCl_2 \cdot 4H_2O$	1	9	11.7
$ZnSO_4 \cdot 7H_2O$	1	0.77	1.001
$FeCl_3$	1	2.16	2.808
$Na_2MoO_4 \cdot 2H_2O$	0.1	430	559
$CoCl_2 \cdot 6H_2O$	0.1	0.17	2.21
$CuSO_4 \cdot 5H_2O$	0.1	0.3	3.9
Boric acid	0.1	1.6	20.8

Vitamins

Chemical component	Stock solution concentration(mM)	Final concentration(uM)	Use volume (uL)
Vitamin B12	0.1	0.000738	9.594
Thiamine hydrochloride	10	0.0296	3.848
Biotin	1	0.00819	10.647
Pyridoxine	1	0.00591	7.683

Table 12 A nitrogen-free medium which was designed for investigating the effect of combined nitrogen sources on cell growth. Several chemical components were optimized for *Botryococcus braunii* cell growth. The final concentration of each component was given.

According to the nitrate concentration in the current culture media and the experimental design for optimizing the combined component, a four level concentration of combined nitrogen experiments was designed (Table. 13). A full map of the four level concentration experiment would include 64 combinations (in duplicate, so a total of 128 bottles).

4 level Concentration			
Concentration level	Nitrate (mM)	Nitrite (mM)	Ammonium (mM)
1	0	0	0
2	2	0.2	0.04
3	10	1	0.2
4	30	5	1

Table 13 A full map of 4-level concentration experiment for combined nitrogen sources.

Prior to studying the combined effect of three nitrogen sources, different single nitrogen sources in a variety of concentrations were investigated (Fig. 55). Trends in single nitrogen source on cell growth were detailed in Table 14.

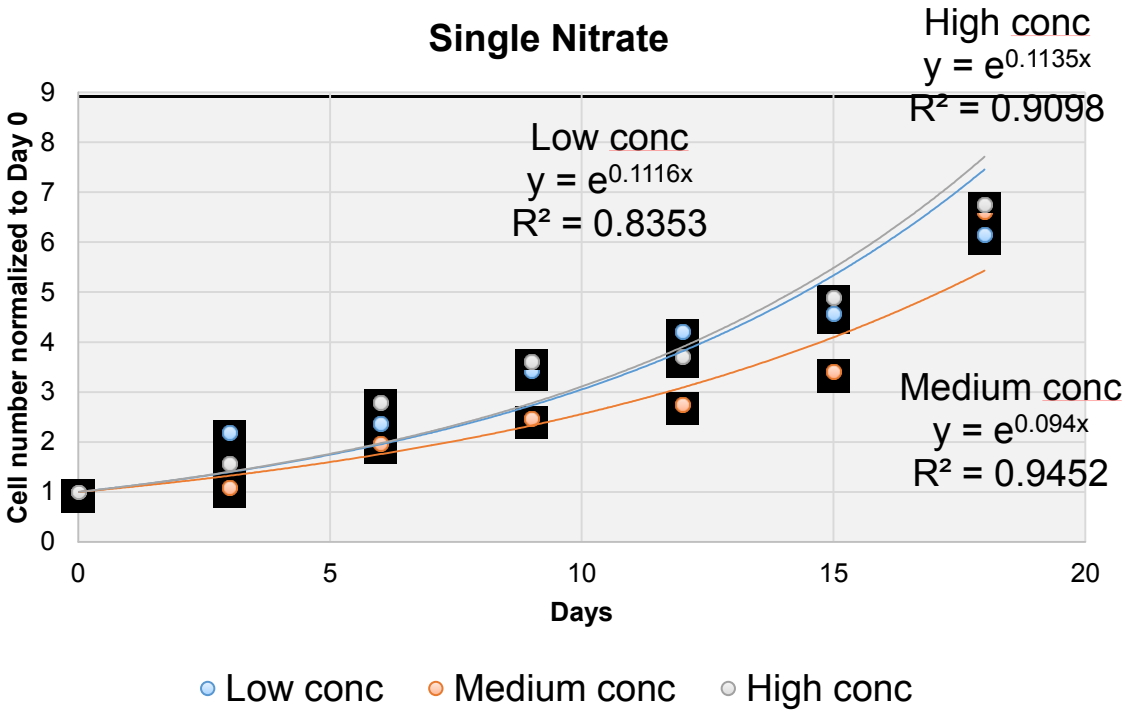
Single Nitrate
High conc
y = e^0.1135x
R² = 0.9098
Low conc
y = e^0.1116x
R² = 0.8353
Medium conc
y = e^0.094x
R² = 0.9452
Cell number normalized to Day 0
Days
0
1
2
3
4
5
6
7
8
9
0
5
10
15
20
Low conc
Medium conc
High conc

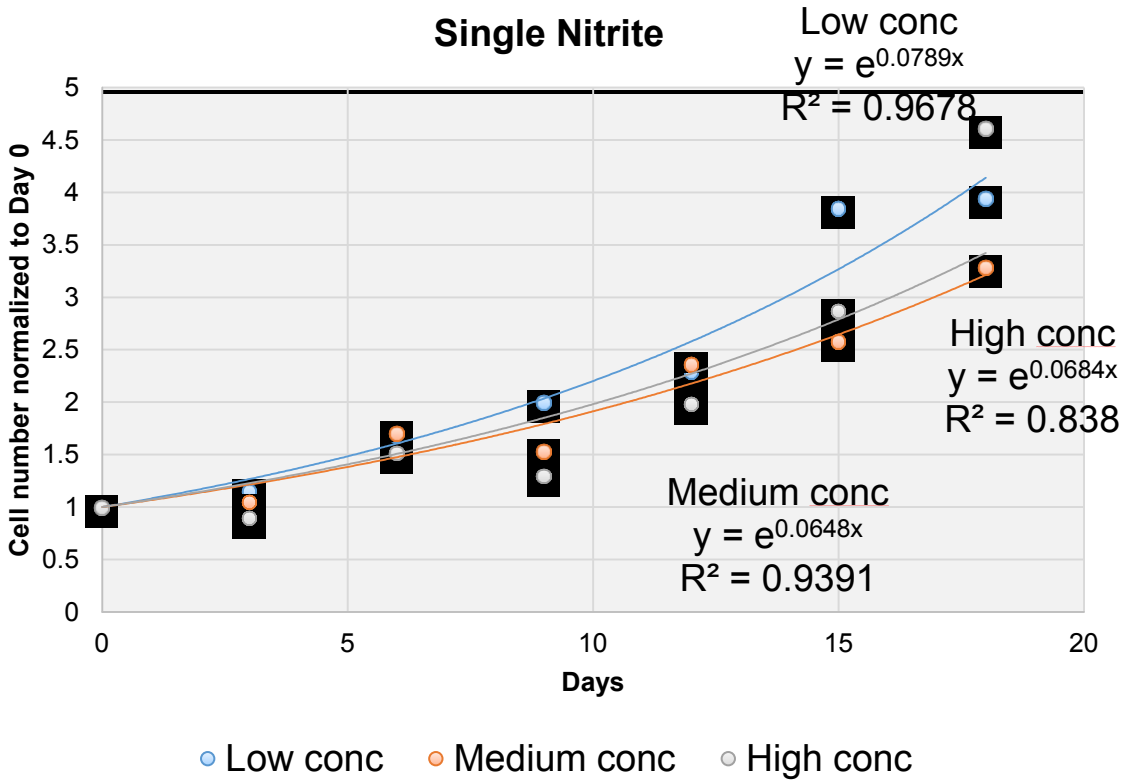
Single Nitrite
Low conc
y = e^0.0789x
R² = 0.9678
High conc
y = e^0.0684x
R² = 0.838
Medium conc
y = e^0.0648x
R² = 0.9391
Cell number normalized to Day 0
Days
0
0.5
1
1.5
2
2.5
3
3.5
4
4.5
5
0
5
10
15
20
Low conc
Medium conc
High conc

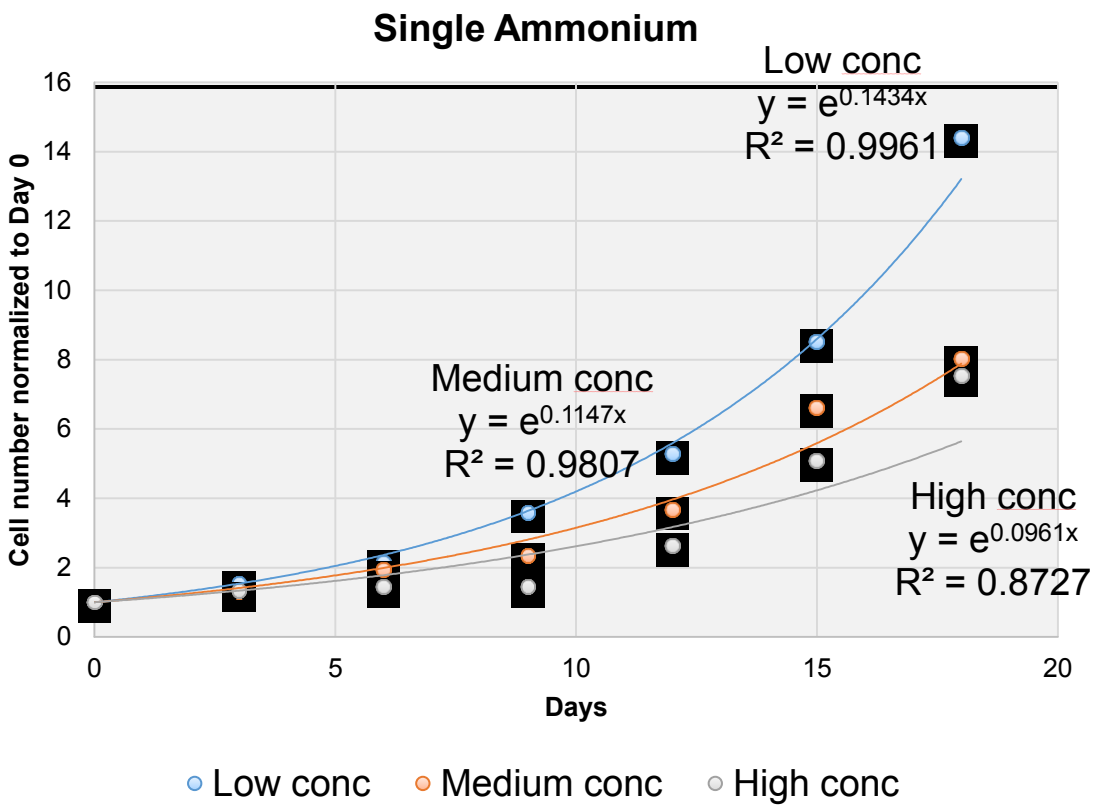

Fig. 55 Plots for cell growth under a single nitrogen source. Y axis represents normalized optical density to Day 0 and X axis represents days. Each non-zero concentration in the map has been studied and cell growth curves plotted.

Conc level	Nitrate(NA)	Nitrite(NI)	Ammonium(AM)
Low Conc	0.1116	0.0789	0.1434
Med Conc	0.094	0.0648	0.1147
High Conc	0.1135	0.0684	0.0961

Table 14 *Botryococcus* growth rates under different single nitrogen sources. Low conc, medium conc and high conc represents concentration levels of 2, 3, 4 of each single nitrogen source.

From the effects of a single nitrogen source on cell growth, we concluded that

- NA↑, GR↑; NI↑, GR↓; AM↑, GR↓ (GR=Growth rate)
- Concentration of nitrite is about six to ten-fold lower than nitrate. Ammonium is about 30 to 50-fold lower than nitrate.
- 0.04mM ammonium could lead to higher cell growth than 30mM nitrate (i.e. 750-fold difference in concentration).

Combined nitrogen sources were studied and we found that several combinations of nitrogen sources could result in significantly higher cell growth (Fig. 56). Therefore, we argue that the use of combined nitrogen sources could be very attractive for efficient, high-yield and low cost cultivation of *Botryococcus braunii.*

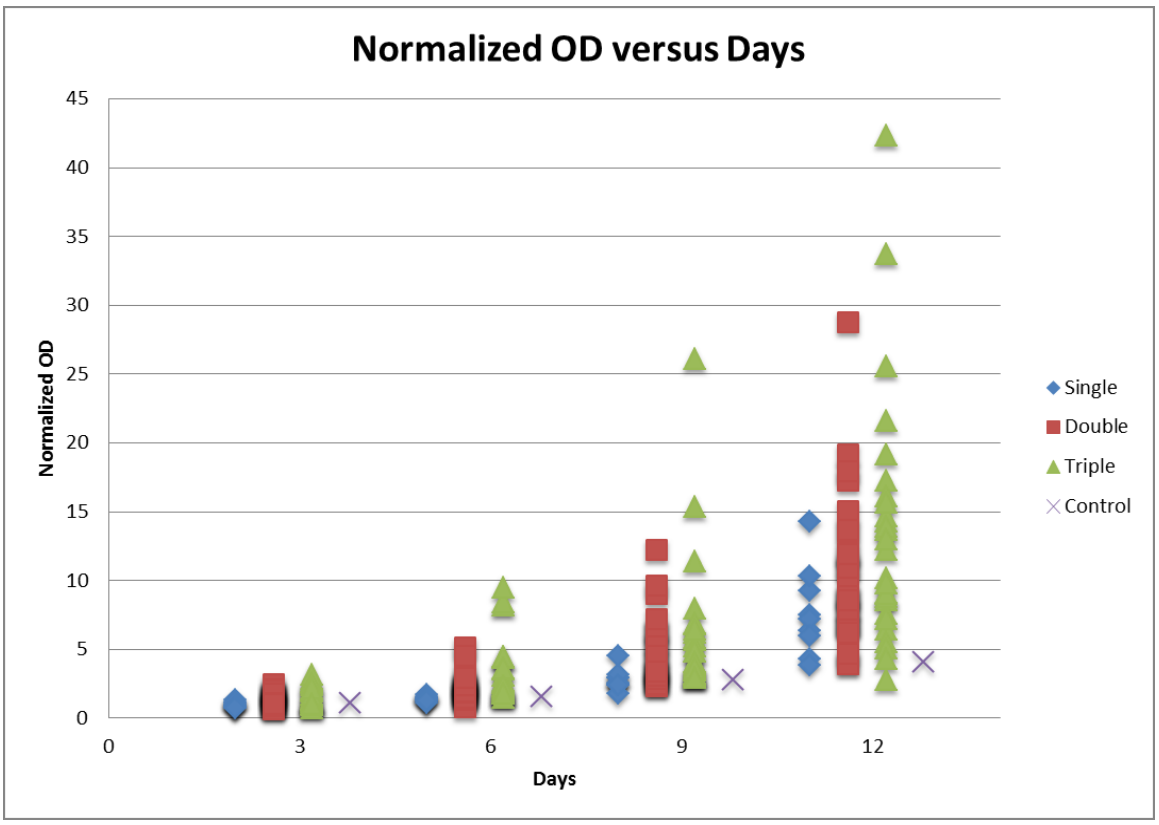

Fig. 56 Cells were treated with different singe/combined nitrogen sources plus the nitrogen-free medium. In the graph, “single” means a single nitrogen source, “double and triple” means two and three combined nitrogen sources respectively. From the result, it seems that combined nitrogen sources work better than single nitrogen sources.

Optical density measured at Day 14 normalized to Day 0 was plotted in the histogram in Fig. 57, where we found that with combined nitrogen sources, we could obtain significantly improved cell growth. And the concentrations of each nitrogen sources in these combinations are listed below (Table 15). Using a combination of 2mM nitrate + 0.2mM nitrite + 1mM ammonium could lead to around seven times more cell numbers compared to 30mM nitrate, and 17 times more when compared to nitrogen-free media.

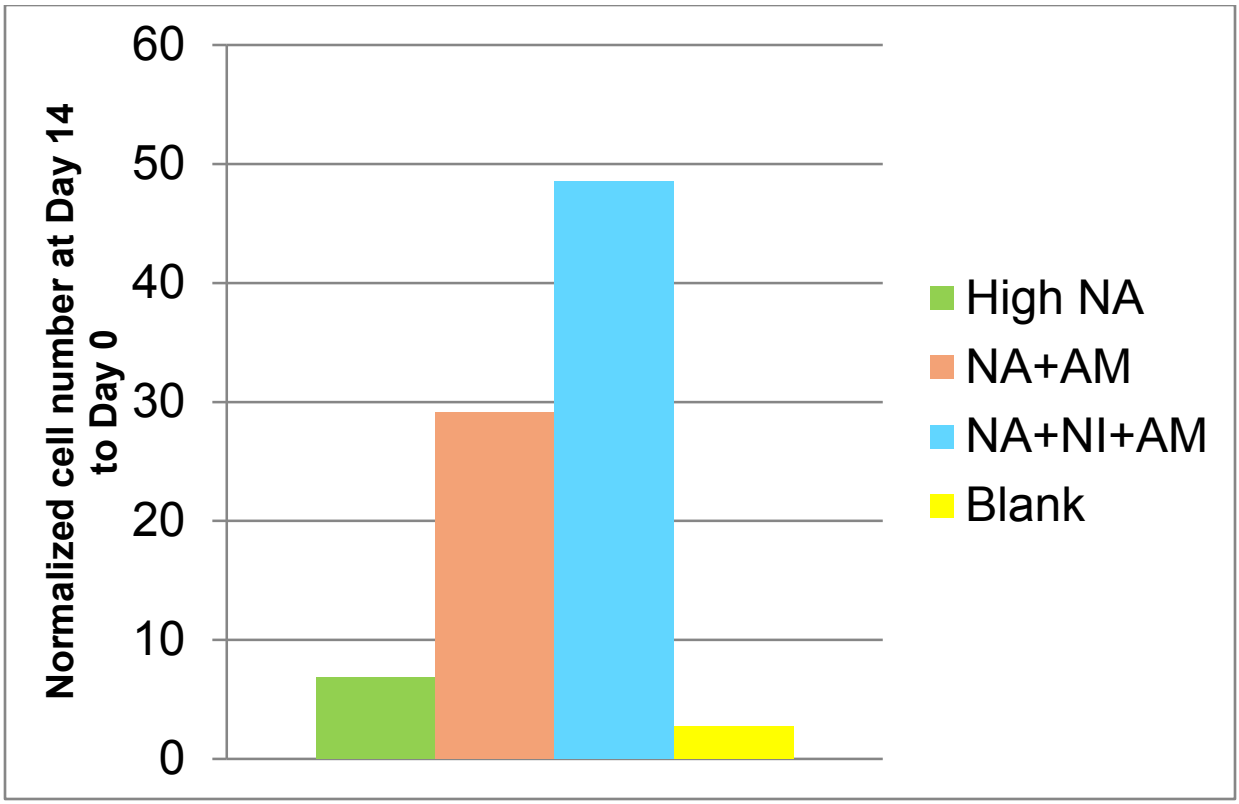

Fig. 57 Optical density of the typical combinations measured at Day 14 normalized to Day 0. The concentrations of each nitrogen source were listed in Table 15.

Combinations	Nitrate (mM)	Nitrite (mM)	Ammonium (mM)	Normalized cell number at Day 14 to Day 0
#1	30	0	0	6.87
#2	2	0	0.2	29.12
#3	2	0.2	1	48.52
#4	0	0	0	2.75

Table 15 Conclusion of using combined nitrogen sources. Concentrations of each component of optimized combinations in N-N-A sources are listed.

5.2 N-N-A Combined nitrogen sources for pH buffer-free medium

A major requirement for microalgae cultivation is the use of pH buffer because nitrogen uptake is closely associated with pH changes in the media solution.

The nitrogen assimilation mechanism of microalgae reflects the intake of nitrate and reductions in the plasma and plastids respectively. This explains the potential increase in pH along with the nitrate uptake. Each ammonium cation (NH_4^+) conversion from nitrate (NO_3^-) requires four protons (H^+) from the media solution. Therefore cells transported protons as long as the nitrate was reduced and the pH in the solution increased over time (Fig. 58).

Media pH was measured during cell growth. Even with the injection of 1% (v/v) CO_2, pH still reached 8.5 which started to inhibit cell growth.

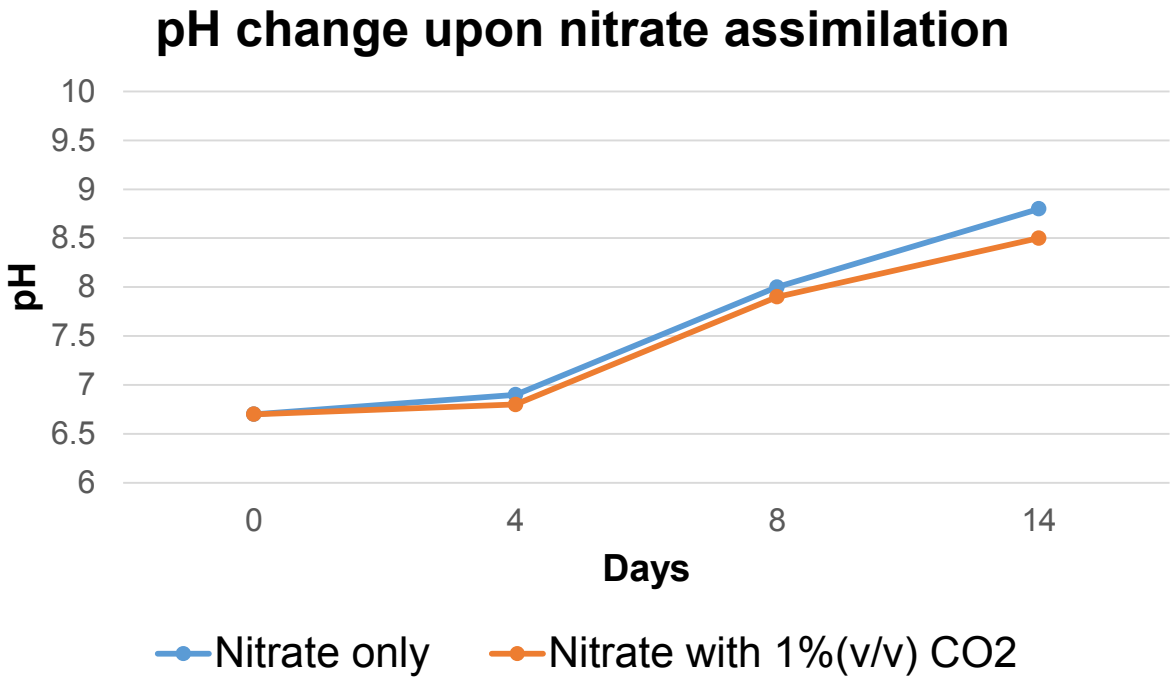

Fig. 58 pH change in the media upon nitrate assimilation. Even with CO_2 injection, pH increased significantly over time. Y axis represented pH and X axis represented Days.

The drawback of the pH changes became apparent when cell growth was enhanced during the heterotrophic phase. The media pH measurement was carried out as citrate increased the cell growth of *Botryococcus braunii* and normalized optical density was monitored to investigate the pH influence on cell growth. Cell growth in the citrate per day group reached a plateau at Day 6 and pH in the media solution was over 8.5 which would inhibit cell growth (Fig. 59). The inhibition effect of pH over 8.5 on cell growth can be seen in the following graph. The blue curve shows the normalized optical density to Day 0 of those *Botryococcus braunii* cells which were titrated to pH=8.5. Cell growth in this group was inhibited when pH raise over 8.5.

Cells treated with citrate each day grew rapidly until Day 6; however, the pH level in their media solution had already reached 8.7 which inhibited cell growth. They were divided into two groups: one, labeled as red curve and red bar, would keep their existing media condition; the other, labeled as green curve and green bar, would be adjusted to a neutral pH media solution. Accordingly we added pH buffer into the culture media of the green group to adjust the pH to 7 at Day 6. Cells started to grow again in contrast with the red group.

These results indicated that the pH increase was the main reason for inhibited cell growth during the heterotrophic phase. As cell numbers accumulated dramatically in the

media solution, *Botryococcus braunii* continuously transported large amounts of nitrate and protons into cells which would consequently raise pH to levels that would eventually inhibit the cell function. Adjusting pH to 7 helped cells to get rid of the basic media condition. As a result cells started to grow again.

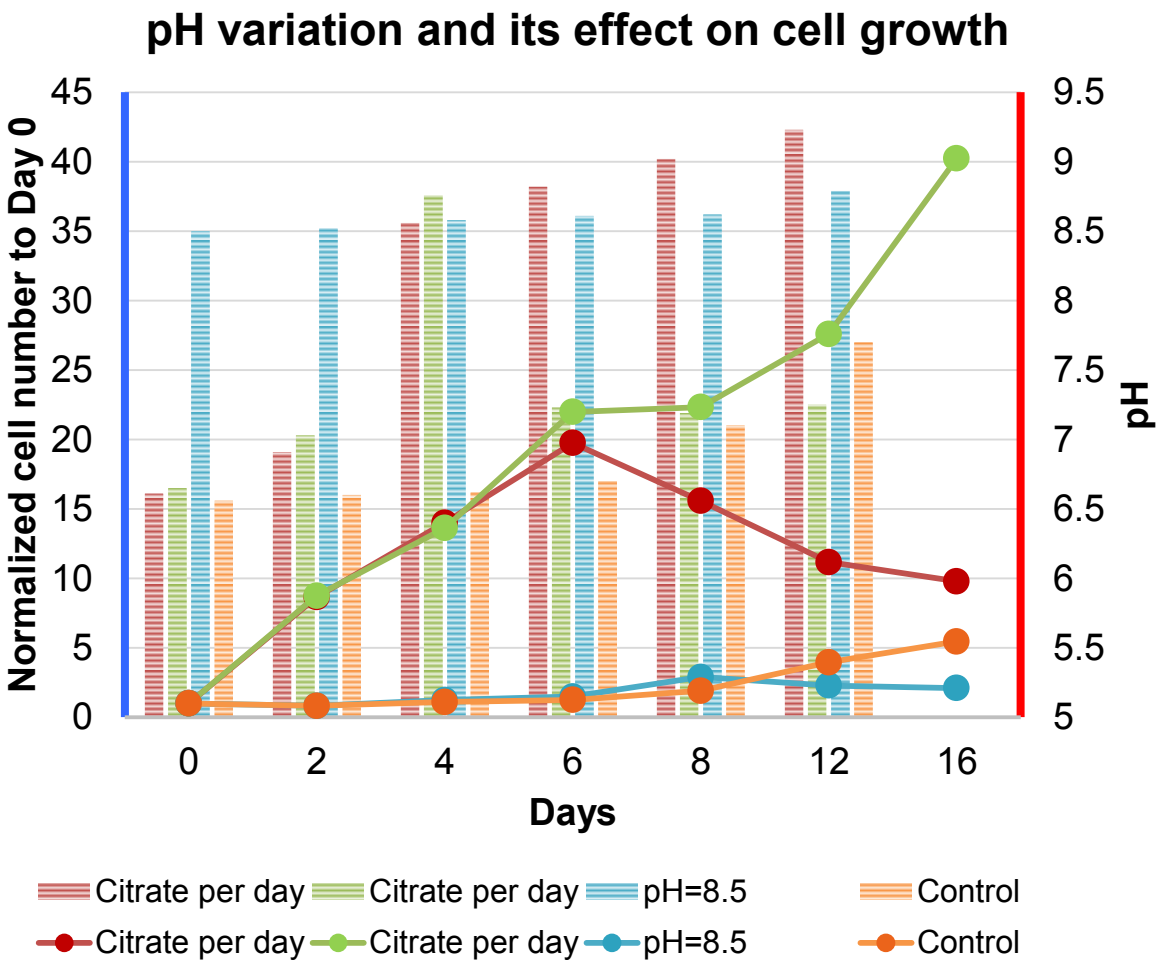

Fig. 59 This shows pH variation in cells and growth curve. Left Y axis represents the normalized optical density to Day 0. The right Y axis represents pH in the media solution and the X axis represents Days. The growth curves of citrate-treated cells began to decline due to pH increase. The citrate-treated cells stopped responding to the citrate stimulation after Day 6 and showed a pH level higher than 8.5. After adjusting the pH back to 7, the citrate stimulation was observed again.

We examined pH variations in *Botryococcus braunii* treated with a single nitrogen source to understand how each nitrogen source would impact pH levels in the media solution (Fig. 60). Low, medium and high concentrations of each single nitrogen source represent concentration levels of 2, 3, and 4 in our design. We concluded:

- Nitrate itself is pH neutral, but nitrate uptake will increase pH.
- Nitrite itself is basic, and nitrite uptake will increase pH.
- Ammonium itself is acidic.

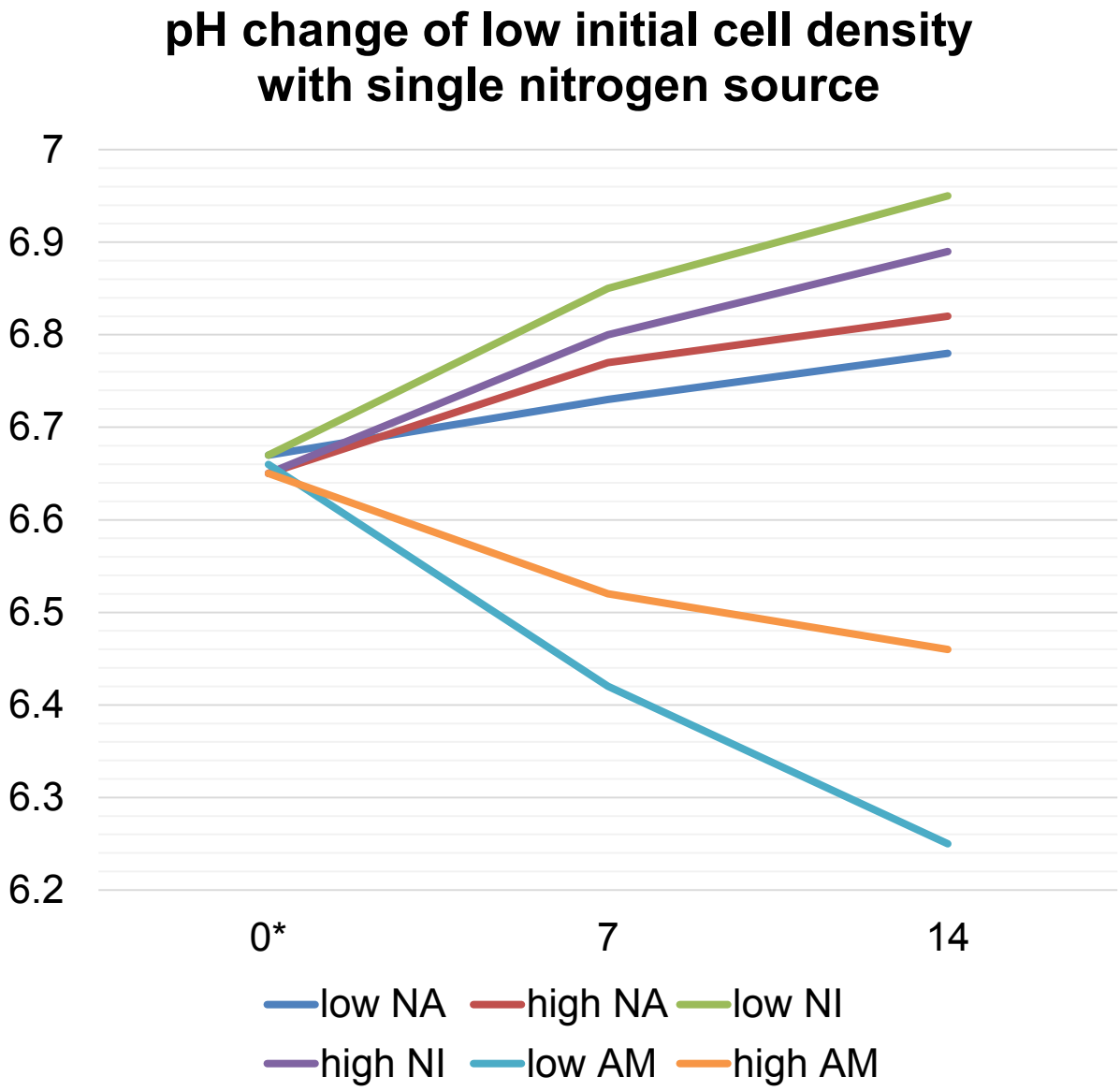

Fig. 60 pH was measured in cells' media solution treated with a single nitrogen source. Y axis represented pH and X axis represented Days. The initial pH is measured before the addition of the nitrogen source.

Based on the above results, we developed N-N-A sources to balance pH variation due to nitrate uptake along with a significant increase in cell growth which we showed in

the previous content. N-N-A combined nitrogen sources helped balance pH in the media solution which effectively eliminated use of pH buffer.

N-N-A sources were tested on *Botryococcus braunii* during the autotrophic phase (Fig. 61). Cell numbers were monitored as well as pH levels in the media solution. Nitrate and ammonium would both change pH in the media solution which corresponded to lower cell growth. Combined use of nitrogen sources not only maintained pH levels in the media solution but also lead to higher cell growth. We list the key parameters of the N-N-A sources tested in Table 16. The concentration of each component in the combination is given in the Table17.

In summary, we developed a N-stoichiometrically-balanced growth media to maintain a constant pH without using buffer. N-N-A sources achieved an optimized growth of cells and maintained pH levels in the media solution. In fed-batch culture, continuous nitrogen feeding is essential to algae growth. As a result, we argue that N-N-A sources could be very attractive and effective in algae cultivation.

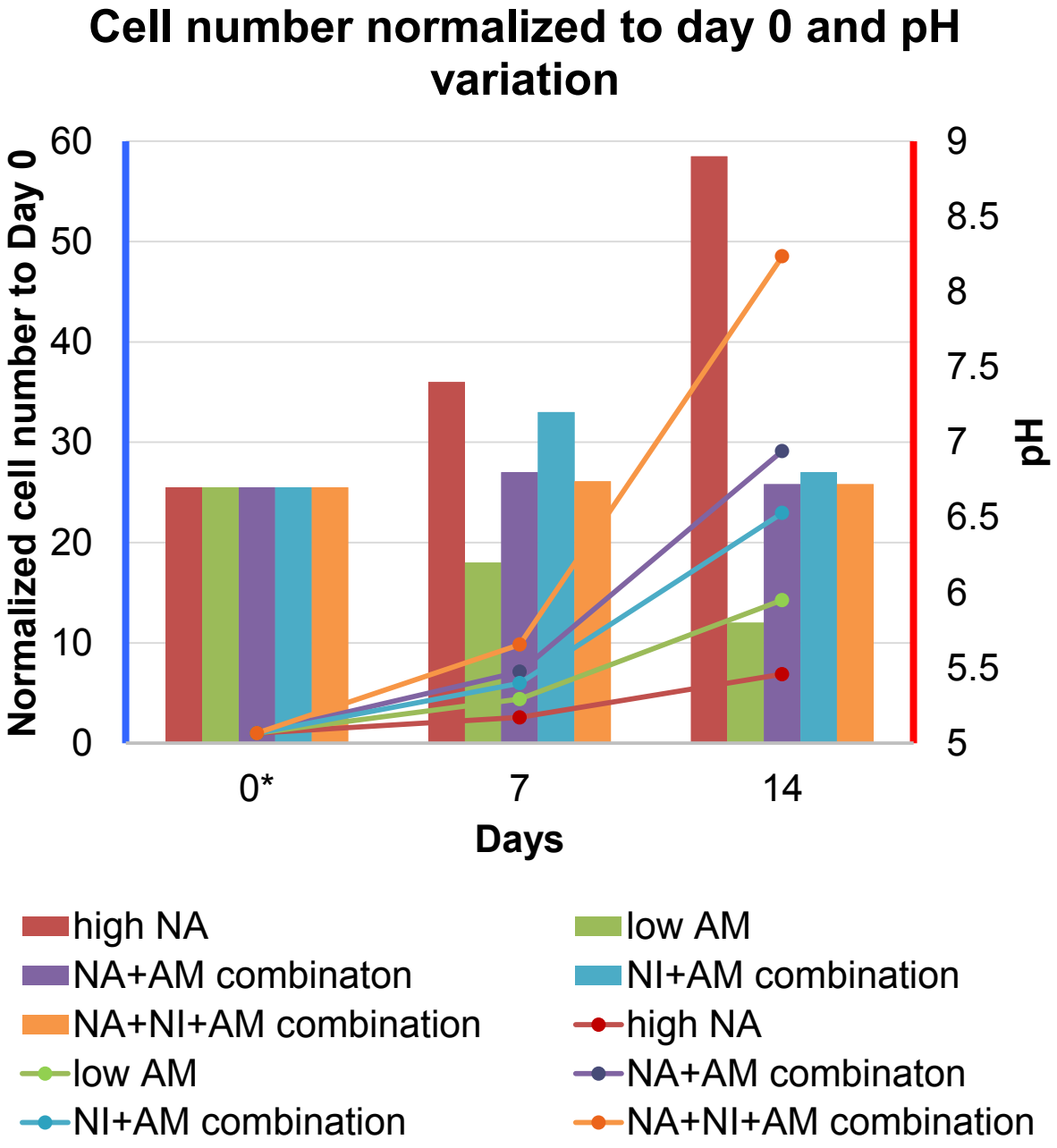

Fig. 61 pH variation and cell growth curve for several selected nitrogen sources, including single nitrogen sources and combined nitrogen sources. Left Y axis represents normalized optical density to Day 0, right Y axis represents pH in the media solution, and X axis represents Days.

	pH at 2wks	Normalized OD at Day 14 to Day 0
High NA	**8.9**	**6.87**
Low AM	**5.8**	**14.26**
NA+AM combination	**6.72**	**29.12**
NA+NI+AM combination	**6.72**	**48.52**
High NA with buffer pH=6.7	**6.75**	**10.91**
Low AM with buffer pH=6.7	**6.62**	**18.27**

Table 16 This shows pH measurement and normalized cell number measurement under single nitrogen sources with pH buffer, without pH buffer, and using N.N.A source as N-stoichiometrically-balanced growth media

Combinations	Nitrate (mM)	Nitrite (mM)	Ammonium (mM)	Normalized cell number at Day 14 to Day 0
High NA	30	0	0	**6.87**
Low AM	0	0	0.04	**14.26**
NA+AM	2	0	0.2	**29.12**
NI+AM	0	1	0.2	**22.94**
NA+NI+AM	2	0.2	1	**48.52**

Table 17 Cell growth under different N.N.A sources. Concentrations of each component are shown.

Chapter 6. Conclusions and future perspectives

The cultivation of microalgae is an interdisciplinary topic that combines many subjects. In this study, we have concluded that

- The green cycle developed for *Botryococcus braunii* could assist in high biofuel production. Heterotrophic growth was induced and then a metal recovery solution was added to convert heterotrophic cells to autotrophic cells.
- We identified the initial condition and solved the data inconsistency problem. We chose 14 days as our time reference. This determined the time duration of each experiment.
- We developed an N-N-A sources media which could achieve enhanced cell growth compared to nitrate as the only nitrogen source. N-N-A sources were able to balance pH variation due to nitrate uptake, so as to maintain pH level in the media solution without use of pH buffer.

By applying these techniques to *Botryococcus braunii*, we were able to achieve an enhanced cell growth 58 times greater than the control (Fig. 62). Cells were treated with N-N-A sources at the beginning, rather than with a single nitrate as for the control. 20mM citrate was added every day for the first week. Normalized optical density can reach up to 24. Metal recovery solution was added at Day 7 and cells were gradually shifted to the autotrophic phase. At Day 14, normalized optical density can reach up to

245.6, which is about 58 times higher than the control. This result substantiated the effect of the green cycle and N-N-A sources on cell growth in *Botryococcus braunii*.

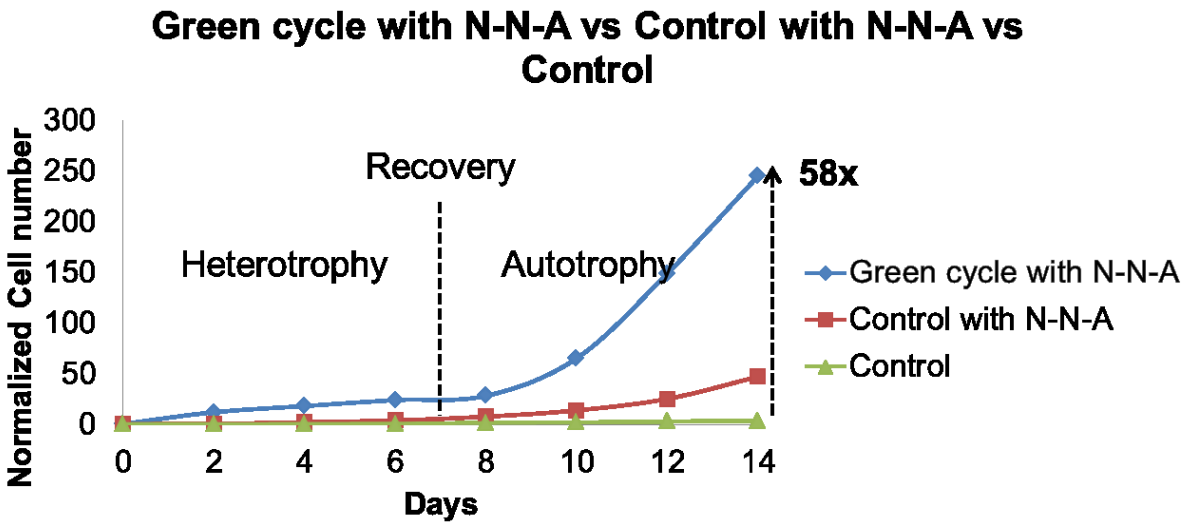

Fig. 62 Cell growth curve under three different conditions: green cycle with N-N-A sources, N-N-A only, control.

The green cycle provides a highly efficient cultivation platform for rapid accumulation of *Botryococcus braunii.* We believe that it can be generalized into microalgae culture technique.

Use of pH buffer in commercial scale microalgae cultivation is expensive and energy-intensive. N-N-A sources can maintain constant pH for the culture media which saves the use of pH buffer thereby facilitating large-scale cultivation. By feeding N-N-A

sources as continuous nitrogen supply, cell culture can reach higher growth and optimized nitrogen uptake efficiency.

Commercial scale microalgae cultivation is the ultimate solution for the microalgae industry. Therefore the search for an efficient cultivation platform is paramount in this field. We have visited many microalgae companies and institutions in the United States and we believe this work could be very important to them.

Fig. 63 A visit to Earthrise farm at Calipatria, California.

Reference

1. Parry M. Millions at Risk, Millions at Risk: Defining critical climate threats and targets. *Global Environmental Change*, **11:** 181-183 (2001)
2. Amin S. Review on biofuel oil and gas production processes from microalgae. *Energy. Convers. Manage.,* **50:** 1834–40 (2009)
3. Hassan MA, Yacob S, Ghani BA. Utilization of biomass in Malaysia-potential for CDM business, *Faculty of Biotechnology* (2005)
4. Global Economics & Climate Change: Energy in 2050, HSBC Global Research, *HSBC Climate change* (2011)
5. An Assessment of World Hydrocarbon Resources, H-H. Rogner, *Annu. Rev. Energy Environ*., **22:** 217–62 (1997)
6. World Energy Outlook 2001, International Energy Agency, *IEA 2001*, p.44 (2001)
7. Malakoff, Yeston, Smith. Getting better to get bigger. *Science*, **329:** 779 (2010)
8. Yeston. A Biofuels Wikis. *Science*, **330:** 428 (2010).
9. Marcuschamer. Technoeconomic analysis of biofuels: A wiki-based platform for lignocellulosic biorefineries, *Biomass Bioenergy*, **34(12):** 1914-21 (2010)
10. Reijnders L. Conditions for the sustainability of biomass based fuel use. *Energy Policy*, **34:** 863–76 (2006)
11. Ozcimen D, Karaosmanoglu F. Production and characterization of bio-oil and biochar from rapeseed cake. *Renew. Energy*, **29:** 779–87 (2004)
12. Jefferson M. Sustainable energy development: performance and prospects. *Renew. Energy*, **31:** 571–82 (2006)
13. Cadenas A, Cabezudo S. Biofuels as sustainable technologies: perspectives for less developed countries. *Technol. Forecast Social Change*, **58:** 83–103 (1998)
14. Difiglio C. Using advanced technologies to reduce motor vehicle greenhouse gas emissions. *Energy Policy*, **25:** 1173–8 (1997)
15. G. Berndes, M. Hoogwijk, R. van den Broek, *Biomass Bioenergy*, **25:** 1 (2003).

16. E. M. W. Smeets, A. P. C. Faaij, I. M. Lewandowski, W. C. Turkenburg, *Prog. Energy Combust. Sci.*, **33:** 56 (2007).
17. J. E. Campbell, D. B. Lobell, R. C. Genova, C. B. Field, *Environ. Sci. Technol.*, **42:** 5791 (2008)
18. International Energy Agency, Energy Technology Perspectives 2008—Scenarios and Strategies to 2050 (*International Energy Agency*, Paris, 2008), pp. 307–338
19. Demirbas A. Biomass resources for energy and chemical industry. *Energy Edu. Sci. Technol.*, **5:** 21–45 (2000)
20. Puppan D. Environmental evaluation of biofuels. *Period. Polytec. Ser. Soc. Man. Sci.,* **10:** 95–116 (2002)
21. Wang D, Czernik S, Montane´ D, Mann M, Chornet E. Biomass to hydrogen via pyrolysis and catalytic steam reforming of the pyrolysis oil and its fractions. *IEC. Res.,* **36:**1507–18 (1997)
22. Wang D, Czernik S, Chornet E. Production of hydrogen from biomass by catalytic steam reforming of fast pyrolysis oils. *Energy Fuels,* **12:** 19–24 (1998)
23. Czernik S, French R, Feik C, Chornet E. Production of hydrogen from biomass by pyrolysis/steam reforming. *Advances in hydrogen energy*, New York, p. 87–91 (2000)
24. Demirbas A. Yields of hydrogen-rich gaseous products via pyrolysis from selected biomass samples. *Fuel,* **80:** 1885–91 (2001)
25. Demirbas A. Hydrogen production via pyrolytic degradation of agricultural residues. *Energy Sources,* **27:** 769–75 (2005)
26. Demirbas A. Hydrogen-rich gas from fruit shells via supercritical water extraction. *Int. J. Hydrogen Energy,* **29:** 1237–43 (2004)
27. Haas MJ, McAloon AJ, Yee WC, Foglia TA. A process model to estimate biodiesel production costs. *Biores. Technol.,* **97:** 671–8 (2006)
28. Prakash CB. A critical review of biodiesel as a transportatıon fuel in Canada. *A technical report. Canada*: GCSI—Global Change Strategies International Inc. (1998)
29. Demirbas A. Diesel fuel from vegetable oil via transesterification and soap pyrolysis. *Energy Sources,* **24:** 835–41 (2002)

30. Meher LC, Sagar DV, Naik SN. Technical aspects of biodiesel production by transesterification—a review. *Renew. Sust. Energy Rev.,* **10:** 248–68 (2006)
31. Madras G, Kolluru C, Kumar R. Synthesis of biodiesel in supercritical fluids. *Fuel,* **83:** 2029–33 (2004)
32. Ali Y, Hanna MA, Cuppett SL. Fuel properties of tallow and soybean oil esters. *JAOCS,* **72:**1557–64 (1995)
33. Usta N, Ozturk E, Can O, Conkur ES, Nas S, Con AH, et al. Combustion of biodiesel fuel produced from hazelnut soapstock/waste sunflower oil mixture in a Diesel engine. *Energy Convers. Manage.,* **46:** 741–55 (2005)
34. Knauf, M. & Moniruzzaman, M. Lignocellulosic biomass processing: a perspective. *Int. Sugar J*., **106:** 147–150 (2004).
35. Sticklen, M. B. in Proc. 2nd Int. Ukrainian Conf. Biomass for Energy, *Ukraine Natl. Acad. Sci., Kiev*,133-6 (2004)
36. Demirbas A. Progress and recent trends in biofuels. *Prog. Energy Combust. Sci.,* **33(1) :**1–18 (2007)
37. W. J. Oswald, C.G. Golueke, Biological transformation of solar energy. *Adv. Appl. Microbiol*., **2:** 223 (1960).
38. J. Sheehan, T. Dunahay, J. Benemann, P. Roesler, A Look Back at the U.S. Department of Energy's Aquatic Species Program: Biodiesel from Algae (Department of Energy, Golden, CO, 1998).
39. N. Usui, M. Ikenouchi, *Energy Convers. Manage*., 38 (suppl. 1), S487 (1997)
40. Q. Hu et al., *Plant J*., **54:** 621 (2008)
41. Y. Chisti, *Biotechnol. Adv*., **25:** 294 (2007)
42. S. Lestari, P. Mäki-Avela, J. Beltramini, G. Q. M. Lu, D. Y. Murzin, *Chem. Sus. Chem*., **2:** 1109 (2009)
43. J. Benemann, *J. Appl. Phycol*., **12:** 291 (2000)
44. M. D. Deng, J. R. Coleman, *Appl. Environ. Microbiol*., **65:** 523 (1999)
45. L. Reijnders, *Trends Biotechnol*., **26:** 349-351 (2008)

46. A. Banerjee, R. Sharma, Y. Chisti, U. C. Banerjee, *Crit. Rev. Biotechnol*., **22:** 245 (2002)

47. O. Pulz, W. Gross, *Appl. Microbiol. Biotechnol*., **65:** 635 (2004)

48. Food and Agriculture Organization of the United Nations, http://faostat.fao.org

49. International Energy Agency (IEA), *Oil Market Report*, 10 June 2010; http://omrpublic.iea.org

50. T. L. Walker, C. Collet, S. Purton, *J. Phycol*., **41:** 1077 (2005)

51. S. S. Merchant et al., *Science,* **318:** 245 (2007)

52. E. V. Armbrust et al., *Science,* **306:** 79 (2004)

53. C. Bowler et al., *Nature,* **456:** 239 (2008)

54. A. Melis, *Plant Sci*., **177:** 272 (2009)

55. M. Tredici, *Biofuels,* **1:** 143 (2010)

56. Q. Hu, A. Richmond, *J. Appl. Phycol*., **8:** 139 (1996)

57. J. W. F. Zijffers et al., *Mar. Biotechnol*., **12(6):** 708–718 (2010)

58. R. H. Wijffels, M. J. Barbosa, M. H. M. Eppink, *Biofuels Bioproducts Biorefining,* **4:** 287 (2010)

59. R. Bosma, M. H. Vermue, J. Tramper, R. H. Wijffels, *Int. Sugar J*., **112:** 74 (2010)

60. K. van Egmond, T. Bresser, L. Bouwman, *Ambio,* **31:** 72 (2002)

61. Wijffels, R.H. & Barbosa, M.J. An outlook on microalgal biofuels. *Science*, **329:** 796 (2010)

62. Miller, S.A. Minimizing land use and nitrogen intensity of bioenergy. *Environ. Sci. Technol.*, **44:** 3932–3939 (2010)

63. Melillo, J.M. et al. Indirect emissions from biofuels: how important? *Science,* **326:** 1397–1399 (2009)

64. Crutzen, P.J., Mosier, A.R., Smith, K.A. & Winiwarter, W. N2O release from agro-biofuel production negates global warming reduction by replacing fossil fuels. *Atmos. Chem. Phys*., **8:** 389–395 (2008)

65. Erisman, J.W., Sutton, M.A., Galloway, J., Klimont, Z. & Winiwarter, W. How a century of ammonia synthesis changed the world. *Nature Geoscience,* **1:** 636–639 (2008)

66. Becker, E.W. Micro-algae as a source of protein. *Biotechnol., Adv.* **25:** 207–210 (2007)

67. Hazelwood, L.A., Daran, J.M., van Maris, A.J.A., Pronk, J.T. & Dickinson, J.R. The Ehrlich pathway for fusel alcohol production: a century of research on Saccharomyces cerevisiae metabolism. *Appl. Environ. Microbiol.,* **74:** 2259–2266 (2008)

68. Atsumi, S., Hanai, T. & Liao, J.C. Non-fermentative pathways for synthesis of branchedchain higher alcohols as biofuels. *Nature,* **451:** 86–89 (2008)

69. Zhang, K., Sawaya, M.R., Eisenberg, D.S. & Liao, J.C. Expanding metabolism for biosynthesis of nonnatural alcohols. *Proc. Natl. Acad. Sci.,* **105:** 20653–58 (2008)

70. Edited by Renewable fuels association. *2010 Ethanol Industry Overlook*. (2010) available at http://www.ethanolrfa.org/pages/annual-industry-outlook

71. Wake LV, Hillen LW. Study of a “bloom” of the oil-rich alga *Botryococcus Braunii* in the Darwin River Reservoir. *Biotechnol. Bioeng.,* **22:**1637–56 (1980)

72. Wake LV, Hillen LW. Nature and hydrocarbon content of blooms of the alga *Botryococcus Braunii* occurring in Australian freshwater lakes. *Aust. J. Mar. Freshwater Res.,* **32(3):** 353–367 (1981)

73. Aaronson S, Berner T, Gold K, Kushner L, Patni NJ, Repak A, Rubin D. Some observations on the green planktonic alga, *Botryococcus Braunii* and its bloom form. *J. Plankton Res.,* **5:** 693–700 (1983)

74. Huszar VLM, Reynolds CS. Phytoplankton periodicity and sequences of dominance in an Amazonian flood-plain lake (Lago Bata, Parà, Brazil): responses to gradual environmental change. *Hydrobiologia,* **346:** 169–181 (1997)

75. Huang Y, Street-Perrott FA, Perrott RA, Metzger P, Eglinton G. Glacial-interglacial environmental changes inferred from molecular and compound-specific $\delta^{13}C$ analyses of sediments from Sacred lake, Mt. Kenya. *Geochim. Cosmochim.,* **63:** 1383–140476 (1999)

76. Metzger P, Largeau C. Chemicals of *Botryococcus Braunii*. In: Cohen Z (ed) Chemicals from microalgae. Taylor & Francis, London, pp 205–260 (1999)

77. Volova TG, Kalacheva GS, Zhila NO. Specificity of lipid composition in two Botryococcus strains, the producers of liquid hydrocarbons. *Russ. J. Plant Physiol.,* **50:** 627–633 (2003)

78. Brown AC, Knights BA. Hydrocarbon content and its vrelationship to physiological state in the green alga *Botryococcus Braunii*. *Phytochemistry,* **8:** 543–547 (1969)

79. Knights BA, Brown AC, Conway E, Middleditch BS. Hydrocarbons from the green form of the freshwater alga *Botryococcus Braunii*. *Phytochemistry,* **9:** 1317–1324 (1970)

80. Metzger P, Casadevall E. Botryococcoid ethers, ether lipids from *Botryococcus Braunii*. *Phytochemistry*, **30:** 1439–1444 (1991)

81. Chisti, Y. An unusual hydrocarbon. *J. Ramsay Society,* **27–28:** 24–26 (1980)

82. Gelpi, E., Schneider, H., Mann, J., and Oro, J. Hydrocarbons of geochemical significance in microscopic algae. *Phytochemistry,* **9:** 603 (1970)

83. Metzger, P., Allard, B., Casadevall, E., Berkaloff, C., and Coute, A. Structure and chemistry of a new chemical race of *Botryococcus Braunii* (chlorophyceae) that produces lycopadiene, a tetraterpenoid hydrocarbon. *J. Phycol.,* **26:** 258 (1990)

84. Metzger, P. and Casadevall, E. Lycopadiene, a tetraterpenoid hydrocarbon from new strains of the green alga *Botryococcus Braunii*. *Tetrahedron Lett.,* **24:** 2305 (1987)

85. Metzger, P., Casadevall, E., and Coute, A. Botryococcene distribution in strains of green alga *Botryococcus Braunii*. *Phytochemistry,* **27:** 1383 (1988)

86. Largeau C, Casadevall E, Berkaloff C, Dhamelincourt P. Sites of accumulation and composition of hydrocarbons in *Botryococcus Braunii*. *Phytochemistry,* **19:** 1043–1051 (1980)

87. Metzger, P., Berkaloff, C., Casadevall, E., and Coute, A. Alkadiene and botryococcene producing races of wild strains of *Botryococcus Braunii*. *Phytochem.,* **24:** 2305 (1985)

88. Metzger, P., Casadevall, E., Pouet, M. J., and Pouet, Y. Structure of some botryococcenes: branched hydrocarbons from the B race of the green alga *Botryococcus Braunii*. *Phytochem,* **24:** 2995 (1985)

89. Grung, M., Metzger, P., and Liaaen-Jensen, S. Algal carotenoids, primary and secondary carotenoids in two races of green alga *Botryococcus Braunii*. Biochem. Sys. Eco., **17:** 263 (1989)

90. Grung, M., Metzger, P., and Liaaen-Jensen, S. Secondary carotenoids in *Botryococcus Braunii* race L, new strain. *Biochem. Sys. Eco.,* **22:** 25 (1994)

91. Tonegawa, I., Okada, S., Murakami, M., and Yamaguchi, K. Pigment composition of the green microalga *Botryococcus Braunii*, Kawaguchi. *Fish Sc.,* **64:** 305 (1998)

92. Wolf, F. R., Nanomura, A. M., and Bassham, J. A. Growth and branched hydrocarbon production in a strain of *Botryococcus Braunii*. *J. Phycol.,* **21:** 388 (1985)

93. Weetal, H. H. 1985. Studies on nutritional requirements of the oil producing alga *Botryococcus Braunii*. *Appl. Biochem. Biotechnol.,* **11:** 377 (1985)

94. Ben-Amotz, A., Torbene, T. G., and Thomas, W. H. Chemical profile of selected species of microalgae with emphasis on lipids. *J. Phycol.,* **21:** 72 (1985)

95. Casadevall, E., Largeau, C., Metzger, P., Chirac, C., Berkaloff, C., and Coute, A. Hydrocarbon production by unicellular microalga *Botryococcus Braunii*. *Biosciences,* **2:** 129 (1983)

96. Brenckman, F., Largeau, C., Casadevall, E., and Berkaloff, C. Effect of nitrogen nutrition on growth and hydrocarbon production of the unicellular microalga *Botryococcus Braunii*. *Comm. Eur. Communities, Energy Biomass,* 717 (1989)

97. Casadevall, E., Dif, D., Largeau, C., Gudin, C., Chamount, D., and Desanti, O. Studies on batch and continuous culture of *Botryococcus Braunii*: hydrocarbon production in relation to physiological state, cell ultrastructure and phosphate nutrition. *Biotechnol. Bioeng.,* **27:** 286 (1985)

98. Wolf, F. R., Nanomura, A. M., and Bassham, J. A. Growth and branched hydrocarbon production in a strain of *Botryococcus Braunii*. *J. Phycol.,* **21:** 388 (1985)

99. Oh, H. M., Kim, S., Park, E. R., Lee, S. T., Kwon, J. S., and Yoon, B. D. Effects of light intensity and nutrients on the growth of *Botryococcus* sp. *Misaengmul Hakhoechi,* **25:** 339 (1997)

100. Kojima, E. and Zhang, K. Growth and hydrocarbon production by microalga *Botryococcus Braunii* in bubble column photobioreactor. *J. Bioscience Bioeng.,* **87:** 811 (1999)

101. Lupi, F. M., Fernandes, H. M. L., Tomme, M. M., Sa Correia, I., and Novais, J. M. Influence of nitrogen source and photoperiod on exopolysaccharide synthesis by the microalga *Botryococcus Braunii*. *Enzyme Microb. Technol.,* **16:** 546 (1994)

102. Lupi, F. M., Fernandes, H. M. L., Sa Correia, I., and Novais, J. M. Temperature profiles of cellular growth exopolysaccharide synthesis by *Botryococcus Braunii*. *J. Phycol.,* **3:** 35 (1991)

103. Wang, X. and Xie, S. Effects of several factors on growth of *Botryococcus Braunii*. *Weishengwuxue Tongbao,* **23:** 275 (1996)

104. Frenz, J., Largeau, C., and Casadevall, E. Hydrocarbon recovery by extraction with a biocompatible solvent from free and immobilized cultures of *Botryococcus Braunii*. *Enzyme Microb. Technol.,* **11:** 717 (1989)

105. Frenz, Z., Largeau, C., Csadevall, C., Kollerup, F., and Daugulis, A. J. Hydrocarbon recovery and biocompatibility of solvents for extraction from cultures of *Botryococcus Braunii*. *Biotechnol. Bioeng.,* **34:** 755 (1989)

106. Chisti, Y. Shear sensitivity. In: *Encyclopedia of Bioprocess Technology: Fermentation, Biocatalysis, and Bioseparation*, vol. 5, Flickinger, M. C. and Drew, S. W., Eds., Wiley, New York, 2379 (1999)

107. Niehaus TD, Okada S, Devarenne TP, Watt DS, Sviripa V, Chappell J. Identification of unique mechanisms for triterpene biosynthesis in *Botryococcus braunii*. *Proc. Natl. Acad. Sci. USA,* **108:** 12260–12265 (2011)

108. Modified Bold 3N Medium recipe online from UTEX, the culture collection of algae: http://www.sbs.utexas.edu/utex/mediaDetail.aspx?mediaID=55

109. Davis, M.S., Solbiati, J., Cronan Jr., J.E. Overproduction of acetyl-CoA carboxylaseactivity increases the rate of fatty acid biosynthesis in *Escherichia coli*. *Journal of Biological Chemistry,* **275 (37):** 28593–28598 (2000)

110. Kim, K.H. Regulation of mammalian acetyl-coenzyme A carboxylase. *Annual Review of Nutrition*, **17:** 77–99 (1997)

111. Li, S.J., Cronan Jr., J.E. Growth rate regulation of *Escherichia coli* acetyl coenzyme A carboxylase, which catalyzes the first committed step of lipid biosynthesis. *Journal of Bacteriology*, **175 (2):** 332–340 (1993)

112. Sendl, A., Schliack, M., Loser, R., Stanislaus, F.,Wagner, H. Inhibition of cholesterol synthesis in vitro by extracts and isolated compounds prepared from garlic and wild garlic. *Atherosclerosis,* **94(1):** 79–85 (1992)

113. Martin DB, Vagelos PR. The Mechanism of Tricarboxylic Acid Cycle Regulation of Fatty Acid Synthesis. *J. Biol. Chem.,* **237:** 1787–92 (1962)

114. Boone AN, Chan A, Kulpa JE, Brownsey RW. Bimodal Activation of Acetyl-CoA Carboxylase by Glutamate. *J. Biol. Chem.,* **275 (15):** 10819–25 (2000)

115. Faergeman NJ, Knudsen J. Role of long chain fatty acyl-CoA esters in the regulation of metabolism and in cell signalling. *Biochem. J.,* **323 (Pt 1):** 1–12 (1997)

116. Sticklen, M. B. Plant genetic engineering for biofuel production: towards affordable cellulosic ethanol. *Nature Reviews Genetics, **9*:** 433-443 (2008)

117. A.L. Ahmad, N.H. Mat Yasin, C.J.C. Derek, J.K. Lim, Microalgae as a sustainable energy source for biodiesel production: A review, *Renewable and Sustainable Energy Reviews*, **15(1):** 584-93 (2011)

118. John A Myers, Brandon S Curtis and Wayne R Curtis, Improving accuracy of cell and chromophore concentration measurements using optical density, *BMC Biophysics*, **6(1):** 4 (2013)

119. Hogg, Stuart. *Essential Microbiology* (2nd ed.). Wiley-Blackwell. p. 86. 2013

120. Fan J, Huang J, Li Y, Han F, Wang J, Li X, Wang W, Li S; Sequential heterotrophy-dilution-photoinduction cultivation for efficient microalgal biomass and lipid production. *Bioresour. Technol*., **112:** 206-11 (2012)

121. Method 1687: Total Kjeldahl Nitrogen in Water and Biosolids by Automated Colorimetry with Preliminary Distillation/Digestion, *US EPA*, EPA-821-R-01-004, 2001

122. Roe, J.H. The determination of sugar in blood and spinal fluid with anthrone reagent. *J. Biol. Chem*., **212(1):** 335-43 (1955)

123. Cawse, P.A. The determination of nitrate in soil solution by ultra-violet spectrometry. *Analyst,* **92:** 311-315 (1967)

124. Snell, F.D. and C.T. Snell. *Colorimetric methods of analysis* 11, 3rd ed. p. 785-790, Van Nostrand, New York, 1949

125. Folin, O. and W. Denis. Nitrogen determination of direct Nesslerization. *J. Biol. Chem.,* **26:** 473-478 (1916)

126. Huo, Y. *et al*. Conversion of proteins into biofuels by engineering nitrogen flux. *Nat. Biotechnol.,* **29:** 346–351 (2011)

127. P. Metzger, C. Largeau. *Botryococcus braunii*: a rich source for hydrocarbons and related ether lipids. *Appl Microbiol Biotechnol.,* **66:** 486–496 (2005)

128. UTEX webpage: Algae details. UTEX 572 http://www.sbs.utexas.edu/utex/algaeDetail.aspx?algaeID=3051

129. Banerjee A, Sharma R, Chisti Y, Banerjee UC. *Botryococcus braunii*: a renewable source of hydrocarbons and other chemicals. *Crit Rev Biotechnol*., **22(3):**245-79 (2002)

130. Medh, J.D. Cal state university, Northridge, CHEM464: Fatty Acid Biosynthesis. Page 3 http://www.csun.edu/~jm77307/Fatty%20Acid%20Biosynthesis.pdf

131. Wikipedia webpage, Control of Acetyl CoA Carboxylase. (public copyright granted) http://en.wikipedia.org/wiki/File:Control_of_Acetyl_CoA_Carboxylase_corrected.png

132. Facemonster webpage, Science>Plant, Photosynthesis. http://www.factmonster.com/ipka/A0775714.html

133. Masanori Sato, Yoshinori Murata, Mika Mizusawa, Hitoshi Iwahash, Shu-ichi Oka. A Simple and Rapid Dual-fluorescence Viability Assay for Microalgae, *Microbiol. Cult. Coll.*, **20(2):** 55-59 (2004)

134. BD Bioscience fluorochrome chart, BD fluorescence Spectrum Viewer, https://www.bdbiosciences.com/research/multicolor/spectrum_viewer/index.jsp

135. Scherholz, Curtis. Achieving pH control in microalgal cultures through fed-batch addition of stoichiometrically-balanced growth media, *BMC Biotechnology* **13:** 39 (2013)

136. Thermo Scientific webpage, Instruction: Micro BCA™ Protein Assay Kit, Thermo Scientific. https://www.piercenet.com/instructions/2160412.pdf

137. Cellsignet webpage, 96 well plate, http://www.cellsignet.com/media/plates/96.jpg

138. Wikipedia webpage, Bicinchoninic acid. (public copyright granted) http://en.wikipedia.org/wiki/File:Structure_of_bicinchoninic_acid.png

139. Fluorophores webpage, SYTOX Green, http://www.fluorophores.tugraz.at/substance/214